A Stochastic Electrodynamics Description of Quantum Teleportation with Continuous Variables

Andy Chia

A thesis submitted in fulfilment of the requirements for the degree of Master of Science in Physics.

The University of Auckland,
April 2005.

Quantum Teleportation.

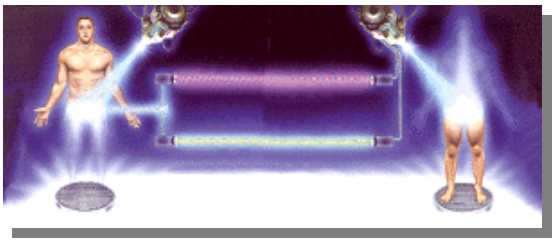

When fantasy becomes reality ....

Abstract

Stochastic electrodynamics is applied to treat continuous-variable teleportation. The approach circumvents the operator algebra that would otherwise be present in a quantum calculation. It brings advantage in the ease with which a broadband treatment of teleportation may be given.

We derive the teleported squeezing spectra and intensity correlation function for both coherent and squeezed vacuum input states. It is shown that the squeezing spectra observed by Victor (the independent verifier) reproduce those obtained from a quantum trajectory formulation of teleportation. Stochastic electrodynamics is expected to fail, however, in its treatment of photo-electron counting experiments. Indeed it miscalculates the intensity correlations measured at the teleporter output.

Preface

On many occasions has the author found himself in a quandary trying to decide on what material to present. This report has not given the author a chance neither to be expansive or to expatiate on certain topics as he would have liked. In compromising, he has tried to be comprehensive with the selected topics.

The readership of this work is defined at the level of a graduate student with conventional background knowledge on non-relativistic quantum mechanics and quantum optics. It also assumes familiarity with all computational tools that have been employed in the calculations. For most part this involves concepts of stochastic processes and preferably stochastic calculus, although this is not essential. Complex analysis is required for integrals that appear in the final derivation of the intensity correlation function in Chap. 6. We do however treat this as an adjunctive calculation and the integrals may be referred to as known results.

An Overview

The thesis begins with an introduction to what the author feels every researcher, in either the area of quantum information science or quantum/atom optics (and perhaps related areas) ought to appreciate — quantum non-locality. Holding such a substantive place in our understanding of nature, the fundamentality of quantum non-locality is manifested through uncountable quantum information networks proposed by physicists today. We introduce the principle of one such network — quantum teleportation. Among the many facets of quantum information processing protocols, teleportation utilizes non-locality to assist the sending of information over large distances; the details of which are revealed in Chap. 2. The attention then drifts towards stochastic electrodynamics and its application to teleportation within a quantum optical setting. The third chapter is intended to be transitory. The analysis and historical account of the subject presented up to the end of Chap. 3 brings the reader up to date and adequately confident to examine teleportation by the more intriguing methods of Chap. 4–6. The transitions between time and frequency domains in our analysis are shown below:

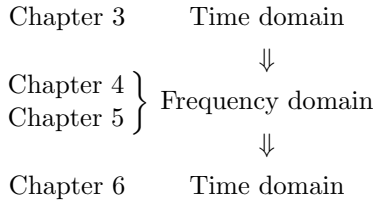

Each of Chap. 5 and 6 is based on a measure of the success of teleportation while Chap. 4 discusses some preliminary assumptions and derives the teleporter output as a function of known inputs in frequency space. In quantifying teleportation, no attempts are made to use "fidelity", as the word has been assigned specific definitions within quantum information. This thesis will relinquish the word to cease ambiguity as to whether it is the technical definition that has been referred or the faithfulness of teleportation.

Teleportation will be verified upon examining the squeezing spectra and intensity correlation function at the output. The two quantities are derived in Chap. 5 and 6. We close this report by summarizing the results obtained in the investigation thus far, and draw some conclusive statements regarding the applicability of stochastic electrodynamics to teleportation in Chap. 7. Possible future elaborations are also suggested therein.

A Note of Caution : I have not taken care with the use of the word "mode", and unfortunately the word is ubiquitous in physics, especially within optics. Technically a mode of the optical field is labelled by a particular frequency, direction of travel, and its polarization. For the majority of the content, we will not be so assiduous with the precise definition. We shall adapt to using mode as synonymous with frequency. However, in Sect. 4.1.2 where a density of modes $g(\omega)$ is used to convert a set of discrete field statistics is into the continuum, the word mode will come to denote all three properties just mentioned. Even more confusing, the word "mode" as used to differentiate single-mode and multi-mode teleportation does not refer to the frequency content of the light at all. All fields are in fact broadband, i.e. multi-frequency. Mode here refers to the use of distinctive pulses of light for teleportation and leads to a dissimilarity in the sequence of steps taken to accomplish teleportation. This is a remark in need to be pointed out if one intends to delve into the literature of teleportation. In general, the meaning of "mode" should be read under context.

Acknowledgements

To Howard : I always knew that I am like a reservoir of energy, endlessly poured into physics. You have just steered the reservoir vent a bit towards theoretical quantum optics. Thanks for understanding my *masochistic* nature in writing a *sexy* thesis. *It takes a perfectionist to understand a perfectionist.* My time spent working with you has given me an opportunity for introspection about my thoughts on physics, in particular quantum optics. Perhaps my opening paragraph *did* express a naive predilection towards Einstein, I believe time will tell as it has always.

To Mathew : I know that in the course of this year I have bothered Howard more than I have bothered you. Nevertheless, the various solutions and explanations you have shown me to the same problem (related or unrelated to teleportation) still scares me. Your quantum field theory course is by far the most exciting, if not the most difficult of all courses. It has been the only paper which I entered the lecture theatre so exuberantly on every allocated session.

To Chang-Suk : It has been a real pleasure to be your colleague. I have certainly benefitted from the many discussions we have had about physics.

To Dr. Bold and Sze Tan : Nobody (with the exception of Howard and Mathew) has shown the dedication you have in educating students. Simply said, your efforts are incomparable and your influence is definitely in this thesis. The numerous laboratory sessions Sze has spent telling me about theory instead of letting me to "just do the lab" is an indispensable character rarely seen.

I would like to give everyone above a Chinese phrase that I have come to love and live by:

真正的財富不是身外之物而是
隱藏在你內心的潛在動力

Auckland *Andy Chia*
April 2005

Contents

List of Figures

Chapter 1

Entanglement: A Departure from Classical Physics

The year 1935 brought to physics perhaps one of the most renowned controversies known of science. The year 1935 was when Einstein stood against profound notions widely accepted by the scientific community but to which he could not concede, these notions being non-locality and indeterminism as proclaimed by quantum mechanics. Einstein, along with two younger supporters, formally put forward his objection, which later became known as the EPR paradox, bearing the name of those who had such radical thoughts about physical reality: A. Einstein, B. Podolsky, and N. Rosen [1].

Unfortunately for EPR, this was also the age of quantum dominance. Quantum mechanics had flourished so vigorously churning out spectacular predictions that most workers in the field did not question the fundamental nature of the theory they were using, i.e. the probabilistic interpretation of quantum mechanics. The estimable EPR paradox arguably known to every graduate student of physics today, had played a subordinate role then, except for Schrödinger, Bohr[1], and perhaps a few of equal rank who communicated with Einstein. The problem, the incompleteness of quantum mechanics, which EPR had so much faith in, was disconnected from the core physics community. There was no impetus in the hearts of many towards any form of resolution. We now discuss the EPR paradox at some length.

1.1 The Einstein-Podolsky-Rosen Paradox

In establishing any theory, or in the case of EPR, a repudiation of another, assumptions are made. Unlike other situations where the assumptions (or approximations) at the outset may often be judged reasonable or not, based on how sensitive they are to variations of pertinent parameters in a model, the assumptions of EPR were no more than an asseveration of their intuition. Let us set out the premise of their argument:

[1]An initial reply to the 1935 EPR paper is documented, for example in [2]. Since then Niels Bohr was known to have communicated with Einstein on the foundations and interpretations of quantum mechanics until the time of his passing.

- **Reality**

  EPR claimed, as a sufficient condition of physical reality, the following [1].

  If, without in any way disturbing a system, we can predict with certainty (i.e., with probability equal to unity) the value of a physical quantity, then there exists an element of physical reality corresponding to this physical quantity.

  An "element of physical reality" is a variable assigned to a physical quantity which describes it at a particular location. The value of this variable is one of the set of possible results of measuring the physical quantity. It is clear then, in the theory of quantum mechanics, that such elements of reality refer to eigenvalues of observables.

- **Locality**

  Locality is often said to be "no-action-at-a-distance". It postulates that the action of measuring one system at one location, does not instantaneously disturb or "influence" another system at a spatially separated location to the former.

- **Completeness**

  Einstein certainly had no doubts about the correctness of quantum mechanics; it was the completeness of the theory which had irritated him. EPR considered the following to be a necessary criterion for a theory to be complete:

  Every element of the physical reality must have a counterpart in the physical theory.

EPR argued that quantum mechanics was incomplete on the grounds of "local realism", which was the combined territory of *reality* and *locality*. Due to D. Bohm and Y. Aharonov, the important workings of the EPR paper are encapsulated in a simple thought-experiment involving two particles (Fig. 1.1) [3]. Consider a source capable of producing two spin-1/2 particles, flying apart in opposite directions with total spin of zero. Denoting the spin of

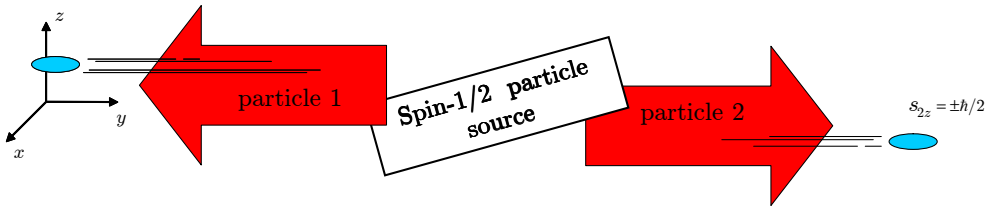

Fig. 1.1: Bohm's version of the EPR paradox. Two particles are emitted into pure linear motion.

particle j ($j = 1, 2$) along the direction of a unit vector $\mathbf{n}$ by s_{jn}, Bohm's recapitulation of the EPR argument proceeds as below:

Suppose two observers, Alice and Bob, each with a Stern-Gerlach magnet standing at opposite ends awaiting particles 1 and 2 respectively. Assuming the particles could travel arbitrarily large distances without being disturbed, Alice and Bob choose to station themselves sufficiently far apart so that after the initial interaction in the source, each particle could be considered an independent system on arrival. Suppose Bob now awaits particle 2 with his Stern-Gerlach magnet orientated to measure the z component of its spin. He finds $s_{2z} = \hbar/2$. By locality, Bob's act of measuring particle 2 could not have causally affected particle 1. Furthermore, conservation of total angular momentum allows Bob to predict with

certainty the z component of the spin of particle 1, thus meeting the criterion of reality; the element of reality in this case being s_{1z}. We see then, given the initial condition, a local realistic argument interprets the evolution of a physical system to be predetermined; expressive of Einstein's thought that the laws of physics be deterministic.

Now suppose Bob now orientates his Stern-Gerlach magnet to first measure s_{2z} and then s_{2x}, at the same location in space. By the same token, Bob now has knowledge of both s_{1z} and s_{1x}. There should then exist two elements of reality, one being s_{1z} and the other s_{1x}. This was an attack against Heisenberg's uncertainty principle; namely that precise knowledge about one of any two observables represented by non-commuting operators precludes knowledge of the other. In other words, the element of reality corresponding to either the z or x component of spin for particle 1, did not enter quantum theory, for if both elements of reality did, both eigenvalues would be simultaneous permissible. Einstein thus proposed that either

(1) *the quantum mechanical description of reality given by the wave function is not complete* or,

(2) *when the operators corresponding to two physical quantities do not commute the two quantities cannot have simultaneous reality.*

Since, abiding by their definition of reality, the above example demonstrates that (2) is false, EPR, in accordance with their necessary condition for a theory to be complete, condemn the wave function of quantum mechanics as holding an incomplete description of reality. The physics mainstream remained oblivious to EPR's claim for almost 30 years, until finally in 1964 while working at CERN, J. Bell put to rest all speculations regarding alternatives to quantum mechanics — the so called **local hidden-variable theories** — with his definitive statement today renowned as **Bell's inequality**.

1.1.1 Defying Locality and Reality

It was in a series of three papers, motivated by the EPR paradox, that Schrödinger introduced the concept of quantum entanglement, and at the same time presented to the world his famous "cat" [4], [5]. Formally, *An entangled state is a state of a compound system whose subsystems are not probabilistically independent* [6]. One such state is

$$|\psi\rangle = c^{(1)}\,|\alpha_1\rangle \otimes |\eta_2\rangle + c^{(2)}\,|\beta_1\rangle \otimes |\chi_2\rangle \ , \tag{1.1a}$$

where $|\psi\rangle$ describes a two particle system with probability amplitudes $c^{(1)}$ and $c^{(2)}$,

$$\left|c^{(1)}\right|^2 + \left|c^{(2)}\right|^2 = 1 \ . \tag{1.1b}$$

Each subsystem is labelled by an arabic subscript, and satisfies

$$\langle\alpha_1|\beta_1\rangle = \delta_{\alpha\beta} \ , \quad \langle\eta_2|\chi_2\rangle = \delta_{\eta\chi} \ . \tag{1.1c}$$

An entangled state is often said to be one that is impossible to factorize into a product, $|a\rangle \otimes |b\rangle$ where $|a\rangle$ and $|b\rangle$ may be general superpositions for subsystem 1 and 2 respectively. This was also put forth qualitatively[2] by Schrödinger in 1935 as the following theorem:

[2]Schrödinger's theorem is a defining *feature* of entanglement but does not *quantify* entanglement by any means of numbers or measures.

An entangled state can never be factorized and a factorized one can never be written as an entangled one.

A proof may be found in Ref. [7].

Let us put the above definitions, i.e. (1.1), in the context of Bohm's two-particle setting. The scenario is described by the spin-singlet state

$$|\psi\rangle = \frac{1}{\sqrt{2}}\Big(|\uparrow_{1n}, \downarrow_{2n}\rangle - |\downarrow_{1n}, \uparrow_{2n}\rangle \Big) \,, \tag{1.2}$$

where $|\uparrow_{1n}, \downarrow_{2n}\rangle = |\uparrow_{1n}\rangle \otimes |\downarrow_{2n}\rangle$, $|\downarrow_{1n}, \uparrow_{2n}\rangle = |\downarrow_{1n}\rangle \otimes |\uparrow_{2n}\rangle$ with $\uparrow_{jn}$ and $\downarrow_{jn}$ denoting $s_{jn} = \hbar/2$ and $s_{jn} = -\hbar/2$ respectively. Note the vital attribute that no direction in space is preferred by spin-singlet states. This very fact is the essence of entanglement. We can draw upon an analogy whereby macroscopic objects may be entangled. Consider three pairs of balls, each ball is entangled with one other in colour; the white entangled with the black, the red with the blue, and finally purple with green. Alice and Bob now each pick out a ball each from a sack and walk off in opposite directions with their balls completely enclosed in their hands. After some distance, Bob decides to loosen his palm and look at his ball. It is white. Alice also decides to look at her ball, and finds it to be black. One could well argue that Alice just coincidentally grabbed the black ball out of the sack; i.e. the colour of Alice's ball was predetermined.

The real factual situation described by quantum mechanics is frightening, for there were six balls initially to be picked from. So let us return all the balls to the sack and bring Alice and Bob to the origin where they are allowed to pick again, without looking, a ball at random. This time Bob looks at his ball and finds its colour to be purple. To his astonishment, after returning to the sack Bob learns that Alice held a green ball. The analogous situation to (1.2) with our entangled balls is simple. The moment of revelation at either Alice's or Bob's end turns the colour of the ball in the other's palm into that of the entangled colour. That is, suppose Alice looks first and finds her ball to be black, she knows Bob must now hold a white one, and if her ball was blue, Bob's will be red. The role of n in (1.2) which observers may choose by orientating their Stern-Gerlach magnets is played out by the myriad of colours one could make available in our balls. The carriage of the ball by Alice or Bob then labels the particle number j. The spin, or more generally the state of the particle corresponds to the endowed colours in our analogy, while the measurement process is the very act of looking at the ball.

An exceedingly non-classical property that is assumed in the foregoing discussion can now be brought to the fore from Bohm's two-particle system, i.e., the measurement postulate in quantum mechanics, which when tied with the conservation of spin (or any other property) so inimically confronts our intuition regarding locality. We demonstrate in the next section, how the comfort-zone of local realism that Einstein (or us) had insisted was demolished.

1.1.2 Superluminal Communication

So does the above imply that faster-than-light communication can be made possible with spin-entangled particles, or for that matter, any variable which can be made to possess such non-local correlations? Perhaps Einstein had introduced the condition of locality into the EPR paradox to pre-empt special relativity being overthrown by quantum mechanics. It should be recognized that to establish communication, a sender must somehow modulate

a physical attribute of some material body. That modulation must then arrive on the doorsteps of a receiver, who is able to read the sender's deliberateness in the signal. Such a task can not be accomplished solely by the shared correlation in the hands of Alice and Bob. At best, Alice and Bob can agree to measure only s_{jz} prior to departure from the source, and assign Alice as the sender. She can then change the quantization axis which she measures as a form of encoding. However, the distant Bob has no way of telling Alice's modulation; all Bob sees is a string of s_{2z} values. Thus, no useful information is transferred.

In addition, special relativity is in no sense violated by the non-locality of entanglement. The implication of Einstein's theory of special relativity is clear: that no moving objects with *finite* rest-mass can attain the speed of light. So either the disturbance transmitted from Alice to Bob has no mass, or, nothing really did propagate — neither violating special relativity.

1.2 Hidden-Variable Theories and Bell's Theorem

We now outline the development of interpretational subtleties in quantum mechanics.

1.2.1 The Meaning of Hidden-Variables

Should one come to terms with the fundamental framework of quantum mechanics — i.e., that the description of physical reality can only be furnished by probabilities of possible events? Some have been uneasy and have suggested that the stochastic nature of quantum mechanics implies that there are, floating around, unknown variables, *hidden-variables*, which must accommodate the probabilities obtained from the time-dependent Schrödinger equation while remaining unobserved. These variables *when* specified, would render dispersion-free states for the observables of a system (i.e. without uncertainties). In other words, with knowledge of the hidden-variables one could predict which of the set $\{a_1, a_2, \ldots a_n\}$ satisfying

$$\hat{A}\,|\psi\rangle = a_i\,|\psi\rangle \ , \quad i = 1, 2, \ldots, n \ , \tag{1.3}$$

would result from a measurement of a system in the state $|\psi\rangle$, corresponding to an observable represented by $\hat{A}$, with unit probability, thus providing a fully deterministic theory of the type Einstein had envisaged.

Prior to the EPR declaration against the completeness of quantum mechanics, hidden-variable considerations had already raised a suspicion that quantum theory may not be safe from any loopholes. The first attempt to dispel such thoughts came from the brilliant mathematician J. von Neumann, who presented a proof in 1932 that hidden-variable theories, local or not, could never reproduce the predictions of quantum mechanics, i.e. hidden-variable theories are impossible [8]. Both von Neumann and EPR's claim had stimulate no effort on the part of others, to pin down in precise terms whether one theory should be preferred over the other. Finally by 1952 D. Bohm had explicitly constructed a *non-local* hidden-variable theory yielding results in parallel to those predicted by quantum mechanics [9], [10]. That Bohm could concoct such a hidden-variable description meant von Neumann's 1932 proof required further scrutiny.

1.2.2 An Inequality to Rule Them All

Two prodigious results arose from the mind of J. Bell. The first came in 1964. A mathematical condition was derived for the two-particle spin system which eliminated the possibility of having a local realistic theory [11]. The second was Bell's reassessment of von Neumann's proof in which an imprudent assumption was identified. The assumption was shown to be an unnecessary restriction to impose on hidden-variable theories [12]. We follow the argument of Bell that led to his critically acclaimed relation. Let us return to the fashionable spin-singlet scenario of Bohm, this time with Bob measuring the spin component of particle 2 at an angle α to the z-axis. The measurement direction will be confined to the xz-plane for simplicity (Fig. 1.1) and the measured spin component denoted by $s_{2\alpha}$.

A successful general proof to show that local hidden-variable theories are impossible must embody determinism, provided by hidden-variables, conventionally written as λ. Thus there should exist a probability density function $p(\lambda)$ with the normalization,

$$\int_\Lambda p(\lambda)\, d\lambda = 1 \,, \tag{1.4}$$

where λ is a continuous variable $\lambda \in \Lambda$. Each pair of particles has a definite but undetectable value of λ, where $p(\lambda)d\lambda$ is the probability that a pair will have their hidden-variable between λ and $\lambda + d\lambda$. It must also be assumed that Alice's and Bob's measurements be independent. In no sense shall $s_{2\alpha}$ have any dependence on the orientation of Alice's Stern-Gerlach apparatus and neither shall Alice's measurement depend on Bob's. Bell began by considering the correlation between s_{1z} and $s_{2\alpha}$,

$$f(\alpha) \equiv \int_\Lambda s_{1z}(\lambda)\, s_{2\alpha}(\lambda)\, p(\lambda)\, d\lambda \,. \tag{1.5}$$

By considering another measurement of the spin component lying at an angle β to the z-axis, we may write

$$f(\alpha) - f(\beta) \,=\, \int_\Lambda \left[s_{1z}(\lambda)\, s_{2\alpha}(\lambda) - s_{1z}(\lambda)\, s_{2\beta}(\lambda)\right] p(\lambda)\, d\lambda \,. \tag{1.6}$$

Since the two particles must conserve spin; $s_{1\alpha}(\lambda) = -s_{2\alpha}(\lambda)$, $s_{1\beta}(\lambda) = -s_{2\beta}(\lambda)$,

$$\begin{aligned} f(\alpha) - f(\beta) \,&=\, \int_\Lambda s_{1z}(\lambda)\left[s_{1\beta}(\lambda) - s_{1\alpha}(\lambda)\right] p(\lambda)\, d\lambda \\ &=\, \int_\Lambda s_{1z}(\lambda)\, s_{1\beta}(\lambda)\left[1 - \frac{4}{\hbar^2}\, s_{1\beta}(\lambda)\, s_{1\alpha}(\lambda)\right] p(\lambda)\, d\lambda \,, \end{aligned} \tag{1.7}$$

where we have also noted $\left[s_{1\beta}(\lambda)\right]^2 = \hbar^2/4$. The magnitude of (1.7) must satisfy

$$\Big|f(\alpha) - f(\beta)\Big| \,\leq\, \int_\Lambda \Big|s_{1z}(\lambda)\, s_{1\beta}(\lambda)\left[1 - \frac{4}{\hbar^2}\, s_{1\beta}(\lambda)\, s_{1\alpha}(\lambda)\right] p(\lambda)\Big| d\lambda \,. \tag{1.8}$$

Since $s_{1\beta}(\lambda)s_{1\alpha}(\lambda) = \pm\hbar^2/4$; we must have $\left[1 - 4\, s_{1\beta}(\lambda)s_{1\alpha}(\lambda)/\hbar^2\right] \geq 0$. The probability distribution is also positive definite, in which case the integrand of (1.8) has to be

$$\Big|s_{1z}(\lambda)\, s_{1\beta}(\lambda)\left[1 - \frac{4}{\hbar^2}\, s_{1\beta}(\lambda)\, s_{1\alpha}(\lambda)\right] p(\lambda)\Big| = \left[\frac{\hbar^2}{4} - s_{1\beta}(\lambda)\, s_{1\alpha}(\lambda)\right] p(\lambda) \,. \tag{1.9}$$

Thus (1.8) becomes

$$\Big|f(\alpha)-f(\beta)\Big| \leq \frac{\hbar^2}{4} + \int_\Lambda s_{1\beta}(\lambda)\, s_{2\alpha}(\lambda)\, p(\lambda)\, d\lambda\ . \tag{1.10}$$

Given that we have restricted Bob's and Alice's measurements ($s_{2\alpha}$ and $s_{2\beta}$) to be coplanar, the expectation value defined by (1.5) will only be a function of the relative angle between Alice's and Bob's measuring device with respect to the z-axis. That is we may write

$$\int_\Lambda s_{1\beta}(\lambda)\, s_{2\alpha}(\lambda)\, p(\lambda)\, d\lambda = f(\alpha-\beta)\ , \tag{1.11}$$

and (1.10) is written more compactly as

$$\Big|f(\alpha)-f(\beta)\Big| - f(\alpha-\beta) \leq \frac{\hbar^2}{4}\ . \tag{1.12}$$

This is **Bell's inequality**. A statement which every local realistic theory must respect.

The question of whether a local hidden-variable theory can be devised to reproduce the predictions of quantum mechanics may now be laid down quantitatively. Can we establish a contradiction of Bell's inequality by quantum mechanics ? Let us calculate the corresponding average values in (1.12) within the formalism of quantum theory. When Alice observes $s_{1z}=-\hbar/2$ or $s_{1z}=\hbar/2$, Bob must find particle 2 to be described by the respective spinors

$$|\uparrow_{2z}\rangle \doteq \begin{bmatrix}1\\0\end{bmatrix}\ , \quad |\downarrow_{2z}\rangle \doteq \begin{bmatrix}0\\1\end{bmatrix}\ , \tag{1.13}$$

where $X \doteq Y$ means Y is a representation of X. The operator $\hat{s}_{2\alpha}$ can be written as a linear combination of $\hat{s}_{2z}$ and $\hat{s}_{2x}$,

$$\begin{aligned}\hat{s}_{2\alpha} &= \hat{s}_{2z}\cos\alpha + \hat{s}_{2x}\sin\alpha\\ &\doteq \frac{\hbar}{2}\begin{bmatrix}\cos\alpha & \sin\alpha\\ \sin\alpha & -\cos\alpha\end{bmatrix}\end{aligned} \tag{1.14}$$

where we have represented spin operators using Pauli matrices. The eigenspinors of $\hat{s}_{2\alpha}$ corresponding to eigenvalues $s_{2\alpha}=\hbar/2$ and $s_{2\alpha}=-\hbar/2$ are respectively given by

$$|\uparrow_{2\alpha}\rangle \doteq \begin{bmatrix}\cos(\alpha/2)\\ \sin(\alpha/2)\end{bmatrix}\ , \quad |\downarrow_{2\alpha}\rangle \doteq \begin{bmatrix}-\sin(\alpha/2)\\ \cos(\alpha/2)\end{bmatrix}\ . \tag{1.15}$$

Hence the eigenstates for the second particle's z component may be expanded as

$$|\uparrow_{2z}\rangle = \cos\left(\frac{\alpha}{2}\right)|\uparrow_{2\alpha}\rangle - \sin\left(\frac{\alpha}{2}\right)|\downarrow_{2\alpha}\rangle\ , \tag{1.16a}$$

$$|\downarrow_{2z}\rangle = \sin\left(\frac{\alpha}{2}\right)|\uparrow_{2\alpha}\rangle + \cos\left(\frac{\alpha}{2}\right)|\downarrow_{2\alpha}\rangle\ . \tag{1.16b}$$

It is now possible to find the conditional probabilities that form the expectation value for $\hat{s}_{1z}\hat{s}_{2\alpha}$ from (1.16), which is

$$f_{\text{QM}}(\alpha) = -\frac{\hbar^2}{4}\Big(\big|\langle\uparrow_{2\alpha}|\uparrow_{2z}\rangle\big|^2 - \big|\langle\downarrow_{2\alpha}|\uparrow_{2z}\rangle\big|^2 - \big|\langle\uparrow_{2\alpha}|\downarrow_{2z}\rangle\big|^2 + \big|\langle\downarrow_{2\alpha}|\downarrow_{2z}\rangle\big|^2\Big)$$

$$= -\frac{\hbar^2}{2}\left[\cos^2\left(\frac{\alpha}{2}\right) - \sin^2\left(\frac{\alpha}{2}\right)\right]$$
$$= -\frac{\hbar^2}{2}\cos\alpha\,. \tag{1.17}$$

It now remains to show that $f_{\rm QM}(\alpha)$ violates the inequality of (1.12). We choose the case of $\alpha = 2\beta$, for which the quantum mechanical prediction is only consistent with that given by a local hidden-variable theory if,

$$\Big|f_{\rm QM}(2\beta) - f_{\rm QM}(\beta)\Big| - f_{\rm QM}(\beta) \le \frac{\hbar^2}{4} \quad\Longrightarrow\quad \Big|\cos(\beta) - \cos(2\beta)\Big| + \cos(\beta) \le \frac{1}{2}\,. \tag{1.18}$$

Equation (1.18) is shown by the blue curve in Fig. 1.2, which clearly demonstrates the incompatibility of quantum theory with Bell's inequality. Out of the genius of Bell, we are

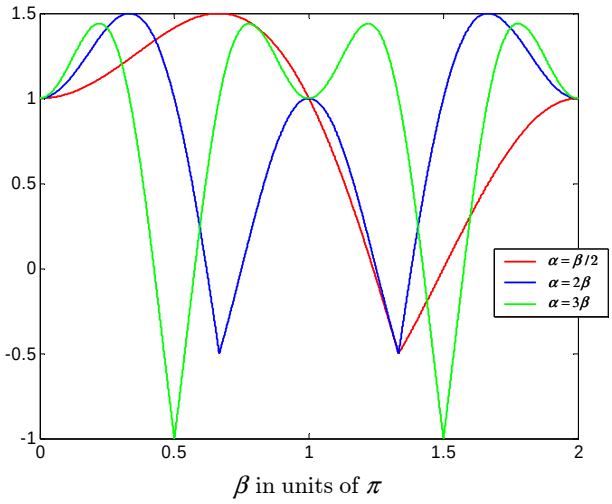

Fig. 1.2: Bell's inequality as calculated from quantum mechanics for the spectrum of spin components specified by β. A violation of (1.12) is clearly shown for some intervals of β.

led to conclusively vindicate quantum mechanics of its postulated inadequacies. The theory may be reinstated more formally:

No theory, while retaining both locality and reality, may replicate the predictions of quantum mechanics for experiments involving such entangled states.

1.3 In the Spirit of Bell

Unfortunately Bell's mathematical demonstration based on Bohm's thought experiment against local realistic theories was inapplicable to realizable experiments. Since any invalidation (or verification) of a theory must ultimately rest upon experiments, equation (1.12) was generalized. This later result is of great practicality and is the form by which Bell's inequality appears in the literature. It is referred to as the **CHSH inequality** (or **generalized Bell's inequality**), named after those who proposed it [13].

Following the spirit of Bell, another distinguished variant, the **GHZ equality** was developed by the trio D. Greenberger, M. Horne, and A. Zeilinger (GHZ), who considered

three-particle correlation experiments [14], [15]. Sadly we do not have enough space to dwell on the intricacies of their work. We note however, the principal point of their result.

In following their analysis, it is worth noting that the GHZ equality has no statistical character. It eradicated the elements of reality with extreme decisiveness, by simply having a quantum mechanical answer in utter contradiction to that obtained from a hidden-variable consideration. The GHZ equality can be shown to refute local realistic theories based on a single outcome; it simply requires no statistical averaging as opposed to (1.18). This is a direct consequence of the fact that no probability distribution, and therefore no statistical measure was introduced in their derivation. Such GHZ correlations have now been verified, and innumerable experiments have tested local realistic theories via Bell's theorem, all of which affirmed quantum theory [16]–[21].

Chapter 2

Teleportation Defined

Now that the reader should have come to terms with entanglement, can we capitalize on such characteristics of quantum mechanics? This question lies at the heart of **quantum information science**, proliferating in exploitations of quantum entanglement. In fact quantum information theorists today have gone beyond Schrödinger's qualitative theorem mentioned under (1.1c), and can extract and quantify entanglement as a physical resource using a measure called *e-bits* (entanglement-bits), defined as one maximally entangled state [22], [23]. Without attempting an explanation we list some commonly discussed tasks [24] (the nomenclature is nevertheless somewhat self-explanatory), some understood more than others, by which robust communication may be promised via entanglement:

- Quantum cryptography
- Quantum teleportation
- Super-dense coding
- Quantum error correction

All such ideas have risen from the will to transcend classical information processing capabilities. The intention here is to concentrate on one implementation — **quantum teleportation** — first announced in 1993.

2.1 Quantum Teleportation of Discrete Variables

Conceived by C. Bennett et al., who showed that quantum correlations in a two dimensional Hilbert space shared between a sender and receiver could be harnessed for the reconstruction of a quantum state at remote and *unknown* locations from the sender [25]. This has the advantage that the physical attributes of a quantum particle may be sent over arbitrarily large distances; unlike classical signal propagation, teleportation does not suffer from effects of attenuation or noise.[1]

It will be instructive to first review the proposal of Bennett et al. for teleporting a qubit, since the qubit is the main resource of interest for quantum information processing today. Furthermore, the continuous-variable teleportation protocol, although differing in architecture as we shall find, involves the same concepts to those designed for qubits.

[1]This assumes the particles used in teleportation reach their destinations intact.

2.1.1 The Posed Problem

Alice the sender has at hand some normalized state,

$$|\psi_1\rangle = a\,|\alpha_1\rangle + b\,|\beta_1\rangle \tag{2.1}$$

where the subscript 1 denotes that her state is carried by particle 1. The Greek letters α and β can label physical properties of the particle such as a spin component, or the polarization of a photon; we shall keep this choice open.[2] Alice would like $|\psi_1\rangle$ to reappear at Bob's location without directly sending particle 1 through a set of intervening space-time points between her and Bob. Alice must not extract information about $|\psi_1\rangle$ by a direct measurement, for that would collapse the state into one of its eigenstates while losing all else. Neither can Alice obtain the complete set of eigenkets for $|\psi_1\rangle$ by reproducing another (or several) particle(s) with the same state $|\psi_1\rangle$ for her to measure; such acts are forbidden as a consequence of quantum mechanics known as the **No-Cloning Theorem** [26].[3]

2.1.2 Principles of Teleportation

The delivery of $|\psi_1\rangle$ to Bob can be accomplished if Alice and Bob share an entangled pair of particles, call them particle 2 and 3, where particle 2 is distributed to Alice and particle 3 to Bob. We shall use a pair in the form of an EPR singlet state (1.2),

$$|\psi_{23^-}\rangle = \frac{1}{\sqrt{2}}\Big(\,|\alpha_2,\beta_3\rangle - |\beta_2,\alpha_3\rangle\,\Big)\,. \tag{2.2}$$

By a "joint measurement", Alice can couple $|\psi_1\rangle$ to her share of the entangled state, i.e. particle 1 to particle 2. Alice's joint measurement is such that the result of her measurement is one of four possible maximally entangled states,

$$|\psi_{12^\pm}\rangle \;=\; \frac{1}{\sqrt{2}}\Big(\,|\alpha_1,\beta_2\rangle \pm |\beta_1,\alpha_2\rangle\,\Big)\,, \tag{2.3a}$$

$$|\phi_{12^\pm}\rangle \;=\; \frac{1}{\sqrt{2}}\Big(\,|\alpha_1,\alpha_2\rangle \pm |\beta_1,\beta_2\rangle\,\Big)\,. \tag{2.3b}$$

Equations (2.3) are a complete orthonormal basis for the two-particle system. They are often referred to as the Bell operator basis, since they were shown to maximally violate Bell's inequality [27]. For this reason a measurement which projects an arbitrary two-particle state onto one of (2.3) is commonly said to be a **Bell-State-Measurement** (BSM). Thus, the total three-particle state before Alice's BSM is given by

$$\begin{aligned}
|\psi_{123}\rangle \;&=\; |\psi_1\rangle \otimes |\psi_{23^-}\rangle \\
&=\; \frac{a}{\sqrt{2}}\Big(\,|\alpha_1,\alpha_2\rangle \otimes |\beta_3\rangle - |\alpha_1,\beta_2\rangle \otimes |\alpha_3\rangle\,\Big) \\
&\quad + \frac{b}{\sqrt{2}}\Big(\,|\beta_1,\alpha_2\rangle \otimes |\beta_3\rangle - |\beta_1,\beta_2\rangle \otimes |\alpha_3\rangle\,\Big)\,.
\end{aligned} \tag{2.4}$$

[2] The symbols α and β label the same physical property and $\{|\alpha_1\rangle, |\beta_1\rangle\}$ is a complete orthonormal set of basis states.

[3] It should be noted that the No-Cloning theorem does not say that no machine may be built to duplicate multiple copies of *any* state. By restricting the cloning device (or process) to be representable by a unitary operator, the theorem states that only orthogonal states may be reproduced while retaining the original copy. It thus prevents the more beneficial case of cloning an arbitrary state.

In order to bring out the essence of Alice's BSM, one should write (2.4) in terms of the Bell operator basis for which the complete three-particle state becomes

$$|\psi_{123}\rangle = \frac{1}{2}\Big[\,|\psi_{12^+}\rangle \otimes \Big(-a\,|\alpha_3\rangle + b\,|\beta_3\rangle\Big) + |\psi_{12^-}\rangle \otimes \Big(-a\,|\alpha_3\rangle - b\,|\beta_3\rangle\Big) + |\phi_{12^+}\rangle \otimes \Big(a\,|\beta_3\rangle - b\,|\alpha_3\rangle\Big) + |\phi_{12^-}\rangle \otimes \Big(a\,|\beta_3\rangle + b\,|\alpha_3\rangle\Big)\Big]\,. \tag{2.5}$$

Quite visibly, Alice's measurement will project Bob's share of the EPR state into one of four possible superpositions shown in (2.5). Each possible state for particle 3 is related to $|\psi_1\rangle$ by a unitary transformation. With a probability of 1/4, Bob will be required to apply one of four unitary transformations represented by $\hat{U}_j$ ($j = 1, 2, 3, \text{or } 4$) depending on the result of the BSM:

(1) Alice measures $|\psi_{12^-}\rangle$. Since the state of particle 3 is only different to that of particle 1 by an overall phase factor that is void of any physical significance, Bob need not perform any alterations. The unitary operator is then the identity $\hat{I}$, understood here to be represented by the 2×2 identity matrix,

$$\hat{U}_1 = \hat{I}\,. \tag{2.6a}$$

(2) Alice measures $|\psi_{12^+}\rangle$. Bob is required to reverse the relative phase occurring in particle 3. This is accomplished by the phase change operator,

$$\hat{U}_2 = e^{i\pi}\,|\alpha_3\rangle\,\langle\alpha_3| + |\beta_3\rangle\,\langle\beta_3|\,. \tag{2.6b}$$

(3) Alice measures $|\phi_{12^-}\rangle$. Bob must perform a state exchange which is effected by,

$$\hat{U}_3 = |\alpha_3\rangle\,\langle\beta_3| + |\beta_3\rangle\,\langle\alpha_3|\,. \tag{2.6c}$$

(4) Alice measures $|\phi_{12^+}\rangle$. Both a phase change and a state exchange are required. Thus one may compose (2.6b) and (2.6c) to obtain

$$\hat{U}_4 = \hat{U}_3\,\hat{U}_2 = e^{i\pi}\,|\beta_3\rangle\,\langle\alpha_3| + |\alpha_3\rangle\,\langle\beta_3|\,. \tag{2.6d}$$

One may also consider performing a state exchange first followed by a phase change since the two operators anti-commute, differing only by an overall phase.

$$\Big[\hat{U}_3\hat{U}_2, \hat{U}_2\hat{U}_3\Big]_+ = 0\,. \tag{2.6e}$$

It is easily checked that $\hat{U}_j^\dagger\hat{U}_j = \hat{U}_j\hat{U}_j^\dagger = \hat{I}$ for all j. Equations (2.6) completes the teleportation protocol.

2.1.3 Discrete Variables Critiqued

Two remarks affirm this protocol not repugnant to any accepted laws of physics. First and foremost, the protocol respects the No-Cloning theorem. Alice's BSM entails particle 1 losing its quantum state. Secondly, Bob must acknowledge Alice's BSM result which requires

at least two bits of classical information.[4] This information is able to be stored, copied, or transmitted by conventional means. That is, Alice may inform Bob about her BSM via a telephone call. This obviously invalidates any attempts to use this protocol as a means of faster-than-light communication.

Limitations

Two inefficacies set a perimeter for qubit teleportation:

(1) The first is fundamental. Only when one uses a maximally entangled state will particle 3 be related to particle 1 via four unitary transformations. This can be seen by using equations (1.1) instead of (2.2) with the appropriate change of subscripts and by setting $c^{(1)} = c^{(2)} = 1/\sqrt{2}$ to arrive at a similar result to (2.5). Any state which is less entangled will reduce the fidelity of teleportation or the range of states that can be teleported. It is clear then, that any such quantum information processing scheme employing EPR correlations shall suffer from this deficiency.

(2) The second applies to schemes using a total of three particles. It is the experimental inability to project the input onto all four Bell-states given by (2.3).[5] The first teleportation experiment used the polarizations of a photon to encode the qubit, and was only capable of identifying the singlet state $|\psi_{12^-}\rangle$ [34]. This was achieved by superimposing the incident photon (particle 1) with particle 2 on a 50/50 beam-splitter. We note below how the identification of $|\psi_{12^-}\rangle$ was possible:

It begins by realizing that of the four polarization states in (2.3), $|\psi_{12^-}\rangle$ is the only antisymmetric one under exchange of particles. If one recalls that the tensor product between the spatial and the polarization states must be overall symmetric for bosons, then the two-particle *spatial state* for $|\psi_{12^-}\rangle$ had to be antisymmetric. This is the situation where one photon is at each output port of a beam-splitter. Similarly we may infer the three remaining two-particle spatial states corresponding to $|\phi_{12^\pm}\rangle$, and $|\psi_{12^+}\rangle$ to be symmetric. This is the case whereby two photons emerge from the same output port. Thus $|\psi_{12^-}\rangle$ could be discriminated experimentally from coincidence counting (simultaneous detections) at the beam-splitter outputs.

A successful Bell-state analyser for teleporting qubits using three particles, where the state to be teleported is carried by a particle external to the teleportation scheme has yet to be devised.

2.2 Teleportation of Continuous Quantum Variables

We now turn to the more general case of teleporting observables with a continuous eigenvalue spectrum such as the position and momentum of a massive particle. The theoretical

[4] Bennett et al. have shown by a "four-way coding scheme" [28] that successful (perfect) teleportation using a classical channel capacity of any lesser than two bits would permit Bob to use the teleported particle to send superluminal messages.

[5] A two-particle scheme proposed by S. Popescu managed to avoid this difficulty [29], [30]. In this scheme however, one of the EPR particles also served to carry the input state. Consequently, only pure states can be teleported; restricting one from considering for example, the (more interesting) case when the input is a member of an entangled pair (one way of realizing "entanglement swapping" [31]–[33]).

possibility was proposed almost a year after Bennett's discrete-variable version by L. Vaidman [35]. Vaidman's vision was then elaborated on by S. Braunstein and H. Kimble first for a single-mode light field [36], and later for a broadband field [37]. It is the latter work of Braunstein and Kimble's that we shall come to appreciate later. For now it will suffice to outline Vaidman's idea.

2.2.1 The Protocol

Instead of the polarization, the motion of a subatomic body will be transferred to another at a distant location.[6] In parallel manner to teleportation of qubits, one is led to consider position and momentum entanglement between particles 2 and 3. One possibility is

$$x_2 + x_3 = 0 \ , \quad p_2 - p_3 = 0 \ , \tag{2.7}$$

where x_j and p_j $(j = 1, 2, 3)$ are eigenvalues for the position and momentum of particle j. Note that like (2.2), (2.7) is a maximally entangle state, since one may infer *with certainty* (x_3, p_3) given precise knowledge of (x_2, p_2), or vice versa.[7] Like (2.2), (2.7) does not define the motional state of any individual particle, but rather the joint property of two, which now lies in an infinite-dimensional Hilbert space.

A third party, Victor the verifier, is hired to prepare particle 1, i.e. he is the sender and receiver. Victor is posed with the same predicament as Alice with discrete variables. It is impossible to measure particle 1 directly since its motional state is specified by two real numbers corresponding to non-commuting operators, thus providing insufficient information for its reconstitution at Bob's end.[8] However he may evade Heisenberg by considering operators in the form of (2.7), because

$$[\hat{x}_i + \hat{x}_j, \hat{p}_i - \hat{p}_j] = 0 \quad \forall \ i, j \tag{2.8}$$

which renders $(x_i + x_j)$ and $(p_i - p_j)$ as properties simultaneously measurable with infinite precision. The analogous BSM for position and momentum are then

$$x_1 + x_2 = \bar{x} \ , \quad p_1 - p_2 = \bar{p}. \tag{2.9}$$

Alice's measurement results are now given by a continuous range of values $(\bar{x}, \bar{p})$. The moment Alice projects particles 1 and 2 onto the joint state of (2.9), particle 3 abruptly jumps to the phase-space coordinate

$$x_3 = x_1 - \bar{x} \ , \quad p_3 = p_1 - \bar{p} \ . \tag{2.10}$$

Hence the EPR particle owned by Bob is now related to particle 1 via an infinite number of possibilities instead of only four. The unitary transformation is now a function of the continuous variables $\bar{x}$ and $\bar{p}$,

$$|x_{\text{T}}, p_{\text{T}}\rangle = \hat{U}(\bar{x}, \bar{p}) \, |x_3, p_3\rangle \ . \tag{2.11}$$

The remaining task is trivial; Alice must transmit her measured results $\bar{x}$ and $\bar{p}$ to Bob, who now displaces his particle in position and momentum by exactly this amount to reproduce the motion of particle 1. This protocol is summarized in Fig. 2.1.

[6] The word "polarization" is used here in the usual relativistic quantum field sense, meaning either the orientation of the electric field vector for a photon or the intrinsic angular momentum of some particle.

[7] The word "state" is used loosely here to refer to the variables (x_j, p_j).

[8] The analogous situation in discrete variables is defined by all cyclic permutations of $[\hat{s}_{jx}, \hat{s}_{jy}] = i\hbar\hat{s}_{jz}$

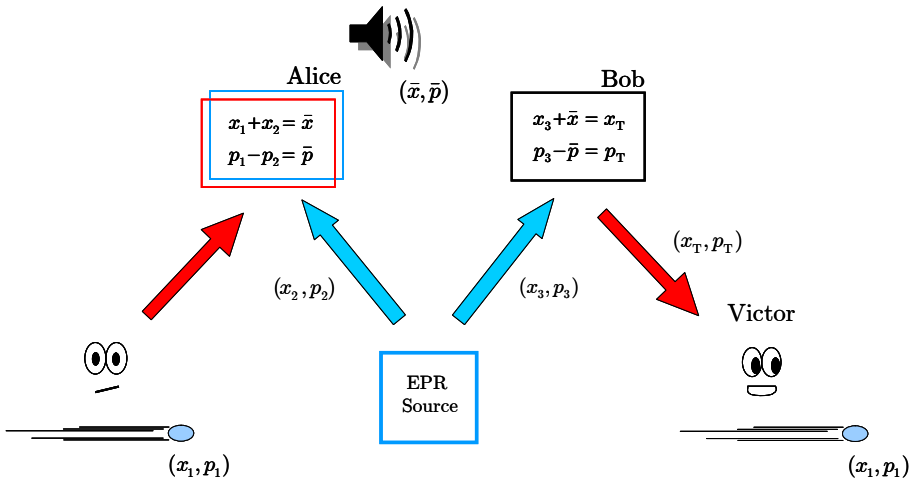

Fig. 2.1: Continuous-variable teleportation scheme. Victor does both the sending and receiving of the quantum state.

2.2.2 Continuous Variables: A Problem or Resolution?

We now recognize that Vaidman's idea runs parallel to that for discrete variables. Quite clearly, teleportation of continuous quantum variables necessitates the transition from two four-state operations (Alice's BSM and Bob's unitary transformation) to two expanded over an infinite number of basis states. One is then naturally led to question whether considering physical attributes lying in an infinite-dimensional Hilbert space resolves the problems threatening the discrete-variable implementation. If we are already unable to identify four states, how do we manage an infinite number of them!? Let us first note what is asked of by (2.3). One must have a device which is capable of not only identifying that one (not which) particle is in one polarization state while the other is in either the orthogonal or the same state, but also providing knowledge of which relative sign in (2.3) was actually detected. No such contrivance exists, and the initial teleportation experiment resorted to examining implications of (2.3) as discussed already.

On a different front, there already exists technology capable of measuring directly, not for massive particles but for photons, the continuous quantities $x_1 + x_2$ and $p_1 - p_2$ with one-to-one correspondence. That is, without resorting to any subsidiary conditions, the results of measuring $\bar{x}$ and $\bar{p}$ are not degenerate. This is the technique of homodyne detection. The existing capability in performing a BSM sets continuous-variable apart from discrete-variable teleportation.

It is clear that in both discrete- and continuous-variable protocols, two conduits can be identified to assist the conveyance of an arbitrary input state to Victor. One classical, given by Alice's communication to Bob, and one quantum, given by the sending of one EPR particle to Bob. Finally, by the same token as the discrete-variable protocol, continuous-variable teleportation eludes all possible contraventions of physical laws.

Chapter 3

Teleportation within Classical Phase-Space

In this chapter we make a transition from introductory principles to the more rigorous expositions of Chap. 4–6 by adopting an explicit model of the teleporter in Sect. 3.1, later followed by a time-domain discussion. The main focus of this report is enunciated in Sect. 3.2 where we relate the teleportation protocol discussed thus far to the theory of **Stochastic Electrodynamics**. It is also at this stage that we convolve the philosophical concepts addressed in Chap. 1 to the implications of stochastic electrodynamics as applied to teleportation.

3.1 Teleportation with Quantum Optics

It is well-known that a mode of the electromagnetic field is formally equivalent to a harmonic oscillator whose frequency of oscillation is equal to the frequency of the field mode. This after all is not so surprising since the classical theory of radiation begins with the dipole oscillator model. A noticeable feature in this connection is the formal equivalence of the position and momentum for a mechanical system to the quadrature phase amplitudes of the optical field. The understanding of photonic states at the quantum optical level allows us to access the principles of teleportation in an experimental setting. Our theory is thus based on a quantum optical implementation of Vaidman's idea originally conceived by Kimble and Braunstein [36]. This scheme teleports the quadrature phase amplitudes of the optical field and is shown in Fig. 3.1. It has now become the "standard" scheme for implementing continuous-variable teleportation, by which a number of experiments have been performed [38]–[40].

A Quantum Optics Toolbox

We outline what quantum optics has to offer at each stage of the protocol, compartmentalized into three main elements:

(1) **EPR correlations:**

The continuous-variable entanglement is embodied in a **two-mode squeezed state**, generated by superimposing squeezed beams of light prepared by a **degenerate para-**

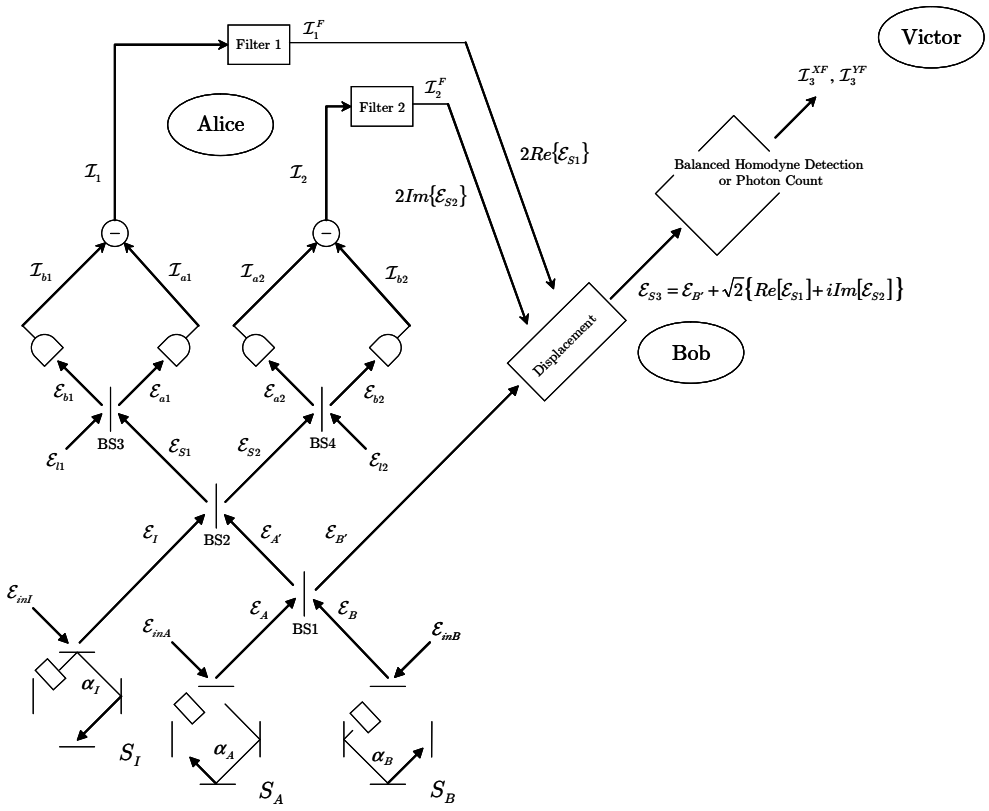

Fig. 3.1: The standard protocol for a continuous-variable teleporter. The squeezing cavities are labelled by S_A and S_B, while squeezing by the input cavity S_I is by choice. Bob must displace his share of the EPR correlation, $\mathcal{E}_{B'}$, based on the set of numbers $(\mathcal{I}_1^F, \mathcal{I}_2^F)$ from Alice to produce $\mathcal{E}_{S3}$. Victor may observe either the squeezing spectrum (via balanced homodyne detection), or intensity correlation function (by a photon counting experiment) of $\mathcal{E}_{S3}$.

metric oscillator (abbreviated DPO, whose terminology we shall come to understand in Chap. 4) via a 50/50 beam-splitter. There is no need to be punctilious here with these DPOs, an understanding of squeezed fluctuations in time will serve amply in observing teleportation. However, a frequency decomposition of its output field in terms of the input will require aid from the more sophisticated **Input-Output Theory**.

(2) **Joint measurement by Alice:**

This is accomplished by employing **balanced homodyne detection**. In this scheme an incoming state with annihilation operator $\hat{\mathcal{E}}_S$ is mixed through a lossless 50/50 beam-splitter with a strong monochromatic local oscillator of coherent amplitude $\mathcal{E}_l = |\mathcal{E}_l|\, e^{i\phi_l}$, set precisely to the frequency of $\hat{\mathcal{E}}_S$. On taking the expectation value with respect to a coherent state, the condition for a strong local oscillator is

$$|\mathcal{E}_l|^2 \gg |\mathcal{E}_S|^2 \ , \tag{3.1}$$

where on the left-hand-side one usually treats the local oscillator classically. Photo-detection then takes place at each beam-splitter output after which one photo-current is subtracted from the other. This has the advantage over ordinary homodyne detection

with its lower noise level on the final output photo-current for the same local oscillator power and beam-splitter transmissivity. This can be seen from calculating the variance of the final photo-currents in both cases [41], [42]. We further include two filters each with a Lorentzian frequency response as a means of modelling Alice's detection bandwidths. These filters produce the currents $\mathcal{I}_1^F$ and $\mathcal{I}_2^F$.

(3) **Field displacement:**

Bob's displacement of $\mathcal{E}_{B'}(t)$ will be straightforward, this involves adding another field of coherent amplitude indicated by Alice's measurement results onto $\mathcal{E}_{B'}(t)$.

3.2 Teleportation within Stochastic Electrodynamics

3.2.1 Introduction to Stochastic Electrodynamics

We intend to treat the standard protocol of Fig. 3.1 not within the formalisms of quantum optics but with **Stochastic Electrodynamics** (SED). It may be incisively said to be a hybrid theory of Maxwellian electrodynamics and that of stochastic processes. Stochastic electrodynamics was given birth to renounce **Quantum Electrodynamics** (QED); thus, it had to be a theory capable of coping with the phenomenon of *vacuum fluctuations* given by the non-zero variance of the quantized electric field $\hat{\mathbf{E}}$ in the vacuum state,

$$\langle \mathbf{0} | \, \hat{\mathbf{E}}^2 \, | \mathbf{0} \rangle - \langle \mathbf{0} | \, \hat{\mathbf{E}} \, | \mathbf{0} \rangle^2 \neq 0 \, , \tag{3.2}$$

where $|\mathbf{n}\rangle \equiv |n_1, n_2, \ldots n_k\rangle$ is the multimode Fock state with n_i being the number of photons with frequency ω_i. These ideas were decent attempts to resurrect the wave nature of light by adding a stochastic component to the classical electric field, after which only its statistical moments are deterministic [43], [44]. SED has had its successes, the most renowned and well documented being its explanation to the Casimir effect [45]–[47]. There is no need to expatiate about the background and application of SED, but the following principal elements of the theory should be noted:

(1) By representing the fields as complex random variables satisfying a set of prescribed statistics, the zero-point field is viewed as a tangible physical entity. It is this tailor-made vacuum fluctuation that distinguishes SED from other classical theories and is the sense in which SED is semi-classical.

(2) Statistical moments in SED are equivalent to quantum operator averages calculated in the Wigner representation, i.e. averages in symmetric ordering [48], [49]. Ordering of course plays no part in SED calculations.

These points will be made clearer in Chap. 5 when we consider squeezing as a classical phenomenon [50].

Research Purpose

Besides pedagogical reasons, our aim is to reproduce the broadband results predicted from **Quantum Trajectory Theory**, reported in Ref. [51] and [52]. In applying SED to describe the standard protocol, there are a number of interesting points ought to be made regarding the classicality of teleportation. These are noted in the following sections.

3.2.2 A Local Hidden-Variable Theory

Phase-space distributions play a large part in quantum optics. Particularly appealing is the interpretation of the phase-space distribution as a probability density in the classical sense when it is positive-definite, in much the same way Schrödinger's wave-function $\psi(x,t)$ is used to interpret $|\psi(x,t)|^2$ as the probability density for a particle to be found at position x at time t. The first person to associate quantum non-locality with the failure of positivity for the Wigner function was Bell [53]. Bell noted that the positive Wigner function provided one with an immediate hidden-variable model for the state. It was later demonstrated by Banaszek and Wódkiewicz that the Wigner distribution of an EPR state produced from non-degenerate parametric amplification, despite being positive everywhere, provided direct evidence of quantum non-locality [54]. Although one can not weld the positivity of the Wigner function for a two-mode squeezed state to its locality, it is possible to remove that non-local character by providing a local realistic theory when the phase-space distribution becomes positive-definite. SED is precisely a local hidden-variable description where one may now consider a rendition of (1.5) in the form,

$$F(\phi_1;\phi_2) = \int_{-\infty}^{+\infty}\int_{-\infty}^{+\infty} \mu_1(\phi_1,\alpha_1)\,\mu_2(\phi_2,\alpha_2)\,W(\alpha_1,\alpha_2)\,d^2\alpha_1\,d^2\alpha_2\ , \tag{3.3}$$

where $\alpha_k = \mathrm{X}_k + i\mathrm{Y}_k$ $(k=1,2)$ are the squeezed coherent amplitudes emerging from the beam-splitter reaching homodyne detector k with local oscillator phase ϕ_k. The measurement results are given by μ_k and $W(\alpha_1,\alpha_2)$ is the Wigner distribution for the hidden variables $(\mathrm{X}_k,\mathrm{Y}_k)$, in equation (1) of Ref. [36]. The Wigner distribution must satisfy

$$\int_{-\infty}^{+\infty}\int_{-\infty}^{+\infty} W(\alpha_1,\alpha_2)\,d^2\alpha_1\,d^2\alpha_2 = 1\ , \tag{3.4}$$

and is shown to be of the form

$$W(\alpha_1,\alpha_2) \propto \delta(\mathrm{X}_1+\mathrm{X}_2)\,\delta(\mathrm{Y}_1-\mathrm{Y}_2) \tag{3.5}$$

in the limit of infinite squeezing power, producing an ideal EPR state.

Since the Wigner function calculates operator averages in symmetrized order, a description of balanced homodyne detection falls within the capabilities of SED [50].[1] Thus, if one restricts to sending only Gaussian states (states having Gaussian Wigner distributions in the phase-space variables) as we shall do, SED provides a local realistic theory of teleportation using the standard protocol.

3.3 Fluctuations in the Classical Phase-Space

In the context of SED, the effect of optical devices on the light as it propagates through the teleporter is to add statistical uncertainty, i.e. noise, to the optical field. These erratic fluctuations of the field are modelled as stochastic processes for which its random evolution may be generated by an appropriate stochastic differential equation [55]. Time-domain simulations of this sort have been carried out by H. Carmichael and H. Nha [56]. A linear mapping

[1] This can be seen by representing the local oscillator as an operator in (3.12).

in the time domain between the teleporter output and input pellucidly demonstrates teleportation. We derive this mapping within SED in a frame rotating at the central frequency $\omega_{\rm C}$ of the input and EPR-correlated fields. This is then the solution to the stochastic differential equation for the teleporter. Since we are working exclusively in the time domain, no explicit time dependence will be shown.

Beam-Splitter Transformations

Provided with the squeezed outputs $\mathcal{E}_A$ and $\mathcal{E}_B$, we now consider the effects of the beam-splitters and carry our field up to Alice for balanced homodyne detection. Consider the situation of Fig. 3.2 where $\mathcal{E}_1$ and $\mathcal{E}_2$ are incident on a beam-splitter with reflection and transmission coefficients r_1, t_1 and r_2, t_2 respectively. There exist variations to which $\mathcal{E}_3$ and

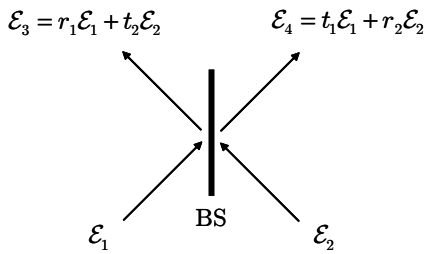

Fig. 3.2: The beam-splitter transformation

$\mathcal{E}_4$ may be expressed in terms of $\mathcal{E}_1$ and $\mathcal{E}_2$ depending on the particular phase transformation on crossing the beam-splitter. However the phase is chosen, conservation of energy bounds the possible alternatives; it demands for a lossless beam-splitter,

$$\begin{aligned} |\mathcal{E}_1|^2 + |\mathcal{E}_2|^2 &= |\mathcal{E}_3|^2 + |\mathcal{E}_4|^2 \\ &= \left(|r_1|^2 + |t_1|^2\right)|\mathcal{E}_1|^2 + \left(|r_2|^2 + |t_2|^2\right)|\mathcal{E}_2|^2 \\ &\quad + \left(r_1^* t_2 + t_1^* r_2\right)\mathcal{E}_1^*\mathcal{E}_2 + \left(r_1 t_2^* + t_1 r_2^*\right)\mathcal{E}_1\mathcal{E}_2^* \ . \end{aligned} \tag{3.6}$$

This imposes conditions for transmission and reflection:

$$|r_1|^2 + |t_1|^2 = |r_2|^2 + |t_2|^2 = 1 \ , \tag{3.7a}$$

$$r_1^* t_2 + t_1^* r_2 = r_1 t_2^* + t_1 r_2^* = 0 \ . \tag{3.7b}$$

By limiting ourselves to 50/50 beam-splitters, and choosing the transmission coefficients to be equal and real, we have

$$t_1 = t_2 = \frac{1}{\sqrt{2}} \ , \qquad |r_1| = |r_2| = \frac{1}{\sqrt{2}} \ . \tag{3.8}$$

Writing $r_1 = e^{i\theta_1}/\sqrt{2}$ and $r_2 = e^{i\theta_2}/\sqrt{2}$, let us choose $\theta_1 = 0$; then (3.7b) implies we must choose $\theta_2 = \pi$. Hence the output fields are given by

$$\mathcal{E}_3 = \frac{1}{\sqrt{2}}\left(\mathcal{E}_1 + \mathcal{E}_2\right) \ , \qquad \mathcal{E}_4 = \frac{1}{\sqrt{2}}\left(\mathcal{E}_1 - \mathcal{E}_2\right) \ . \tag{3.9a}$$

Excursion 3.1 The transition to quantum mechanics can be made in two ways: Either by transforming the field states incident on the beam-splitter[2], or by treating (3.9) as operator equations that preserve the commutation relations

$$\left[\hat{\mathcal{E}}_1, \hat{\mathcal{E}}_1^\dagger\right] = \left[\hat{\mathcal{E}}_2, \hat{\mathcal{E}}_2^\dagger\right] = 1 \,, \quad \left[\hat{\mathcal{E}}_3, \hat{\mathcal{E}}_3^\dagger\right] = \left[\hat{\mathcal{E}}_4, \hat{\mathcal{E}}_4^\dagger\right] = 1 \,, \tag{3.10a}$$

and

$$\left[\hat{\mathcal{E}}_1, \hat{\mathcal{E}}_2\right] = \left[\hat{\mathcal{E}}_1, \hat{\mathcal{E}}_2^\dagger\right] = 0 \,, \quad \left[\hat{\mathcal{E}}_3, \hat{\mathcal{E}}_4\right] = \left[\hat{\mathcal{E}}_3, \hat{\mathcal{E}}_4^\dagger\right] = 0 \,. \tag{3.10b}$$

Equation (3.10a) assumes ideal monochromatic fields and (3.10b) expresses the independence of fields at the beam-splitter input and output ports.

Repetitive use of equations (3.9) at BS1 and BS2 would give us the fields entering the homodyne detectors at the location of Alice,

$$\mathcal{E}_{S1} \,=\, \frac{1}{\sqrt{2}}\,\mathcal{E}_I + \frac{1}{2}\left(\mathcal{E}_A + \mathcal{E}_B\right) \,, \tag{3.11a}$$

$$\mathcal{E}_{S2} \,=\, \frac{1}{\sqrt{2}}\,\mathcal{E}_I - \frac{1}{2}\left(\mathcal{E}_A + \mathcal{E}_B\right) \,. \tag{3.11b}$$

Balanced Homodyne Detection Without Filtering

From the currents $\mathcal{I}_{aj} \equiv |\mathcal{E}_{aj}|^2$ and $\mathcal{I}_{bj} \equiv |\mathcal{E}_{bj}|^2$ with $j = 1, 2$, we form the homodyned outputs (Fig. 3.1)

$$\mathcal{I}_1 \,\equiv\, \mathcal{I}_{b1} - \mathcal{I}_{a1} \,=\, \left|\bar{\mathcal{E}}_{l1}\right| \left(\mathcal{E}_{S1}\, e^{-i\phi_{l1}} + \mathcal{E}_{S1}^*\, e^{i\phi_{l1}}\right) \,, \tag{3.12a}$$

$$\mathcal{I}_2 \,\equiv\, \mathcal{I}_{a2} - \mathcal{I}_{b2} \,=\, \left|\bar{\mathcal{E}}_{l2}\right| \left(\mathcal{E}_{S2}\, e^{-i\phi_{l2}} + \mathcal{E}_{S2}^*\, e^{i\phi_{l2}}\right) \tag{3.12b}$$

where in the rotating frame, the local oscillator is written as $\mathcal{E}_{lj} = \left|\bar{\mathcal{E}}_{lj}\right| e^{i\phi_{lj}}$.

For now we leave the spectral content of $\mathcal{I}_j$ unaltered by setting filters 1 and 2 to have infinite bandwidths. The information sent to Bob is thus given by

$$\mathcal{I}_1^F \,=\, G_1 \left|\bar{\mathcal{E}}_{l1}\right| \left[\frac{2}{\sqrt{2}}\,\mathcal{E}_I^{(\phi_{l1})} + \mathcal{E}_A^{(\phi_{l1})} + \mathcal{E}_B^{(\phi_{l1})}\right] \,, \tag{3.13}$$

$$\mathcal{I}_2^F \,=\, G_2 \left|\bar{\mathcal{E}}_{l2}\right| \left[\frac{2}{\sqrt{2}}\,\mathcal{E}_I^{(\phi_{l2})} - \mathcal{E}_A^{(\phi_{l2})} - \mathcal{E}_B^{(\phi_{l2})}\right] \tag{3.14}$$

where we have introduced the definition of the quadrature amplitudes

$$\mathcal{E}^{(\theta)} \equiv \frac{1}{2}\left(\mathcal{E} e^{-i\theta} + \mathcal{E}^* e^{i\theta}\right) \,, \tag{3.15}$$

and a constant filter gain G_j.

It shall now be convenient to write the real and imaginary parts of the fields in terms of their quadrature amplitudes. The real and imaginary parts of some field $\mathcal{E} = \mathcal{E}_X + i\mathcal{E}_Y$ can readily shown to be

$$\mathcal{E}_X \,=\, \mathcal{E}^{(\theta)} \cos\theta - \mathcal{E}^{(\theta+\pi/2)} \sin\theta \,, \tag{3.16a}$$

$$\mathcal{E}_Y \,=\, \mathcal{E}^{(\theta)} \sin\theta + \mathcal{E}^{(\theta+\pi/2)} \cos\theta \,, \tag{3.16b}$$

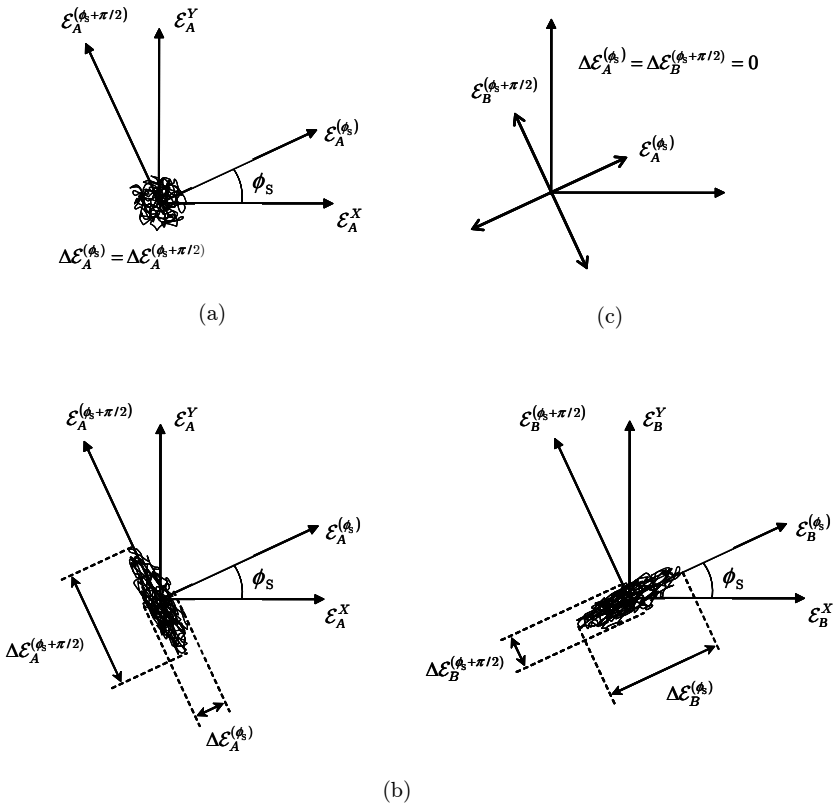

Fig. 3.3: Fluctuations as jittery motion accumulated over time in phase-space. A coherent state must stay within the Heisenberg uncertainty bound. (a) A vacuum coherent state at the output of cavity S_A. (b) Moderately squeezed output fields of S_A and S_B. (c) As squeezing increases indefinitely, the squeezed quadratures exhibit no jittery motion along that direction in phase-space. The random variable must then have its realization along a perpendicular quadrature.

where $\mathcal{E}^{(\theta)}$ is the component of $\mathcal{E}$ at an angle θ in the anticlockwise direction to the real axis. Hence

$$\mathcal{E} = \mathcal{E}_X + i\mathcal{E}_Y = \left[\mathcal{E}^{(\theta)} + i\mathcal{E}^{(\theta+\pi/2)}\right] e^{i\theta} \ . \tag{3.17}$$

Letting S_A and S_B produce squeezing in the $\phi_{\rm s}$ and $\phi_{\rm s} + \pi/2$ quadratures respectively (Fig. 3.3), Bob should consider the following displacement

$$\begin{aligned}\mathcal{E}_{S3} &= \mathcal{E}_{B'} + \frac{1}{\sqrt{2}}\left(\mathcal{I}_1^F + i\mathcal{I}_2^F\right) e^{i\phi_{\rm s}} \\ &= \frac{1}{\sqrt{2}}\left[\mathcal{E}_A^{(\phi_{\rm s})} - \mathcal{E}_B^{(\phi_{\rm s})}\right] e^{i\phi_{\rm s}} + G_1\left|\bar{\mathcal{E}}_{l1}\right|\left\{\mathcal{E}_I^{(\phi_{l1})} + \frac{1}{\sqrt{2}}\left[\mathcal{E}_A^{(\phi_{l1})} + \mathcal{E}_B^{(\phi_{l1})}\right]\right\} e^{i\phi_{\rm s}} \\ &\quad + i\left[\mathcal{E}_A^{(\phi_{\rm s}+\pi/2)} - \mathcal{E}_B^{(\phi_{\rm s}+\pi/2)}\right] e^{i\phi_{\rm s}} + iG_2\left|\bar{\mathcal{E}}_{l2}\right|\left\{\mathcal{E}_I^{(\phi_{l2})} - \frac{1}{\sqrt{2}}\left[\mathcal{E}_A^{(\phi_{l2})} + \mathcal{E}_B^{(\phi_{l2})}\right]\right\} e^{i\phi_{\rm s}} \ .\end{aligned} \tag{3.18}$$

[2]Coherent states in fact transform to coherent states after traversing the beam-splitter [57]

It is now that we can come to appreciate homodyning as a phase-sensitive measurement by which Alice would ideally set the local oscillator to have phases $\phi_{l1} = \phi_{\rm s}$ and $\phi_{l2} = \phi_{\rm s} + \pi/2$. She would also like to be able to produce the gains $G_1 = \left|\bar{\mathcal{E}}_{l1}\right|^{-1}$ and $G_2 = \left|\bar{\mathcal{E}}_{l2}\right|^{-1}$, since under these conditions (3.18) simplifies to

$$\mathcal{E}_{S3} = \frac{2}{\sqrt{2}} \left[\mathcal{E}_A^{(\phi_{\rm s})} - i\mathcal{E}_B^{(\phi_{\rm s}+\pi/2)}\right] e^{i\phi_{\rm s}} + \left[\mathcal{E}_I^{(\phi_{\rm s})} + i\mathcal{E}_I^{(\phi_{\rm s}+\pi/2)}\right] e^{i\phi_{\rm s}} \,. \tag{3.19}$$

Writing the output fields of S_A and S_B in the form of a time average plus fluctuations,

$$\mathcal{E}_A^{(\phi_{\rm s})} = \left\langle \mathcal{E}_A^{(\phi_{\rm s})} \right\rangle + \Delta\mathcal{E}_A^{(\phi_{\rm s})} \,, \quad \mathcal{E}_B^{(\phi_{\rm s}+\pi/2)} = \left\langle \mathcal{E}_B^{(\phi_{\rm s}+\pi/2)} \right\rangle + \Delta\mathcal{E}_B^{(\phi_{\rm s}+\pi/2)} \tag{3.20}$$

evidently shows one should consider squeezed vacuum states, for which

$$\left\langle \mathcal{E}_A^{(\phi_{\rm s})} \right\rangle = \left\langle \mathcal{E}_B^{(\phi_{\rm s}+\pi/2)} \right\rangle = 0 \,. \tag{3.21}$$

In the limit of perfectly correlated EPR fields,

$$\Delta\mathcal{E}_A^{(\phi_{\rm s})} \longrightarrow 0 \,, \quad \Delta\mathcal{E}_B^{(\phi_{\rm s}+\pi/2)} \longrightarrow 0 \tag{3.22}$$

completely eliminating the first square-bracket term in (3.19), giving the final output to be passed to Victor as

$$\mathcal{E}_{S3} = \left[\mathcal{E}_I^{(\phi_{\rm s})} + i\mathcal{E}_I^{(\phi_{\rm s}+\pi/2)}\right] e^{i\phi_{\rm s}} \,. \tag{3.23}$$

By using a homodyne detector Victor should discover that teleportation is impeccable where the phase-space trail set by the input is flawlessly adhered to by the output. Equation (3.19) is said to be derived under conditions of unit-gain and no filtering.

EPR Correlations with Classical Fields

From the beam-splitter transformations of (3.9), it can now be seen that (2.7) is realized as

$$\left[\mathcal{E}_{A'}^{(\phi_{\rm s})} + \mathcal{E}_{B'}^{(\phi_{\rm s})}\right] = \sqrt{2}\,\Delta\mathcal{E}_A^{(\phi_{\rm s})} \,, \quad \left[\mathcal{E}_{A'}^{(\phi_{\rm s}+\pi/2)} - \mathcal{E}_{B'}^{(\phi_{\rm s}+\pi/2)}\right] = \sqrt{2}\,\Delta\mathcal{E}_B^{(\phi_{\rm s}+\pi/2)} \tag{3.24}$$

taken the limit of (3.22). The fluctuations given by $\Delta\mathcal{E}_B^{(\pi/2)}$ for example, may be generated from the Stratonovich stochastic differential equations

$$d\mathcal{E}_B \;=\; \sqrt{2\kappa}\,\alpha_B + d\mathcal{E}_{inB} \,, \tag{3.25a}$$

$$d\alpha_B \;=\; -\kappa\,(\alpha_B - \lambda\,\alpha_B^*)\,dt - \sqrt{2\kappa}\,d\mathcal{E}_{inB} \tag{3.25b}$$

where α_B and $\mathcal{E}_{inB}$ are the intra-cavity and input fields of S_B. The output and intra-cavity fields have complex increments $d\mathcal{E}_B$ and $d\alpha_B$ over a time step of dt. The input has complex Wiener increment $d\mathcal{E}_{inB}$ which satisfies

$$\left\langle d\mathcal{E}_{inB}\,d\mathcal{E}_{inB}\right\rangle = \left\langle d\mathcal{E}_{inB}^*\,d\mathcal{E}_{inB}^*\right\rangle \;=\; 0 \,, \tag{3.26a}$$

$$\left\langle d\mathcal{E}_{inB}^*\,d\mathcal{E}_{inB}\right\rangle \;=\; \frac{1}{2}\,dt \,. \tag{3.26b}$$

We shall be content with the form (3.25) for the moment, they are discussed in Chap. 5.1; what should be noted is the finite zero-point energy given by the right-hand-side of (3.26b).

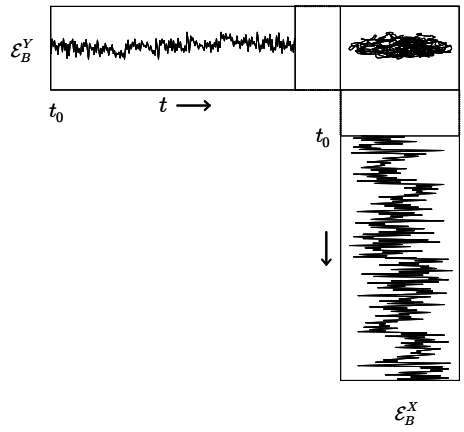

Fig. 3.4: Squeezing of the imaginary part generated from (3.25). The arrow indicates the direction of time flow.

Equations (3.25) and (3.26) model squeezing as erratic fluctuations in phase-space, as shown by Fig. 3.4.

Quantum mechanics differs to a classical formulation in that the identification of a "state" diverges into two classes of mathematical artefacts, namely operators and kets. Classical mechanics makes no such distinction; the dynamical variable itself is the "state". The rudimentary analysis leading up to (3.23) may then be thought of as classical, or in the Heisenberg picture of quantum mechanics, where operators evolve.

Chapter 4

The Linear Mapping in Fourier Space

Chapters 4 and 5 will examine teleportation in frequency space. We wish to describe the broadband nature of the teleportation protocol. Our first task is to derive a linear mapping in which we seek to relate each frequency component of the teleported field to that of the DPO inputs. The mapping follows by exactly the same approach as that in Sect. 3.3 except all fields are now frequency decomposed. We begin with the construction of the DPO output field and its specifications. This will pave a convenient route towards future calculations. Sect. 4.2 will account for Alice's joint measurement with finite detection bandwidths, after which we arrive at Bob's location. The last section then deals with the final procedure of field displacement and Victor's receipt of the teleported field.

4.1 The Degenerate Parametric Oscillator

4.1.1 The Model

We first discuss the basic working model of a cavity generating squeezed states and the approximations involved in the mathematical description that follow. The system is depicted in Fig. 4.1. Except for the output coupling mirror, which is slightly transmitting, all other mirrors are approximated to have unit reflectivity. The fraction of intensity that leaks out per second is proportional to κ. For teleportation we will work with squeezed vacuum, thus the responsible physical process is degenerate parametric down conversion driven by a monochromatic pump $\mathcal{E}_p(t)$ of frequency $2\omega_{\rm C}$, with $\omega_{\rm C}$ on the order of optical frequencies ($\omega_{\rm C} \sim 10^{14}$). The signal field $\mathcal{E}_s(t)$ has zero mean, containing only the indestructible vacuum energy. The intra-cavity field labelled as $\varphi(t)$, thus carries a pump mode at $2\omega_{\rm C}$, and the down-converted *quasi*-mode (sometimes referred to as the subharmonic) at $\omega_{\rm C}$, which is the mode of interest.

Excursion 4.1 Parametric down-conversion differs from the more general case of squeezing an intense coherent state, in which case a signal photon *stimulates* a two-photon emission, with one photon (normally called the idler) having its frequency given by the difference between that of the pump and the signal. In our application the down-converted light is weaker

as it results from *spontaneous* two-photon emission.

It shall be assumed that the bandwidth of the particular cavity *quasi*-mode centred on $\omega_{\rm C}$ is sufficiently narrow: Let Δ be in general the spectral separation between a cavity mode frequency of interest and those of the adjacent quasi-modes. Taking the full width at half maximum (FWHM) to be a measure of its bandwidth BW, it is then favourable to have,

$$\frac{BW}{\Delta} \ll 1 \, . \tag{4.1}$$

For our particular setting shown in Fig. 4.2 (b) $\Delta \sim 10^{14}$ Hz and typical values for the FWHM are on the order of MHz. The relatively minuscule bandwidth of the down-converted light is made possible by experimental techniques of phase-matching such that the majority of photons produced from the non-linear interaction have frequency $\omega_{\rm C}$. When (4.1) is valid, we speak of the subharmonic as the cavity mode for the spectral region of interest ($\omega \approx \omega_{\rm C}$), and the cavity is said to be single mode. From now on, it should be remembered that it is $\omega_{\rm C}$ and its immediate vicinity that we will be working in; thus we label the subharmonic/cavity mode distinctively as $\alpha(t)$. This is the first of two principal approximations involved in the following treatment. The other issue one could be wary of is the spectral response of

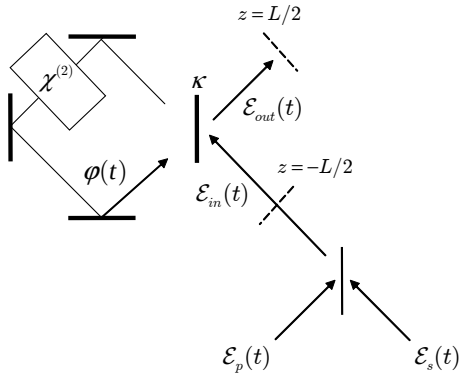

Fig. 4.1: A sample squeezing cavity showing the boundary condition imposed on the fields. The spatial dependence of all fields has been omitted for clarity. This construction and other possible variations based on similar non-linear optical mechanisms is referred to as an Optical Parametric Oscillator. When the non-linear interaction described by $\chi^{(2)}$ produces two photons of the same frequency, the cavity is called a Degenerate Parametric Oscillator.

the output coupling mirror. Letting the cavity round trip length be $L_{\rm C}$, and the non-linear crystal have refractive index $n_\chi(\omega)$ and length l in the direction of propagation of $\varphi(t)$, the cavity round trip time is

$$\begin{aligned} t_{\rm C} &= \text{time spent in vacuum} + \text{time spent in traversing the crystal} \\ &= \frac{L_{\rm C} - l}{c} + \frac{n_\chi l}{c} \\ &= \frac{L_{\rm C} + l\,[n_\chi - 1]}{c} \, . \end{aligned} \tag{4.2}$$

We *define* the rate at which energy leaks out of the cavity to be

$$\frac{T(\omega)}{t_{\rm C}} = \frac{c\,T(\omega)}{L_{\rm C} + l\,[n_\chi(\omega) - 1]} \, , \tag{4.3}$$

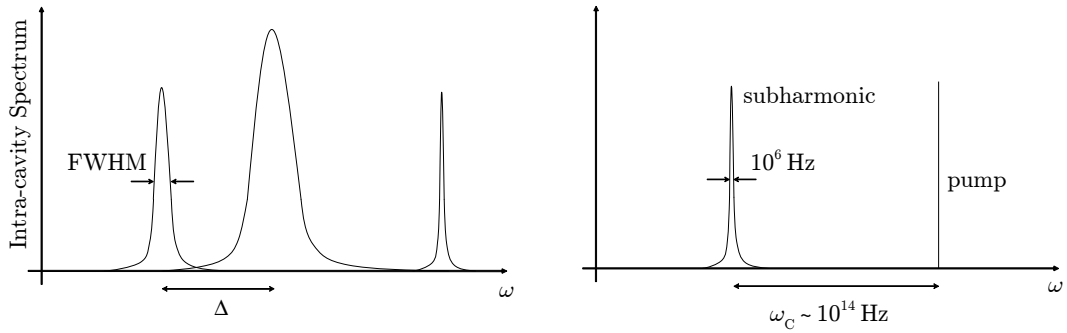

Fig. 4.2: (a) Arbitrary mode structure. The FWHM should be sufficiently smaller than Δ so a profile of interest (e.g. the quasi-mode with resonance frequency $\omega_{\rm C}$ in our case) does not overlap with adjacent ones. (b) Situation for the DPO. The validity of (4.1) hinges on the size of $\Delta \sim \omega_{\rm C}$ and the spread in frequencies of the down-converted light. The pump laser is to a good approximation single mode.

where $T(\omega)$ is the output mirror transmissivity. The spectrum of $\alpha(t)$ will be approximated as delta function with respect to $T(\omega)$. Put more quantitatively, the quasi-mode nature of the subharmonic is such that

$$\left|\frac{dT}{d\omega}\right| \ll \left|\frac{d\left|\mathcal{A}\right|^2}{d\omega}\right| \quad \forall\, \omega :\ \omega_{\rm C} - \frac{BW}{2} < \omega < \omega_{\rm C} + \frac{BW}{2} \tag{4.4}$$

where $\mathcal{A}(\omega)$ is the mode amplitude of $\alpha(t)$.[1] Equation (4.4) says that over the range of frequencies for which $\mathcal{A}(\omega)$ varies; $T(\omega)$ is a slowly varying function. Let Ω denote the interval of frequencies for which the mirror transmission would vary significantly, then $\left|\mathcal{A}(\omega)\right|^2$ must satisfy

$$\frac{BW}{\Omega} \ll 1\ , \tag{4.5}$$

in which case, we may to an extremely good approximation take

$$T(\omega) \approx T(\omega_{\rm C}) \equiv T\ , \tag{4.6}$$

and *define*, with the factor of two being a matter of preference, the cavity damping rate to be

$$2\kappa \equiv \frac{T}{t_{\rm C}}\ . \tag{4.7}$$

Excursion 4.2 In the foregoing discussion it was implicitly assumed that the intensity spectrum for $\alpha(t)$ is symmetric, which is itself an approximation. Once again, this is contingent upon the spectral behaviour of some other variable associated with the power spectral density. To identify this contingency variable we return now to the fundamental physical process by which squeezing is obtained — parametric down conversion. Generally it is not

[1] Note that (4.4) assumes the discrete modes of $\alpha(t)$ are adequately dense so that the its derivative exists. In other words, (4.4) is in the continuous limit.

always the case that a pump photon will trade us two photons each precisely of frequency $\omega_{\rm C}$. From conservation of energy, for every subharmonic photon at $\omega_{\rm C}+d\omega$; there must be a photon *simultaneously* produced at $\omega_{\rm C}-d\omega$. This would give us a photon number spectrum, which we denote by $\bar{n}(\omega)$, that is symmetric about $\omega_{\rm C}$. To translate $\bar{n}(\omega)$ into an intensity spectrum we simply need to multiply $\bar{n}(\omega)$ by the energy per photon $E(\omega)=\hbar\omega$, which is a monotonically increasing function of ω. This immediately suggests that a spectrum in terms of energy for the cavity mode has to be asymmetric. The situation is that of Fig. 4.3. The

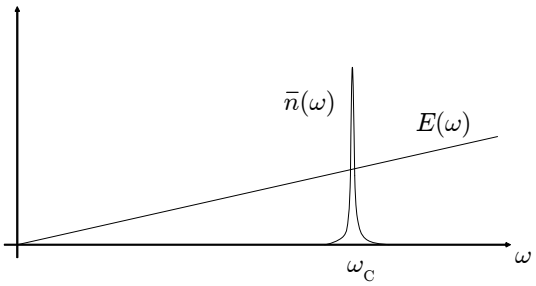

Fig. 4.3: In general terms, the monotonically increasing photon energy would give rise to an asymmetric intensity distribution in frequency.

precise question may now be addressed. It is whether or not over the bandwidth of $\bar{n}(\omega)$, one can set the energy per photon to be a constant. Since $E(\omega)$ is a linear function, we can phrase the question more definitively to ask if,

$$\left| E\left(\omega_{\rm C}-\frac{BW}{2}\right)-E\left(\omega_{\rm C}+\frac{BW}{2}\right)\right| / \hbar\omega_{\rm C} \ll 1 \; . \tag{4.8}$$

Today's experiments can in fact produce photon number bandwidths consistent with (4.8) to give unerringly symmetric power spectral densities.

One may have noticed by now the recurring argument of the subharmonic field to be single mode in the few respects discussed above. Such a single-mode approximation is made commonly in quantum optics. For example, the quantum treatment of decomposing an external laser field into its so called source- and free-fields makes an approximation exactly the same as (4.6) in order to deal with an integral over source-field frequencies [58].

4.1.2 Field Specification

Returning now to the output field sought for, the model of Fig. 4.1 also assumes an undepleted pump and a lossless non-linear medium. Reminding ourselves that it is in the proximity of $\omega_{\rm C}$ that we are working, the vacuum fluctuation is assumed to be *white*. It is also assumed to be *ergodic*.

Periodic boundary conditions are imposed on the input and output fields over a length of L (i.e., $\mathcal{E}(z=-L/2,t)=\mathcal{E}(z=L/2,t)$ where $\mathcal{E}$ stands for $\mathcal{E}_{in}$ or $\mathcal{E}_{out}$). The full real, input *stochastic* field has the mode expansion

$$\mathcal{E}_{in}^{(F)}(z,t)=\sqrt{\frac{c}{L}}\sum_{n=-\infty}^{+\infty} f(\omega_n)\, e^{-i\omega_n(t-z/c)} \; , \tag{4.9}$$

where n is the set of all integers with the special case $n = \text{C}$ for the resonance frequency. The mode labelled by $n = 0$ is dc ($\omega_0 = 0$). It is conventional to split the full field as,

$$\mathcal{E}_{in}^{(F)}(z,t) = \mathcal{E}_{in}(z,t) + \mathcal{E}_{in}^{*}(z,t) \,, \tag{4.10a}$$

$$\mathcal{E}_{in}(z,t) \equiv \sqrt{\frac{c}{L}} \sum_{n=0}^{+\infty} f(\omega_n)\, e^{-i\omega_n(t-z/c)} \,, \tag{4.10b}$$

$$\mathcal{E}_{in}^{*}(z,t) \equiv \sqrt{\frac{c}{L}} \sum_{n=1}^{+\infty} f(-\omega_n)\, e^{i\omega_n(t-z/c)} \,. \tag{4.10c}$$

$\mathcal{E}_{in}(z,t)$ and $[\mathcal{E}_{in}(z,t)]^*$ are referred to as the positive and negative frequency parts and $f(-\omega_n) = f^*(\omega_n)$. The mode amplitudes are discrete Gaussian complex random variables of zero mean, and covariances given by

$$\langle f(\omega_n) \rangle = 0 \,, \tag{4.11a}$$

$$\langle f(\omega_n) f(\omega_m) \rangle = \langle f^*(\omega_n) f^*(\omega_m) \rangle = 0 \,, \tag{4.11b}$$

$$\langle f^*(\omega_n) f(\omega_m) \rangle = \frac{1}{2}\,\delta_{nm} \,. \tag{4.11c}$$

Recall that ergodicity means the left hand sides of (4.11) may be thought of either as the time average of a single realization of $f(\omega_n)$ or as an ensemble average over all possible paths. It is these input statistics, in particular (4.11c), which defines the input as vacuum. Note how the factor of $\sqrt{c/L}$ is reminiscent of the quantization volume which normally appears in the field operator of a second quantized theory. In our one-dimensional model, L will be referred to as the quantization length and c/L scales the field intensity to photon flux units. Taking the coupling mirror to have negligible transmission for $\mathcal{E}_{in}(z,t)$, and using (4.6), the positive frequency part of the cavity output may be constructed as

$$E_{out}(z,t) = e^{i\phi_{\text{R}}} \mathcal{E}_{in}(z,t) + \sqrt{2\kappa}\, e^{i\phi_{\text{T}}} \alpha(z,t) \tag{4.12}$$

where $e^{i\phi_{\text{R}}}$ and $e^{i\phi_{\text{T}}}$ are phase changes from mirror reflection and transmission coefficients and $\alpha(z,t)$ belongs to $\alpha^{(F)}(z,t)$, decomposed in a similar fashion to (4.10):

$$\alpha^{(F)}(z,t) = \alpha(z,t) + \alpha^{*}(z,t) \,, \tag{4.13a}$$

$$\alpha(z,t) = \sum_{n=0}^{+\infty} \mathcal{A}(\omega_n)\, e^{-i\omega_n(t-z/c)} \,, \tag{4.13b}$$

$$\alpha^{*}(z,t) = \sum_{n=1}^{+\infty} \mathcal{A}(-\omega_n)\, e^{i\omega_n(t-z/c)} \,. \tag{4.13c}$$

For calculative convenience, we define

$$\mathcal{E}_{out}(z,t) \equiv e^{-i\phi_{\text{T}}} E_{out}(z,t) \tag{4.14a}$$

and

$$\Lambda(\omega_n) \equiv e^{i(\phi_{\text{R}} - \phi_{\text{T}})} \sqrt{\frac{c}{L}}\, f(\omega_n) + \sqrt{2\kappa}\, \mathcal{A}(\omega_n) \,, \tag{4.14b}$$

so the output may be written with ease as:

$$\mathcal{E}^{(F)}_{out}(z,t) \;=\; \mathcal{E}_{out}(z,t) + \mathcal{E}^{*}_{out}(z,t)\;, \tag{4.15a}$$

$$\mathcal{E}_{out}(z,t) \;=\; \sum_{n=0}^{+\infty} \Lambda(\omega_n)\, e^{-i\omega_n(t-z/c)}\;, \tag{4.15b}$$

$$\mathcal{E}^{*}_{out}(z,t) \;=\; \sum_{n=1}^{+\infty} \Lambda(-\omega_n)\, e^{i\omega_n(t-z/c)}\;. \tag{4.15c}$$

From (3.7), it can now be seen that $\phi_{\rm R} - \phi_{\rm T} = \pm\pi/2$.

It is preferable to work in the continuous limit by inserting the density of modes $g(\omega)$ such that $g(\omega)d\omega$ is the number of modes lying between frequency ω to $\omega + d\omega$. By considering a quantization length of L, it can be shown that for travelling wave modes,

$$g(\omega) = \frac{1}{\Delta\omega} = \frac{L}{2\pi c}\;, \tag{4.16}$$

where $\Delta\omega \equiv \omega_{n+1} - \omega_n$ and $\omega_n = 2n\pi c/L$. This is of course the well established result for the free spectral range of a Fabry-Perot interferometer, except L here only serves to be a theoretical construct. The full real fields given by (4.10) and (4.15) are then cast into integrals,

$$\mathcal{E}^{(F)}_{in}(t) \;=\; \sqrt{\frac{c}{L}} \int_{-\infty}^{+\infty} g(\omega) f(\omega)\, e^{-i\omega t}\, d\omega\;, \tag{4.17a}$$

$$\mathcal{E}^{(F)}_{out}(t) \;=\; \int_{-\infty}^{+\infty} g(\omega)\Lambda(\omega)\, e^{-i\omega t}\, d\omega\;. \tag{4.17b}$$

To help make the linear mapping transparent, the fields will now be displaced to be centred on the origin ($\omega = 0$) and we evaluate all fields at $z = 0$.[2] Dropping the spatial dependence, (4.15) become

$$\mathcal{E}^{(F)}_{out}(t) \;=\; \mathcal{E}_{out}(t) + \mathcal{E}^{*}_{out}(t)\;, \tag{4.18a}$$

$$\mathcal{E}_{out}(t) \;=\; \frac{L}{2\pi c} \int_{-\omega_{\rm C}}^{+\infty} \Lambda(\omega_{\rm C} + \omega)\, e^{-i(\omega_{\rm C}+\omega)t}\, d\omega\;, \tag{4.18b}$$

$$\mathcal{E}^{*}_{out}(t) \;=\; \frac{L}{2\pi c} \int_{-\infty}^{\omega_{\rm C}} \Lambda^{*}(\omega_{\rm C} - \omega)\, e^{i(\omega_{\rm C}-\omega)t}\, d\omega\;. \tag{4.18c}$$

Since $\omega_{\rm C}$ is incommensurably larger than the bandwidth, we may extend the integrals in (4.18b) and (4.18c) to $-\infty$ and $+\infty$ respectively. This would then allow us to define the

[2]Note that the spectrum corresponding to the negative frequency part, $|\Lambda(-\omega)|^2$ is centred on $-\omega_{\rm C}$ while that of the positive part is at $\omega_{\rm C}$, in which case $\mathcal{E}_{out}(t)$ and $[\mathcal{E}_{out}(t)]^*$ must be transformed independently. This centring of the spectra will also make the mechanics of input-output theory in Chap. 5 clear.

Fourier transform of $\mathcal{E}_{out}(t)$.[3]

$$\Lambda(\omega_{\rm C}+\omega) \equiv \mathcal{F}\Big\{\mathcal{E}_{out}(t)\Big\} = \frac{c}{L}\int_{-\infty}^{+\infty}\mathcal{E}_{out}(t)\,e^{i(\omega_{\rm C}+\omega)t}dt\ . \tag{4.19}$$

To facilitate future calculations and for ease of reference, we introduce an extra index ξ such that

$$\xi \in \{I, A, B\}\ , \tag{4.20}$$

to distinguish the fields entering and leaving cavities S_I, S_A, and S_B of Fig. 3.1.[4] The linear mapping is most suitably derived in a frame rotating at frequency $\omega_{\rm C}$ by defining the positive frequency output field of cavity S_ξ as

$$\tilde{\mathcal{E}}_\xi(t) \equiv \mathcal{E}_\xi(t)\,e^{i\omega_{\rm C}t} \equiv \frac{L}{2\pi c}\int_{-\infty}^{+\infty}\tilde{\Lambda}_\xi(\omega)\,e^{-i\omega t}\,d\omega \tag{4.21}$$

where all modes now carry the index ξ with a similar definition as (4.14b),

$$\tilde{\Lambda}_\xi(\omega) \equiv \sqrt{\frac{c}{L}}\,\tilde{f}_\xi(\omega) + \sqrt{2\kappa_\xi}\,\tilde{\mathcal{A}}_\xi(\omega)\ , \quad \tilde{f}_\xi(\omega) \equiv i\bar{f}_\xi(\omega)\ . \tag{4.22}$$

The modes $\bar{f}(\omega)$ and $\tilde{\mathcal{A}}(\omega)$ satisfy the following Fourier transform pairs. The positive frequency part of the cavity mode is given by

$$\begin{aligned}\tilde{\mathcal{A}}_\xi(\omega) &\equiv \mathcal{A}_\xi(\omega_{\rm C}+\omega)\\ &\equiv \mathcal{F}\Big\{\tilde{\alpha}_\xi(t)\Big\} = \frac{c}{L}\int_{-\infty}^{+\infty}\tilde{\alpha}_\xi(t)\,e^{i\omega t}\,dt\ ,\end{aligned} \tag{4.23a}$$

$$\tilde{\alpha}_\xi(t) \equiv \mathcal{F}^{-1}\Big\{\tilde{\mathcal{A}}_\xi(\omega)\Big\} = \frac{L}{2\pi c}\int_{-\infty}^{+\infty}\tilde{\mathcal{A}}_\xi(\omega)\,e^{-i\omega t}\,d\omega\ , \tag{4.23b}$$

and the vacuum input,

$$\begin{aligned}\bar{f}_\xi(\omega) &\equiv f_\xi(\omega_{\rm C}+\omega)\\ &\equiv \mathcal{F}\left\{\tilde{\mathcal{E}}_{in\xi}(t)\right\} = \sqrt{\frac{c}{L}}\int_{-\infty}^{+\infty}\tilde{\mathcal{E}}_{in\xi}(t)\,e^{i\omega t}\,dt\ ,\end{aligned} \tag{4.24a}$$

$$\tilde{\mathcal{E}}_{in\xi}(t) \equiv \mathcal{F}^{-1}\Big\{\bar{f}_\xi(\omega)\Big\} = \frac{1}{2\pi}\sqrt{\frac{L}{c}}\int_{-\infty}^{+\infty}\bar{f}_\xi(\omega)\,e^{-i\omega t}\,d\omega\ . \tag{4.24b}$$

From now on all field amplitudes with a tilde will be in the rotating frame. To complete the specification, we present the DPO input statistics given by (4.11) in the continuous limit.

[3] We require $\omega_{\rm C}$ to be sufficiently large so that boundary terms are vanishingly small, permitting the relation $(1/2\pi)\int_{-\omega_{\rm C}}^{+\infty}\exp[i\omega(t-t')]d\omega \approx \delta(t-t')$. This is necessary for the Fourier transform pair to be defined.

[4] This convention will be beneficial when we come to calculate the squeezing spectra in Chap. 5.

Field Statistics in the Continuum

One must be more attentive in translating the input statistics given by (4.11) correctly into the continuum. Simply regarding ω as a continuous variable and converting the Kronecker delta of (4.11c) into a Dirac delta function will not do. To make the translation clear, let us restore the mean photon number per mode $\bar{n}(\omega)$ for the moment. Taking (4.10) as it stands but treating ω as a continuous variable by inserting $g(\omega)$ and letting $\delta_{nm} \longrightarrow \delta(\omega - \omega')$ in (4.11) gives

$$\left\langle \mathcal{E}^*_{in}(t)\mathcal{E}_{in}(t) \right\rangle = \frac{c}{L} \int_{-\infty}^{+\infty} \left[\bar{n}(\omega) + \frac{1}{2} \right] g^2(\omega)\, d\omega \,. \tag{4.25}$$

What we would like in the integrand is $\bar{n}(\omega)\, g(\omega)$ so that

$$\begin{aligned} \bar{n}(\omega)\, g(\omega)\, d\omega \;&=\; \begin{pmatrix} \text{number of photons} \\ \text{per mode} \end{pmatrix} \begin{pmatrix} \text{number of modes in the frequency} \\ \text{interval } \omega \text{ to } \omega + d\omega \end{pmatrix} \\ &=\; \begin{pmatrix} \text{number of photons with frequency} \\ \text{lying in the interval } \omega \text{ to } \omega + d\omega \end{pmatrix} , \end{aligned} \tag{4.26}$$

which would allow us to interpret $\langle \mathcal{E}^*_{in}(t)\mathcal{E}_{in}(t) \rangle$ as the average number of photons in $\mathcal{E}_{in}(t)$ crossing a length of L per second. The extra factor of $g(\omega)$ makes this impossible. This is due to incorrect scaling of the amplitudes. The relationship between modes and frequency is not one-to-one, in fact we know that $g(\omega)$ is the number of modes with the same frequency ω. In other words, $g(\omega)$ is a degeneracy factor, as it is sometimes called in statistical mechanics. The discrete sum adds all the amplitudes mode by mode whereas the integral does the same by first grouping the modes with the same frequency. The total number of modes accounted for must of course be conserved in both cases. Having said this, if $\langle f^*(\omega_n) f(\omega_m) \rangle$ in (4.11) is to go inside a double sum, then it should have units corresponding to the square of amplitude per mode, which it does. If on the other hand, we wish to account for all the mode amplitudes by counting frequencies, then we must account for the total amplitude corresponding to a particular frequency, that is $g(\omega)f(\omega)$. The same is true for the photon number per mode on the right hand side of (4.11c). Hence the translation from a sum to an integral should be complemented by,

$$\left\langle g(\omega) \bar{f}_\xi(\omega) \right\rangle = 0 \,, \tag{4.27a}$$

$$\left\langle g(\omega) \bar{f}_\xi(\omega)\, g(\omega') \bar{f}_{\xi'}(\omega') \right\rangle = 0 \,, \tag{4.27b}$$

$$\left\langle g(\omega) \left[\bar{f}_\xi(\omega) \right]^* g(\omega') \left[\bar{f}_{\xi'}(\omega') \right]^* \right\rangle = 0 \,, \tag{4.27c}$$

$$\left\langle g(\omega) \left[\bar{f}_\xi(\omega) \right]^* g(\omega') \bar{f}_{\xi'}(\omega') \right\rangle = \left[\bar{n}(\omega) + \frac{1}{2} \right] g(\omega)\, \delta(\omega - \omega')\, \delta_{\xi\xi'} \tag{4.27d}$$

where for our purposes, $\bar{n}(\omega) = 0$. Formally, if one works with the mode sum in calculating the intensity, then the integral form simply results from the definition of the limit of the

resulting Riemann sum:

$$\begin{aligned}\left\langle [\mathcal{E}_{in}(t)]^* \, \mathcal{E}_{in}(t) \right\rangle &= \lim_{\Delta\omega \to 0} \frac{\Delta\omega}{2\pi} \sum_{n=-\infty}^{+\infty} \left[\bar{n}(\omega_n) + \frac{1}{2} \right] \\ &= \frac{c}{L} \int_{-\infty}^{+\infty} g(\omega) \left[\bar{n}(\omega) + \frac{1}{2} \right] d\omega \, , \end{aligned} \tag{4.28}$$

where we have multiplied and divided by cL after taking the limit. We have persisted with writing $g(\omega)$ for the mode density instead of explicit factors of $L/2\pi c$ to emphasize the generality of these results, in particular equations (4.27).

4.2 Balanced Homodyning with Finite Bandwidths

In the present notation (3.11a) and (3.11b) are

$$\tilde{\mathcal{E}}_{S1} = \frac{1}{\sqrt{2}} \tilde{\mathcal{E}}_I + \frac{1}{2} \left(\tilde{\mathcal{E}}_A + \tilde{\mathcal{E}}_B \right) \, , \tag{4.29a}$$

$$\tilde{\mathcal{E}}_{S2} = \frac{1}{\sqrt{2}} \tilde{\mathcal{E}}_I - \frac{1}{2} \left(\tilde{\mathcal{E}}_A + \tilde{\mathcal{E}}_B \right) \, . \tag{4.29b}$$

All local oscillators are approximated to be monochromatic fields tuned precisely to $\omega_{\rm c}$, the central frequency of $\mathcal{E}_{S1}$ and $\mathcal{E}_{S2}$,

$$\mathcal{E}_{lj}(t) = \bar{\mathcal{E}}_{lj} \, e^{-i\omega_{\rm c} t} = |\bar{\mathcal{E}}_{lj}| e^{i(\phi_{lj} - \omega_{\rm c} t)} \, , \tag{4.30}$$

where $j = 1, 2$ and $\bar{\mathcal{E}}_{lj} \equiv |\bar{\mathcal{E}}_{lj}| e^{i\phi_{lj}}$. In the rotating frame all local oscillators are then dc fields. The final photocurrents from homodyning are

$$\begin{aligned}\mathcal{I}_j &\equiv \tilde{\mathcal{E}}^*_{Sj} \, \tilde{\mathcal{E}}_{lj} + \tilde{\mathcal{E}}_{Sj} \, \tilde{\mathcal{E}}^*_{lj} \\ &= |\bar{\mathcal{E}}_{lj}| \frac{L}{2\pi c} \int_{-\infty}^{+\infty} \left\{ \frac{1}{\sqrt{2}} \left(\tilde{\Lambda}_I(\omega) \, e^{-i\phi_{lj}} + \left[\tilde{\Lambda}_I(-\omega) \right]^* \, e^{i\phi_{lj}} \right) \right. \\ &\quad \pm \frac{1}{2} \left(\tilde{\Lambda}_A(\omega) \, e^{-i\phi_{lj}} + \left[\tilde{\Lambda}_A(-\omega) \right]^* \, e^{i\phi_{lj}} \right) \\ &\quad \left. \pm \frac{1}{2} \left(\tilde{\Lambda}_B(\omega) \, e^{-i\phi_{lj}} + \left[\tilde{\Lambda}_B(-\omega) \right]^* \, e^{i\phi_{lj}} \right) \right\} e^{-i\omega t} \, d\omega \end{aligned} \tag{4.31}$$

where in the integrand $+1/2$ applies if $j = 1$, and $-1/2$ if $j = 2$. Filters 1 and 2 produce currents governed by the Stratonovich stochastic differential equation

$$d\mathcal{I}^F_j = -n_j \kappa_\xi \left(\mathcal{I}^F_j \, dt - G_j \, dq_j \right) \, , \tag{4.32}$$

where $d\mathcal{I}^F_j$ is the filtered current increment and dq_j is the amount of charge entering Filter j in time step dt. The filter bandwidth is $n_j \kappa_\xi$ with n_j being any positive real number to specify the filter bandwidth in units of κ_ξ. Alice can then set her detection bandwidths to be symmetric by letting $n_1 = n_2$. We have also included a constant filter gain G_j to

produce unit-gain teleportation. Equation (4.32) can be solved using ordinary calculus by multiplying $\exp(n_j\kappa_\xi t)$ and integrating formally to give

$$\mathcal{I}_j^F(t) = G_j\,\mathcal{I}_j^F(0)\,e^{-n_j\kappa_\xi t} + G_j n_j\kappa_\xi \int_0^t e^{-n_j\kappa_\xi(t-t')}\,\mathcal{I}_j(t')\,dt' \,. \tag{4.33}$$

This simply says that the first term can be made arbitrarily small by waiting long enough. Hence, in the long-time limit and going to the frequency domain by writing,

$$\mathcal{I}_j(t) \equiv \frac{\gamma_j}{2\pi}\int_{-\infty}^{+\infty} \bar{\mathcal{I}}_j(\omega)\,e^{-i\omega t}\,d\omega \,, \quad \bar{\mathcal{I}}_j(\omega) \equiv \frac{1}{\gamma_j}\int_{-\infty}^{+\infty} \mathcal{I}_j(t)\,e^{i\omega t}\,dt \tag{4.34}$$

(4.33) becomes

$$\begin{aligned}\mathcal{I}_j^F(t) &= G_j\frac{\gamma_j\,n_j\kappa_\xi}{2\pi}\int_{-\infty}^{+\infty} d\omega\bar{\mathcal{I}}_j(\omega)\,e^{-n_j\kappa_\xi t}\int_0^t dt' e^{(n_j\kappa_\xi - i\omega)t'} \\ &= G_j\,\frac{\gamma_j}{2\pi}\int_{-\infty}^{+\infty}\bar{\mathcal{I}}_j(\omega)\,\frac{n_j\kappa_\xi}{n_j\kappa_\xi - i\omega}\,e^{-i\omega t}\,d\omega \,.\end{aligned} \tag{4.35}$$

It can be seen from (4.35) and (4.33) that the stochastic differential equation (4.32) reproduces a familiar result of linear systems theory, i.e. (4.32) convolves the signal $\mathcal{I}_j$ with a decaying exponential which in frequency space must be the product of the corresponding Fourier transforms. Thus one could have arrived at (4.35) directly instead of the above demonstration, which shows the compatibility of the Stratonovich stochastic differential equation with ordinary calculus. The process of filtering is shown in Fig. 4.4. From equa-

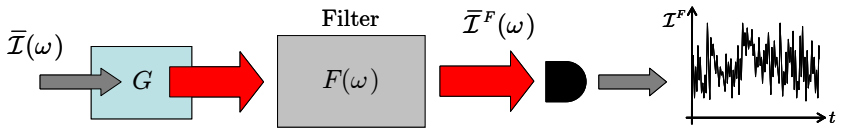

Fig. 4.4: Filter described by (4.32). The filtered photocurrent is $\bar{\mathcal{I}}^F(\omega) = GF(\omega)\bar{\mathcal{I}}(\omega)$, where we take $F(\omega) = n\kappa/(n\kappa - i\omega)$. The indices have been omitted.

tions (4.31) and (4.34), we can make the identifications

$$\gamma_j = |\bar{\mathcal{E}}_{lj}|\frac{L}{c} \,, \tag{4.36a}$$

and

$$\begin{aligned}\bar{\mathcal{I}}_j(\omega) \;=\; &\frac{1}{\sqrt{2}}\left\{\tilde{\Lambda}_I(\omega)\,e^{-i\phi_{lj}} + \left[\tilde{\Lambda}_I(-\omega)\right]^*\,e^{i\phi_{lj}}\right\} \pm \frac{1}{2}\left\{\tilde{\Lambda}_A(\omega)\,e^{-i\phi_{lj}} + \left[\tilde{\Lambda}_A(-\omega)\right]^*\,e^{i\phi_{lj}}\right\} \\ &\pm\frac{1}{2}\left\{\tilde{\Lambda}_B(\omega)\,e^{-i\phi_{lj}} + \left[\tilde{\Lambda}_B(-\omega)\right]^*\,e^{i\phi_{lj}}\right\} \,,\end{aligned} \tag{4.36b}$$

where (4.36b) adopts the same sign convention as (4.31).

4.3 Field Displacement and the Teleported Modes

Bob's act of displacing $\mathcal{E}_{B'}$ is most conveniently expressed by writing all fields in terms of real and imaginary parts. To do so, we note from the two-photon optics considered in Ref. [59] and [60]. The classical two-mode quadrature phase amplitude can be introduced as

$$\beta_\theta(\omega) \equiv \frac{1}{2}\left\{A(\omega_{\rm C}+\omega)\,e^{-i\theta} + [A(\omega_{\rm C}-\omega)]^*\,e^{i\theta}\right\}\,, \tag{4.37}$$

for some complex mode amplitude $A(\omega_{\rm C}+\omega)$ and arbitrary phase θ. Note the quadrature amplitudes are generally complex except when on resonance ($\omega=\omega_{\rm C}$). Bob's share of the EPR field shall be written as

$$\begin{aligned}\mathcal{E}_{B'}(t) &= \frac{1}{\sqrt{2}}\left[\tilde{\mathcal{E}}_A(t) - \tilde{\mathcal{E}}_B(t)\right]\\ &= \frac{1}{\sqrt{2}}\left\{\frac{1}{2}\left(\tilde{\mathcal{E}}_A(t)+\left[\tilde{\mathcal{E}}_A(t)\right]^*\right) - \frac{1}{2}\left(\tilde{\mathcal{E}}_B(t)+\left[\tilde{\mathcal{E}}_B(t)\right]^*\right)\right\}\\ &\quad + \frac{i}{\sqrt{2}}\left\{\frac{1}{2i}\left(\tilde{\mathcal{E}}_A(t)-\left[\tilde{\mathcal{E}}_A(t)\right]^*\right) - \frac{1}{2i}\left(\tilde{\mathcal{E}}_B(t)-\left[\tilde{\mathcal{E}}_B(t)\right]^*\right)\right\}\,.\end{aligned} \tag{4.38}$$

Let us define our preferred quadratures to be of phases zero and $\pi/2$, in which case Alice would measure the real and imaginary part of $\mathcal{E}_{S1}$ and $\mathcal{E}_{S2}$ respectively. The quadrature amplitudes for the vacuum field are

$$x_\xi(\omega) \equiv \frac{1}{2}\left\{\tilde{f}_\xi(\omega)+\left[\tilde{f}_\xi(-\omega)\right]^*\right\}\,,\quad y_\xi(\omega)\equiv\frac{1}{2i}\left\{\tilde{f}_\xi(\omega)-\left[\tilde{f}_\xi(-\omega)\right]^*\right\}\,, \tag{4.39a}$$

and similarly for the subharmonic,

$$X_\xi(\omega) \equiv \frac{1}{2}\left\{\tilde{\mathcal{A}}_\xi(\omega)+\left[\tilde{\mathcal{A}}_\xi(-\omega)\right]^*\right\}\,,\quad Y_\xi(\omega)\equiv\frac{1}{2i}\left\{\tilde{\mathcal{A}}_\xi(\omega)-\left[\tilde{\mathcal{A}}_\xi(-\omega)\right]^*\right\}\,. \tag{4.39b}$$

With these definitions we find

$$\frac{1}{2}\left\{\tilde{\Lambda}_\xi(\omega)+\left[\tilde{\Lambda}_\xi(-\omega)\right]^*\right\} = \sqrt{\frac{c}{L}}\,x_\xi(\omega)+\sqrt{2\kappa_\xi}\,X_\xi(\omega)\,, \tag{4.40a}$$

$$\frac{1}{2i}\left\{\tilde{\Lambda}_\xi(\omega)-\left[\tilde{\Lambda}_\xi(-\omega)\right]^*\right\} = \sqrt{\frac{c}{L}}\,y_\xi(\omega)+\sqrt{2\kappa_\xi}\,Y_\xi(\omega)\,. \tag{4.40b}$$

For our purposes, the damping of S_A and S_B will be kept the same, i.e. $\kappa_A=\kappa_B\equiv\kappa$, and independent of κ_I. Hence (4.38) can be written as

$$\mathcal{E}_{B'}(t) = \mathcal{E}^X_{B'}(t) + i\mathcal{E}^Y_{B'}(t)\,, \tag{4.41a}$$

where $\mathcal{E}_{B'}(t)$ has real and imaginary parts with a frequency decomposition in terms of quadrature modes,

$$\begin{aligned}\mathcal{E}^X_{B'}(t) = \frac{1}{\sqrt{2}}\int_{-\infty}^{+\infty} g(\omega)\Bigg\{&\left[\sqrt{\frac{c}{L}}\,x_A(\omega)+\sqrt{2\kappa}\,X_A(\omega)\right]\\ &-\left[\sqrt{\frac{c}{L}}\,x_B(\omega)+\sqrt{2\kappa}\,X_B(\omega)\right]\Bigg\}e^{-i\omega t}\,d\omega\,,\end{aligned} \tag{4.41b}$$

$$\mathcal{E}^Y_{B'}(t) = \frac{1}{\sqrt{2}} \int_{-\infty}^{+\infty} g(\omega) \left\{ \left[\sqrt{\frac{c}{L}}\, y_A(\omega) + \sqrt{2\kappa}\, Y_A(\omega) \right] - \left[\sqrt{\frac{c}{L}}\, y_B(\omega) + \sqrt{2\kappa}\, Y_B(\omega) \right] \right\} e^{-i\omega t}\, d\omega \; . \tag{4.41c}$$

Bob's displacement of $\mathcal{E}_{B'}$ in phase-space is straightforwardly given by

$$\mathcal{E}_{S3}(t) = \mathcal{E}_{B'}(t) + \frac{1}{\sqrt{2}} \left[\mathcal{I}^F_1(t) + i\mathcal{I}^F_2(t) \right] \; . \tag{4.42}$$

It will be helpful to explicitly define the real functions $\mathcal{E}^X_{S3}(t)$ and $\mathcal{E}^Y_{S3}(t)$ so that

$$\mathcal{E}_{S3}(t) = \mathcal{E}^X_{S3}(t) + i\mathcal{E}^Y_{S3}(t) \; , \tag{4.43a}$$

where the real and imaginary parts of $\mathcal{E}_{S3}(t)$ are thus given by

$$\begin{aligned} \mathcal{E}^X_{S3}(t) &= \mathcal{E}^X_{B'}(t) + \frac{\mathcal{I}^F_1(t)}{\sqrt{2}} \\ &= \frac{1}{\sqrt{2}} \int_{-\infty}^{+\infty} g(\omega) \left\{ \left[\sqrt{\frac{c}{L}}\, x_A(\omega) + \sqrt{2\kappa}\, X_A(\omega) \right] \right. \\ &\quad \left. - \left[\sqrt{\frac{c}{L}}\, x_B(\omega) + \sqrt{2\kappa}\, X_B(\omega) \right] + G_1 |\bar{\mathcal{E}}_{l1}|\, \bar{\mathcal{I}}_1(\omega) \frac{n_1\kappa}{n_1\kappa - i\omega} \right\} e^{-i\omega t}\, d\omega \; , \end{aligned} \tag{4.43b}$$

and

$$\begin{aligned} \mathcal{E}^Y_{S3}(t) &= \mathcal{E}^Y_{B'}(t) + \frac{\mathcal{I}^F_2(t)}{\sqrt{2}} \\ &= \frac{1}{\sqrt{2}} \int_{-\infty}^{+\infty} g(\omega) \left\{ \left[\sqrt{\frac{c}{L}}\, y_A(\omega) + \sqrt{2\kappa}\, Y_A(\omega) \right] \right. \\ &\quad \left. - \left[\sqrt{\frac{c}{L}}\, y_B(\omega) + \sqrt{2\kappa}\, Y_B(\omega) \right] + G_2 |\bar{\mathcal{E}}_{l2}|\, \bar{\mathcal{I}}_2(\omega) \frac{n_2\kappa}{n_2\kappa - i\omega} \right\} e^{-i\omega t}\, d\omega \; . \end{aligned} \tag{4.43c}$$

Equation (4.36b) becomes, for $j = 1$, $\phi_{l1} = 0$,

$$\begin{aligned} \bar{\mathcal{I}}_1(\omega) &= \frac{2}{\sqrt{2}} \left[\sqrt{\frac{c}{L}}\, x_I(\omega) + \sqrt{2\kappa_I}\, X_I(\omega) \right] \\ &\quad + \left[\sqrt{\frac{c}{L}}\, x_A(\omega) + \sqrt{2\kappa}\, X_A(\omega) \right] + \left[\sqrt{\frac{c}{L}}\, x_B(\omega) + \sqrt{2\kappa}\, X_B(\omega) \right] \; , \end{aligned} \tag{4.44a}$$

and for $j = 2$, $\phi_{l2} = \pi/2$,

$$\begin{aligned} \bar{\mathcal{I}}_2(\omega) &= \frac{2}{\sqrt{2}} \left[\sqrt{\frac{c}{L}}\, y_I(\omega) + \sqrt{2\kappa_I}\, Y_I(\omega) \right] \\ &\quad - \left[\sqrt{\frac{c}{L}}\, y_A(\omega) + \sqrt{2\kappa}\, Y_A(\omega) \right] - \left[\sqrt{\frac{c}{L}}\, y_B(\omega) + \sqrt{2\kappa}\, Y_B(\omega) \right] \; . \end{aligned} \tag{4.44b}$$

A chief routine of verification will be to observe the teleported squeezing spectra. Interrogating teleportation by examining the intensity correlation function will be reserved as the topic of Chap. 6. Thus, Victor will now perform the last stage of homodyning and filtering. This will prepare the teleported field in the form suitable for the derivation of squeezing spectra in the next chapter. Victor's procedure will be accounted for by extending the value of j to 3, with the same definitions of current and local oscillator. The final filtered current $\mathcal{I}_3^F(t)$ corresponding to $\phi_{l3} = 0$, along with it's Fourier component will be denoted respectively as

$$\mathcal{I}_3^{XF}(t) = 2G_3|\bar{\mathcal{E}}_{l3}|\left[\mathcal{E}_{S3}^X(t) \star e^{-n_3\kappa t}\right] = \frac{G_3\gamma_3}{2\pi}\int_{-\infty}^{+\infty}\bar{\mathcal{I}}_3^X(\omega)\frac{n_3\kappa}{n_3\kappa - i\omega}\,e^{-i\omega t}\,d\omega\,, \quad (4.45a)$$

$$\bar{\mathcal{I}}_3^X(\omega) = \left[\sqrt{\frac{c}{L}}\,x_A(\omega) + \sqrt{2\kappa}\,X_A(\omega)\right] - \left[\sqrt{\frac{c}{L}}\,x_B(\omega) + \sqrt{2\kappa}\,X_B(\omega)\right] + G_1|\bar{\mathcal{E}}_{l1}|\,\bar{\mathcal{I}}_1(\omega)\frac{n_1\kappa}{n_1\kappa - i\omega}\,, \quad (4.45b)$$

where $f(t) \star g(t)$ denotes the convolution of $f(t)$ and $g(t)$. Similarly for the case of $\phi_{l3} = 0$:

$$\mathcal{I}_3^{YF}(t) = 2G_3|\bar{\mathcal{E}}_{l3}|\left[\mathcal{E}_{S3}^Y(t) \star e^{-n_3\kappa t}\right] = \frac{G_3\gamma_3}{2\pi}\int_{-\infty}^{+\infty}\bar{\mathcal{I}}_3^Y(\omega)\frac{n_3\kappa}{n_3\kappa - i\omega}\,e^{-i\omega t}\,d\omega\,, \quad (4.46a)$$

$$\bar{\mathcal{I}}_3^Y(\omega) = \left[\sqrt{\frac{c}{L}}\,y_A(\omega) + \sqrt{2\kappa}\,Y_A(\omega)\right] - \left[\sqrt{\frac{c}{L}}\,y_B(\omega) + \sqrt{2\kappa}\,Y_B(\omega)\right] + G_2|\bar{\mathcal{E}}_{l2}|\,\bar{\mathcal{I}}_2(\omega)\frac{n_2\kappa}{n_2\kappa - i\omega}\,, \quad (4.46b)$$

where γ_3 is given by

$$\gamma_3 = \frac{2L|\bar{\mathcal{E}}_{l3}|}{c\sqrt{2}}\,. \quad (4.47)$$

Let us say a few words about the linear mapping presented by equations (4.45) and (4.46). First, the departure from unit-gain teleportation is expressed by the deviation of the product $G_j|\bar{\mathcal{E}}_{lj}|$ from unity and how accurately the phase space displacement given by (4.42) can be generated. Secondly, although $\mathcal{E}_{S3}^X(t)$ and $\mathcal{E}_{S3}^Y(t)$ are interpreted as classical stochastic fields, they do not contravene the Heisenberg's uncertainty principle. The product of the quadrature variances in Heisenberg's uncertainty relation is duplicated as a direct consequence of the extra 1/2 appearing in (4.27). This is most conspicuous in the case of vacuum fields where $\Delta\mathcal{E}_{S3}^X\,\Delta\mathcal{E}_{S3}^Y$ is expected to vanish within the realm of pure classical notions because zero-point fluctuations should not appear. Stochastic electrodynamics regards $\mathcal{E}_{S3}^X$ and $\mathcal{E}_{S3}^Y$ as coexisting complementary hidden variables for which the commutator

$$\left[\hat{\mathcal{E}}_{S3}^X, \hat{\mathcal{E}}_{S3}^Y\right] = \frac{i}{2} \quad (4.48)$$

is absent. More will be said about SED and its relation to quantum mechanical operators in Sect. 5.4.

Being the prevailing concept of classical theories, SED permits simultaneous knowledge of both quadratures. However, on accepting (or with hindsight) that quantum mechanics

is complete in describing the real factual situation, the application of (4.45) and (4.46) is then bounded by the above commutator of (4.48). That is, Victor may inquire about any two quadratures simultaneously by the use of a beam-splitter, for which he will retrieve the coordinates of a coherent state, squeezed or not, with fluctuations predicted by Heisenberg's uncertainty principle.

It should also be stressed that the homodyne current records are classical information, represented by a series of real numbers in time. Finally, the linear mapping has been derived in the rotating frame, which in the quantum formulation is equivalent to working in the interaction picture. We will have more to say on this subject in Chap. 5.

Chapter 5

Quadrature Teleportation

We saw in Chap. 3, as a precursor to teleportation of stochastic fields where we visualized field fluctuations over time. If the phase-space trajectory of the teleported field can be made to exactly overlap that of the input, perfect teleportation is claimed. This was easy to understand because one only deals with the total field — the integral over all frequencies. The Fourier space description provides an alternative explanation to these time domain functions by requiring each mode between the teleporter input and output to be identical. The linear mapping of Chap. 4 now provides an analytical expression for the observable squeezing spectra of the teleported quadratures. With these formulas at hand, the significance of multimode squeezing and filtering bandwidths become transparent. We devote Sect. 5.2 to deriving these relations and Sect. 5.3 will explore these issues with the aid of some plots for the analytical expressions.

The linear mapping of Chap. 4 began with the fields entering the squeezers and involves tracking these fields through the various stages of the teleportation protocol, expressing the output modes in terms of input ones at each stage. The most difficult of these input-output relations lie in the DPOs; for which we are yet to relate the emitted modes to those entering it. To begin, it would be instructive to sketch out the internal workings of these squeezing cavities as provided by stochastic electrodynamics.

5.1 Input-Output Theory within Stochastic Electrodynamics

Due mainly to Collett and Gardiner, we now have at our disposal what is formally known as **Input-Output Theory** [61], [62]. In their original formulation, the authors were primarily interested in the squeezed output of a DPO. By relating the intra-cavity dynamics to the input field, they were able to derive the emanated squeezing spectra. Collett and Gardiner derived their results treating the optical field to be comprised of photons; we on the other hand, will derive the corresponding quantities in the view that our field is composed of classical waves. Although we do not follow a quantum field treatment the hindsight granted to us by the quantum mechanical model is invaluable and we will, when opportunities arise, note the quantum-classical correspondences. The terminology "input-output theory" does imply a sense of generality for the formalism, and indeed one need not be restricted to a cavity-based system. A theoretical treatment of such "input-output" type was done for

an electronic circuit connected to a lossy transmission line prior to the work of Collett and Gardiner [63]. The utility of input-output theory is demonstrated for various optical instruments in Ref. [64] for instance. Nevertheless, the designation of such techniques as input-output theory is now exclusive to quantum optics.

5.1.1 Classical Langevin Equations

The rigorous formalities of input-output theory would stretch the thesis beyond its intended scope. We will begin with an assertion of the classical Langevin equations for the cavity mode and be meticulous about its form and origin. The reader who is interested in its formal abstraction and mathematical rigour should consult the second of the two-paper series on the subject [62]. Recapitulating our model of a DPO discussed in Sect. 4.1, the correct equations of motion for the negative and positive frequency parts (one being the complex conjugate of the other) read,

$$\frac{d\alpha_\xi^*}{dt} = i\omega_{\rm C}\,\alpha_\xi^* - \kappa_\xi\,\alpha_\xi^* \pm \kappa_\xi\lambda_\xi\,\alpha_\xi\,e^{i2\omega_{\rm C}t} + i\sqrt{2\kappa_\xi}\,\mathcal{E}_{in\xi}^*\,, \tag{5.1a}$$

$$\frac{d\alpha_\xi}{dt} = \underbrace{-i\omega_{\rm C}\,\alpha_\xi}_{\text{free evolution}} - \underbrace{\kappa_\xi\,\alpha_\xi}_{\text{damping}} \pm \underbrace{\kappa_\xi\lambda_\xi\,\alpha_\xi^*\,e^{-i2\omega_{\rm C}t}}_{\text{non-linear interaction}} - \underbrace{i\sqrt{2\kappa_\xi}\,\mathcal{E}_{in\xi}}_{\text{source term}}\,. \tag{5.1b}$$

The first term in (5.1b) represents the free evolution of the field; i.e., the amplitude simply varies on its own at a frequency of $\omega_{\rm C}$. Classically, this is precisely the sinusoidal wave motion. The non-unit reflectivity of the output mirror provides a means of decay for the intra-cavity field. Thus the second term is straightforwardly $-\kappa_\xi\alpha_\xi$ where its magnitude tells us the amplitude is damped at half the rate of the intensity. This can be seen by multiplying (5.1a) by α_ξ and (5.1b) by α_ξ^*:

$$\begin{aligned}\frac{d\,|\alpha_\xi|^2}{dt} &= \alpha_\xi\frac{d\alpha_\xi^*}{dt} + \frac{d\alpha_\xi}{dt}\,\alpha_\xi^* \\ &= -2\kappa_\xi\,|\alpha_\xi|^2 \pm 2\kappa_\xi\lambda_\xi\,|\alpha_\xi|^2\cos\left[2\left(\omega_{\rm C}t+\phi_\alpha\right)\right] + i\sqrt{2\kappa_\xi}\left[\mathcal{E}_{in\xi}^*\,\alpha_\xi - \mathcal{E}_{in\xi}\,\alpha_\xi^*\right].\end{aligned} \tag{5.2}$$

where we have written $\alpha_\xi = |\alpha_\xi|\,e^{i\phi_\alpha}$. Thus we see that in the absence of the non-linear interaction and the driving field, a cavity initially filled with energy $|\alpha_\xi|^2(0)$ has an intensity loss rate given by

$$|\alpha_\xi|^2(t) = |\alpha_\xi|^2(0)\,e^{-2\kappa_\xi t}\,. \tag{5.3}$$

Appearing in the non-linear interaction is λ_ξ, a real, positive, and dimensionless quantity. It is proportional to the magnitude of the pump $|\mathcal{E}_p|$, the cavity finesses of the pump and subharmonic, and the non-linear susceptibility $\chi^{(2)}$. It may be thought of as an effective pump strength and shall be referred to as the pump parameter. The sign of the non-linear interaction will be clear when we come to calculate the squeezing spectra. For the moment, we shall say that it is to be taken as plus or minus corresponding to squeezing in the Y- or X-quadrature respectively.

It is the long time limit of (5.1) that will be of interest, and upon solving these equations in the steady-state one is led to discover various solutions given different values of the pump parameter. The values of λ_ξ correspond to whether the round-trip parametric gain $\kappa_\xi\lambda_\xi t_{\rm C}$, is greater or less than the round-trip loss $\kappa_\xi t_{\rm C}$, respectively referred to as above or below

threshold. We will operate the DPO in the regime below threshold; i.e. $\lambda_\xi < 1$. This prevents the DPO from self-sustained oscillation.

Setting $\lambda_\xi = 1$ in (5.2) we see that the intra-cavity intensity varies with a sinusoidal component, in which case the sum of the first two terms will generally be negative. Two extremes are given by those times for which $\cos[2(\omega_C t + \phi_\alpha)] = 1$, when the overall contribution from the first two terms exactly vanishes or doubles.

For $0 < \lambda_\xi < 1$, the resulting effect of the non-unit reflectivity of the output mirror and the non-linear interaction is to damp $|\alpha_\xi|^2$, which if $d|\alpha_\xi|^2/dt$ is to be zero, will depend on the driving term. In corpuscular terms, the non-linear crystal is pumped at a rate such that the number of photons gained solely from the non-linear interaction in a time interval of t_C is less than the number of photons of the *subharmonic mode* seeping out of the cavity in the same time period. The non-linear interaction term can be elucidated further with hindsight of the quantum description for parametric down conversion. We leave this explanation to the subsection below. Finally, the last term in (5.1) is the transmission of $\mathcal{E}_{in\xi}$ (which in our case is a vacuum field) into the DPO, where the complex number i accounts for the relative phase shift of $\pi/2$ with respect to the cavity mode. The square root over $2\kappa_\xi$ accommodates our choice to scale $\mathcal{E}_{in\xi}$ such that $\langle \mathcal{E}^*_{in\xi}\mathcal{E}_{in\xi}\rangle$ has units of photon flux.

5.1.2 Degenerate Parametric Amplification from Heisenberg's Equation of Motion

For simplicity, the non-linear interaction can be understood to generate squeezing by solely considering a degenerate parametric amplifier with a classical pump. Just for this section operators shall be written without a circumflex. From Ref. [65], [66] and [67], the amplifier Hamiltonian may be split into a part which is independent of time, H_0 and one *explicitly* time-dependent[1]

$$\begin{aligned} H_s &= H_0 + V(t) \\ &= \hbar\omega_C\, a^\dagger a + \frac{i\hbar}{2}\left[\zeta\left(a^\dagger\right)^2 e^{-i2\omega_C t} - \zeta^* a^2 e^{i2\omega_C t}\right] . \end{aligned} \tag{5.4}$$

Where ζ accounts for both the classical pump amplitude and the non-linear susceptibility. We allow ζ to be complex with a magnitude different from $\kappa\lambda$ to exclude properties intrinsic to a cavity construction. Equation (5.4) is a macroscopic model where only the bulk material property and incoming and outgoing photons appear. Note the inclusion of the conjugate process, second harmonic generation, to ensure H_s is Hermitian. The Heisenberg equations of motion for the subharmonic field are,

$$\frac{da}{dt} = \frac{1}{i\hbar}[a, H_s] = -i\omega_C\, a + \zeta a^\dagger e^{-i2\omega_C t} , \tag{5.5a}$$

$$\frac{da^\dagger}{dt} = \frac{1}{i\hbar}\left[a^\dagger, H_s\right] = i\omega_C\, a^\dagger + \zeta^* a\, e^{i2\omega_C t} \tag{5.5b}$$

where (5.5a) and (5.5b) are Hermitian conjugates since $H_s = H_s^\dagger$. It is most convenient to work in a rotating frame given by

$$\tilde{a}(t) \equiv a(t)\, e^{i\omega_C t} , \tag{5.6a}$$

[1] This is mentioned for the purpose of *Excursion 5.1.*

where $a(t)$ denotes the subharmonic field in the Heisenberg picture. Equations (5.5) then become

$$\frac{d\tilde{a}}{dt} = \zeta \tilde{a}^\dagger \ , \qquad \frac{d\tilde{a}^\dagger}{dt} = \zeta^* \tilde{a} \ . \tag{5.6b}$$

To observe squeezing, we write $\zeta = |\zeta| e^{i\phi}$ and note the general definition of the quadrature phase operator defined by

$$\beta_\theta(t) \equiv \frac{1}{2}\left[\tilde{a}(t)e^{-i\theta} + \tilde{a}^\dagger(t)e^{i\theta}\right] \ . \tag{5.7}$$

Equations (5.6b) are then used to obtain

$$\frac{d\beta_\upsilon(t)}{dt} = |\zeta|\, \beta_\upsilon(t) \ , \qquad \frac{d\beta_{\upsilon+\pi/2}(t)}{dt} = -|\zeta|\, \beta_{\upsilon+\pi/2}(t) \tag{5.8}$$

with respective solutions exhibiting squeezing,

$$\beta_\upsilon(t) = \beta_\upsilon(0)\, e^{|\zeta| t} \ , \qquad \beta_{\upsilon+\pi/2}(t) = \beta_{\upsilon+\pi/2}(0)\, e^{-|\zeta| t} \ , \tag{5.9}$$

where $\upsilon = \phi/2$. Equations (5.8) and (5.9) stand as operator equations stipulated by

$$\left[\beta_\upsilon, \beta_{\upsilon+\pi/2}\right] = \frac{i}{4}\left([\tilde{a}, \tilde{a}^\dagger] - [\tilde{a}^\dagger, \tilde{a}] \right) = \frac{i}{2} \tag{5.10}$$

and hence the Heisenberg uncertainty principle

$$\Delta\beta_\upsilon \, \Delta\beta_{\upsilon+\pi/2} \geq \frac{1}{4} \ , \tag{5.11}$$

where the quadrature phase fluctuations are taken with respect to an arbitrary field state $|\psi\rangle$,

$$\Delta\beta_\upsilon \equiv \left[\langle\psi|\, \beta_\upsilon^2 \, |\psi\rangle - \langle\psi|\, \beta_\upsilon \, |\psi\rangle^2 \right]^{\frac{1}{2}} \ . \tag{5.12}$$

For squeezed states, equations (5.7), (5.9) and (5.12) give

$$\Delta\beta_\upsilon = \frac{e^{|\zeta| t}}{2} \ , \qquad \Delta\beta_{\upsilon+\pi/2} = \frac{e^{-|\zeta| t}}{2} \tag{5.13}$$

from which we obtain the familiar result $\Delta\beta_\upsilon = \Delta\beta_{\upsilon+\pi/2} = 1/2$ in the absence of the non-linear interaction ($\zeta = 0$).

Excursion 5.1 To go into a rotating frame is equivalent to transforming from the Heisenberg to interaction picture. Via this transformation, the free Hamiltonian H_0 carries full time dependence arising from H_s — it is an operator in the Heisenberg picture, written as $H_0(t)$.[2] The interaction picture operator is then defined in terms of operators in the Heisenberg picture as

$$a_{\rm I}(t) \equiv e^{-iH_0(t)t/\hbar}\, a(t)\, e^{iH_0(t)t/\hbar} \ , \tag{5.14a}$$

and evolves according to

$$\frac{da_{\rm I}(t)}{dt} = \frac{1}{i\hbar}\left[a_{\rm I}(t), V_{\rm H}(t)\right] \tag{5.14b}$$

[2] This is because $[H_0, H_s] \neq 0$.

where $V_{\rm H}(t) \equiv e^{iH_s t/\hbar}\, V(t)\, e^{-iH_s t/\hbar}$. Using the decomposition in (5.4) it can be shown that equations (5.14) are the same as (5.6), as it must.

Equations (5.5) constitute the core for the final form of da/dt. We now turn the parametric amplifier into a problem of damping by confining the subharmonic field within some physical boundary laid by mirrors, like the configuration of Fig. 4.1 for example. We can then construct Heisenberg's equation of motion phenomenologically by tacking on the dissipation and driving terms:

$$\begin{aligned}\frac{da}{dt} &= \frac{1}{i\hbar}\,[a, H_s] - \bar{\kappa} a - i\sqrt{2\bar{\kappa}}\,\Gamma \\ &= -i\omega_{\rm C}\, a + \bar{\kappa}\lambda a^{\dagger} e^{-i2\omega_c t} - \bar{\kappa} a - i\sqrt{2\bar{\kappa}}\,\Gamma\ . \end{aligned} \tag{5.15}$$

We may consider H_s to be given by (5.4) with $\zeta = \zeta^* = \kappa\lambda$, and Γ is the bath operator coupling to a. The form of the source term assumes the same coupling strength of a to Γ across all modes. In the rotating frame,

$$\frac{d\tilde{a}}{dt} = -\bar{\kappa}\tilde{a} + \bar{\kappa}\lambda\tilde{a}^{\dagger} - i\sqrt{2\bar{\kappa}}\,\tilde{\Gamma} \tag{5.16}$$

where $\tilde{\Gamma}(t) \equiv \Gamma(t)\, e^{i\omega_c t}$. The prefactors of Γ may, as a matter of preference, be absorbed into its definition. We see then, (5.15) and its Hermitian conjugate appear almost identical to (5.1a) and (5.1b). The quantum treatment is vitally distinguished by (5.10) and (5.13). Replicas of (5.9) also exist in the most primitive form of classical electromagnetism but commutation relations (and therefore Heisenberg's uncertainty relation) are by contrast absent with β_υ and $\beta_{\upsilon+\pi/2}$ being ordinary complex numbers. Stochastic electrodynamics however, works on a higher level of sophistication by conforming to the Heisenberg uncertainty relation through its tailor-made vacuum fluctuations. Thus, because of (4.27), (5.1a) and (5.1b) mimic Heisenberg's equations of motion even more closely than a "pure" classical theory.

While we have provided the reader with a phenomenological model of the DPO, it should be noted that the above procedures leading to (5.16) may be repeated within the formalisms of classical field theory, where the terms in (5.15) may be accounted for systematically by considering a Hamiltonian density and using Hamilton's equation of motion. Poisson brackets would then appear in place of commutator brackets. This would have been the preferred route to deriving the classical Langevin equations.[3]

Returning to (5.1), we now relate Fourier components of the intra-cavity mode amplitude to the amplitudes of the input modes. Cavity S_A will squeeze the X-quadrature, and S_B the Y-quadrature. Going to a rotating frame, which may be effected either by setting $\omega_{\rm C} = 0$ and allowing $\alpha_\xi \longrightarrow \tilde{\alpha}_\xi$, $\mathcal{E}_{in\xi} \longrightarrow \tilde{\mathcal{E}}_{in\xi}$, or by multiplying both sides of (5.1) by an exponential. Equations (4.23) and (4.24) give for the Fourier transform (5.1b) to

$$-(\kappa_\xi - i\omega)\tilde{\mathcal{A}}_\xi(\omega) \pm \kappa_\xi\lambda_\xi \left[\tilde{\mathcal{A}}_\xi(-\omega)\right]^* - \sqrt{\frac{2\kappa_\xi c}{L}}\,\tilde{f}_\xi(\omega) = 0\ . \tag{5.17a}$$

Taking the complex conjugate and letting $\omega \longrightarrow -\omega$ (or multiply (5.1a) by c/L and integrate against $e^{i\omega t}$) returns

$$-(\kappa_\xi - i\omega)\left[\tilde{\mathcal{A}}_\xi(-\omega)\right]^* \pm \kappa_\xi\lambda_\xi\tilde{\mathcal{A}}_\xi(\omega) - \sqrt{\frac{2\kappa_\xi c}{L}}\,\left[\tilde{f}_\xi(-\omega)\right]^* = 0 \tag{5.17b}$$

[3]Time constraints have prevented the author to rework the equations leading to (5.15) within the context of a classical field theory. The reader should also be aware that Gardiner and Collett derived a more general *quantum* Langevin equation involving commutators by which (5.15) is a special case of their result.

where we take the plus sign for the second term if $\xi = B$, and minus for $\xi = A$. Ideally, cavities S_A and S_B should share the same pump parameter ($\lambda_A = \lambda_B$) to maximize the correlation between their outputs. The above sign convention shall be adopted throughout future calculations. Since $\tilde{\mathcal{E}}_I$ will be prepared independently, the modes to be teleported will satisfy,

$$-(\kappa_I - i\omega)\tilde{\mathcal{A}}_I(\omega) \pm \kappa_I\lambda_I \left[\tilde{\mathcal{A}}_I(-\omega)\right]^* - \sqrt{\frac{2\kappa_I c}{L}}\, \tilde{f}_I(\omega) = 0 \,, \tag{5.18a}$$

$$-(\kappa_I - i\omega) \left[\tilde{\mathcal{A}}_I(-\omega)\right]^* \pm \kappa_I\lambda_I \tilde{\mathcal{A}}_I(\omega) - \sqrt{\frac{2\kappa_I c}{L}}\, \left[\tilde{f}_I(-\omega)\right]^* = 0 \tag{5.18b}$$

with its own pump parameter λ_I. Equations (5.18a) and (5.18b) constrains the direction of squeezing in phase-space to be either along the real or imaginary axis. It will be best to solve (5.17) and (5.18) for quadrature modes. After some algebra we arrive at

$$X_\xi(\omega) = -\sqrt{\frac{2\kappa_\xi c}{L}} \frac{x_\xi(\omega)}{\kappa_\xi(1 \mp \lambda_\xi) - i\omega} \,, \quad Y_\xi(\omega) = -\sqrt{\frac{2\kappa_\xi c}{L}} \frac{y_\xi(\omega)}{\kappa_\xi(1 \pm \lambda_\xi) - i\omega} \,. \tag{5.19}$$

Equation (5.19) completes our linear mapping since we can now express the teleported quadrature modes entirely as a function of those incident on the entanglement source and the input cavity. We now proceed to calculate the spectra of squeezing which will be our measure of authenticity for teleportation.

5.2 Derivation of Teleported Spectra of Squeezing

The X-quadrature squeezing spectrum at Bob's location will be calculated first. The Y-quadrature spectrum then follows with appropriate replacements in signs and variable labelling. Recalling (4.43) which gives the displaced field

$$\mathcal{E}_{S3}(t) = \mathcal{E}^X_{S3}(t) + i\mathcal{E}^Y_{S3}(t) \,, \tag{5.20}$$

let us write

$$\mathcal{E}^X_{S3}(t) = \int_{-\infty}^{+\infty} g(\omega)\, \bar{\mathcal{E}}^X_{S3}(\omega)\, e^{-i\omega t}\, d\omega \,, \tag{5.21a}$$

$$\mathcal{E}^Y_{S3}(t) = \int_{-\infty}^{+\infty} g(\omega)\, \bar{\mathcal{E}}^Y_{S3}(\omega)\, e^{-i\omega t}\, d\omega \tag{5.21b}$$

where we now define the X-quadrature amplitudes for $\mathcal{E}_{S3}$ to be (letting $\kappa_A = \kappa_B \equiv \kappa$ as before)

$$\bar{\mathcal{E}}^X_{S3}(\omega) = \frac{1}{\sqrt{2}} \left\{ \left[\sqrt{\frac{c}{L}}\, x_A(\omega) + \sqrt{2\kappa}\, X_A(\omega)\right] - \left[\sqrt{\frac{c}{L}}\, x_B(\omega) + \sqrt{2\kappa}\, X_B(\omega)\right] + \bar{\mathcal{I}}_1(\omega) \frac{G_1 |\bar{\mathcal{E}}_{l1}|\, n_1\kappa}{n_1\kappa - i\omega} \right\} \,, \tag{5.22a}$$

and similarly for the Y-quadrature,

$$\bar{\mathcal{E}}^{Y}_{S3}(\omega) = \frac{1}{\sqrt{2}}\left\{\left[\sqrt{\frac{c}{L}}\, y_A(\omega) + \sqrt{2\kappa}\, Y_A(\omega)\right] - \left[\sqrt{\frac{c}{L}}\, y_B(\omega) + \sqrt{2\kappa}\, Y_B(\omega)\right] + \bar{\mathcal{I}}_2(\omega)\frac{G_2\left|\bar{\mathcal{E}}_{l2}\right| n_2\kappa}{n_2\kappa - i\omega}\right\} . \tag{5.22b}$$

The currents $\bar{\mathcal{I}}_1(\omega)$ and $\bar{\mathcal{I}}_2(\omega)$ are given by (4.44a) and (4.44b) respectively. In the continuous limit, the **Wiener-Khinchine Theorem** will be helpful in identifying the spectrum of squeezing [68]. The auto-correlation function for the X-quadrature is [4]

$$\left\langle \left[\mathcal{E}^{X}_{S3}(t)\right]^{*} \mathcal{E}^{X}_{S3}(t+\tau)\right\rangle = \int_{-\infty}^{+\infty}\int_{-\infty}^{+\infty}\left\langle g(\omega)\left[\bar{\mathcal{E}}^{X}_{S3}(\omega)\right]^{*} g(\omega')\,\bar{\mathcal{E}}^{X}_{S3}(\omega')\right\rangle e^{-i(\omega'-\omega)t}\, e^{-i\omega'\tau}\, d\omega\, d\omega' \tag{5.23}$$

where

$$\begin{aligned}\left\langle g(\omega)\left[\bar{\mathcal{E}}^{X}_{S3}(\omega)\right]^{*} g(\omega')\,\bar{\mathcal{E}}^{X}_{S3}(\omega')\right\rangle &= \frac{1}{2}\Bigg\langle g(\omega)\Bigg\{\left[\sqrt{\frac{c}{L}}\, x_A(\omega) + \sqrt{2\kappa}\, X_A(\omega)\right]^{*} \\ &\quad - \left[\sqrt{\frac{c}{L}}\, x_B(\omega) + \sqrt{2\kappa}\, X_B(\omega)\right]^{*} + \left[\bar{\mathcal{I}}_1(\omega)\right]^{*}\frac{G_1\left|\bar{\mathcal{E}}_1\right| n_1\kappa}{n_1\kappa + i\omega}\Bigg\} \\ &\quad \times g(\omega')\Bigg\{\left[\sqrt{\frac{c}{L}}\, x_A(\omega') + \sqrt{2\kappa}\, X_A(\omega')\right] \\ &\quad - \left[\sqrt{\frac{c}{L}}\, x_B(\omega') + \sqrt{2\kappa}\, X_B(\omega')\right] + \left[\bar{\mathcal{I}}_1(\omega')\right]\frac{G_1\left|\bar{\mathcal{E}}_1\right| n_1\kappa}{n_1\kappa - i\omega'}\Bigg\}\Bigg\rangle .\end{aligned} \tag{5.24}$$

To simplify (5.24), note that not all terms survive on expansion due to the independence of the DPO vacuum inputs. We first compute the non-zero terms. From (4.39a) along with the DPO input statistics given by (4.27) we find [5]

$$\begin{aligned}\left\langle g(\omega)\left[x_\xi(\omega)\right]^{*} g(\omega')\, x_{\xi'}(\omega')\right\rangle &= \frac{1}{4}\left\langle g(\omega)\left\{\left[\tilde{f}_\xi(\omega)\right]^{*} + \tilde{f}_\xi(-\omega)\right\} g(\omega')\left\{\tilde{f}_{\xi'}(\omega') + \left[\tilde{f}_{\xi'}(-\omega')\right]^{*}\right\}\right\rangle \\ &= \frac{1}{4}\, g(\omega)\,\delta(\omega-\omega')\,\delta_{\xi\xi'} ,\end{aligned} \tag{5.25a}$$

Using (5.19), the covariances taken between quadratures external and internal to cavity S_ξ can be computed,

$$\left\langle g(\omega)\left[x_\xi(\omega)\right]^{*} g(\omega')\, X_{\xi'}(\omega')\right\rangle = -\frac{1}{\kappa_\xi(1 \mp \lambda_{\xi'}) - i\omega'}\sqrt{\frac{2\kappa_\xi c}{L}}\,\frac{1}{4}\, g(\omega)\,\delta(\omega-\omega')\,\delta_{\xi\xi'} , \tag{5.25b}$$

[4] Remembering that $\mathcal{E}^{X}_{S3}(t)$ and $\mathcal{E}^{Y}_{S3}(t)$ are real by construction.

[5] Obviously (4.27) is preserved for $\tilde{f}(\omega) \equiv i\bar{f}(\omega)$.

$$\Big\langle g(\omega)\, x_\xi(\omega)\, g(\omega')\, [X_{\xi'}(\omega')]^* \Big\rangle = \Big\langle g(\omega)\, [x_\xi(\omega)]^*\, g(\omega')\, X_{\xi'}(\omega') \Big\rangle^*$$
$$= -\frac{1}{\kappa_\xi(1 \mp \lambda_{\xi'}) + i\omega'} \sqrt{\frac{2\kappa_\xi c}{L}}\, \frac{1}{4}\, g(\omega)\, \delta(\omega - \omega')\, \delta_{\xi\xi'}\ , \quad (5.25c)$$

and also the portion of intra-cavity energy density contained in the X-quadrature,

$$\Big\langle g(\omega)\, [X_\xi(\omega)]^*\, g(\omega')\, X_{\xi'}(\omega') \Big\rangle$$
$$= \frac{1}{[\kappa_\xi(1 \mp \lambda_\xi) + i\omega]\, [\kappa_\xi(1 \mp \lambda_{\xi'}) - i\omega']} \frac{2\kappa_\xi c}{L}\, \frac{1}{4}\, g(\omega)\, \delta(\omega - \omega')\, \delta_{\xi\xi'}\ . \quad (5.25d)$$

On expanding (5.24), all terms will be of the form

$$\Big\langle g(\omega) \Big[\sqrt{\frac{c}{L}}\, x_\xi(\omega) + \sqrt{2\kappa_\xi}\, X_\xi(\omega)\Big]^* g(\omega') \Big[\sqrt{\frac{c}{L}}\, x_{\xi'}(\omega') + \sqrt{2\kappa_\xi}\, X_{\xi'}(\omega')\Big] \Big\rangle$$
$$= \frac{c}{L} \Big\langle g(\omega)\, [x_\xi(\omega)]^*\, g(\omega')\, x_{\xi'}(\omega') \Big\rangle + \sqrt{\frac{2\kappa_\xi c}{L}} \Big\langle g(\omega)\, [x_\xi(\omega)]^*\, g(\omega')\, X_{\xi'}(\omega') \Big\rangle$$
$$+ \sqrt{\frac{2\kappa_\xi c}{L}} \Big\langle g(\omega)\, [X_\xi(\omega)]^*\, g(\omega')\, x_{\xi'}(\omega') \Big\rangle + 2\kappa_\xi \Big\langle g(\omega)\, [X_\xi(\omega)]^*\, g(\omega')\, x_{\xi'}(\omega') \Big\rangle$$
$$= \frac{c}{L} \Big\{ 1 - \frac{2\kappa_\xi}{\kappa_\xi(1 \mp \lambda_\xi) - i\omega'} - \frac{2\kappa_\xi}{\kappa_\xi(1 \mp \lambda_\xi) + i\omega}$$
$$+ \frac{(2\kappa_\xi)^2}{[\kappa_\xi(1 \mp \lambda_\xi) + i\omega]\, [\kappa_\xi(1 \mp \lambda_\xi) - i\omega']} \Big\} \frac{1}{4}\, g(\omega)\, \delta(\omega - \omega')\, \delta_{\xi\xi'}$$
$$= \frac{1}{4}\, \Omega^X_\xi(\omega, \omega')\, g(\omega)\, \delta(\omega - \omega')\, \delta_{\xi\xi'}\ . \quad (5.26a)$$

where we define,

$$\Omega^X_\xi(\omega, \omega') \equiv \frac{c}{L} \Big\{ 1 - \frac{2\kappa_\xi}{\kappa_\xi(1 \mp \lambda_\xi) - i\omega'} - \frac{2\kappa_\xi}{\kappa_\xi(1 \mp \lambda_\xi) + i\omega}$$
$$+ \frac{(2\kappa_\xi)^2}{[\kappa_\xi(1 \mp \lambda_\xi) + i\omega]\, [\kappa_\xi(1 \mp \lambda_\xi) - i\omega']} \Big\}\ , \quad (5.26b)$$

reminding ourselves of the sign convention mentioned in (5.17) and (5.18).

Excursion 5.2 For the purpose of obtaining (5.25), (4.27) provided a complete description of the external vacuum field for our DPO. It should be mentioned for completeness, that the quantum calculation must be complemented by the boson commutation relations

$$\Big[g(\omega) \hat{\bar{f}}_\xi(\omega), g(\omega') \hat{\bar{f}}_{\xi'}(\omega') \Big] = 0\ , \quad (5.27a)$$
$$\Big[g(\omega) \hat{\bar{f}}^\dagger_\xi(\omega), g(\omega') \hat{\bar{f}}^\dagger_{\xi'}(\omega) \Big] = 0\ , \quad (5.27b)$$
$$\Big[g(\omega) \hat{\bar{f}}_\xi(\omega), g(\omega') \hat{\bar{f}}^\dagger_{\xi'}(\omega') \Big] = g(\omega)\, \delta(\omega - \omega')\, \delta_{\xi\xi'}\ . \quad (5.27c)$$

whereby the same relation to (5.11) is expected for the cavity inputs $\hat{x}_\xi(\omega) = \Delta\hat{x}_\xi(\omega)$ and $\hat{y}_\xi(\omega) = \Delta\hat{y}_\xi(\omega)$. The ensemble averages must then be realized from a density operator $\rho_{\rm R}$

for the reservoir such that

$$\begin{aligned}\Big\langle g(\omega)\hat{\bar{f}}_\xi(\omega)\, g(\omega')\hat{\bar{f}}_{\xi'}(\omega')\Big\rangle &= \mathrm{tr}\Big\{\rho_{\mathrm{R}}\, g(\omega)\hat{\bar{f}}_\xi(\omega)\, g(\omega')\hat{\bar{f}}_{\xi'}(\omega')\Big\} \\ &= 0\,, \end{aligned} \tag{5.28a}$$

$$\begin{aligned}\Big\langle g(\omega)\hat{\bar{f}}^\dagger_\xi(\omega)\, g(\omega')\hat{\bar{f}}^\dagger_{\xi'}(\omega')\Big\rangle &= \mathrm{tr}\Big\{\rho_{\mathrm{R}}\, g(\omega)\hat{\bar{f}}^\dagger_\xi(\omega)\, g(\omega')\hat{\bar{f}}^\dagger_{\xi'}(\omega')\Big\} \\ &= 0\,, \end{aligned} \tag{5.28b}$$

$$\begin{aligned}\Big\langle g(\omega)\hat{\bar{f}}^\dagger_\xi(\omega)\, g(\omega')\hat{\bar{f}}_{\xi'}(\omega')\Big\rangle &= \mathrm{tr}\Big\{\rho_{\mathrm{R}}\, g(\omega)\hat{\bar{f}}^\dagger_\xi(\omega)\, g(\omega')\hat{\bar{f}}_{\xi'}(\omega')\Big\} \\ &= g(\omega)\,\bar{n}(\omega)\,\delta(\omega-\omega')\,\delta_{\xi\xi'}\,. \end{aligned} \tag{5.28c}$$

Note that it is no longer legitimate to add the extra 1/2 to the average number of photons per mode. It is now a manifestation of the above boson commutators.

5.2.1 Classical Squeezing

A few remarks about (5.26a) and the squeezed states of light can be made. Noting the quadrature mode amplitudes have zero mean, the X-quadrature spectra of squeezing on the output of our DPO are furnished directly from (5.26). The two-time correlation function of $\tilde{\mathcal{E}}^X_\xi(t)$ is

$$\begin{aligned}&\Big\langle\Big[\tilde{\mathcal{E}}^X_\xi(t)\Big]^*\,\tilde{\mathcal{E}}^X_\xi(t+\tau)\Big\rangle \\ &\qquad= \int_{-\infty}^{+\infty}\int_{-\infty}^{+\infty}\Big\langle g(\omega)\left[\sqrt{\frac{c}{L}}\,x_\xi(\omega)+\sqrt{2\kappa_\xi}\,X_\xi(\omega)\right]^* \\ &\qquad\quad\times g(\omega')\left[\sqrt{\frac{c}{L}}\,x_\xi(\omega')+\sqrt{2\kappa_\xi}\,X_\xi(\omega')\right]\Big\rangle\, e^{i(\omega-\omega')t}\,e^{-i\omega'\tau}\,d\omega\,d\omega'\,. \end{aligned} \tag{5.29}$$

Substituting in (5.26) and integrating with respect to ω' gives

$$\Big\langle\Big[\tilde{\mathcal{E}}^X_\xi(t)\Big]^*\,\tilde{\mathcal{E}}^X_\xi(t+\tau)\Big\rangle = \frac{1}{2\pi}\int_{-\infty}^{+\infty}\left\{\frac{1}{4}\frac{\big[(\kappa_\xi(1\mp\lambda_\xi)\big]^2+\omega^2}{\big[(\kappa_\xi(1\pm\lambda_\xi)\big]^2+\omega^2}\right\}\,e^{-i\omega\tau}\,d\omega\,, \tag{5.30}$$

where we have substituted (4.16) for the density of modes. For the continuing derivation below, it is wise to further define

$$\bar{\Omega}^X_\xi(\omega) \equiv \frac{\big[(\kappa_\xi(1\mp\lambda_\xi)\big]^2+\omega^2}{\big[(\kappa_\xi(1\pm\lambda_\xi)\big]^2+\omega^2} \quad\Longrightarrow\quad \Omega^X_\xi(\omega,\omega')\big|_{\omega=\omega'} = \bar{\Omega}^X_\xi(\omega)\frac{c}{L}\,, \tag{5.31}$$

where (5.31) is consistent with (5.26) in signs. The Wiener-Khinchine theorem for a stationary process delivers the DPO outgoing squeezing spectrum from (5.30) as

$$\big|\Delta\mathcal{E}^X_\xi(\bar{\omega})\big|^2 = \frac{1}{4}\frac{(1\mp\lambda_\xi)^2+\bar{\omega}^2}{(1\pm\lambda_\xi)^2+\bar{\omega}^2}\,, \tag{5.32}$$

where $\bar{\omega}\equiv\omega/\kappa_\xi$ specifies the optical frequency in units of the amplitude decay rate. First we note that each Fourier component satisfies

$$\big|\Delta\mathcal{E}^X_\xi(\bar{\omega})\big|\,\big|\Delta\mathcal{E}^Y_\xi(\bar{\omega})\big| = \frac{1}{4}\,. \tag{5.33}$$

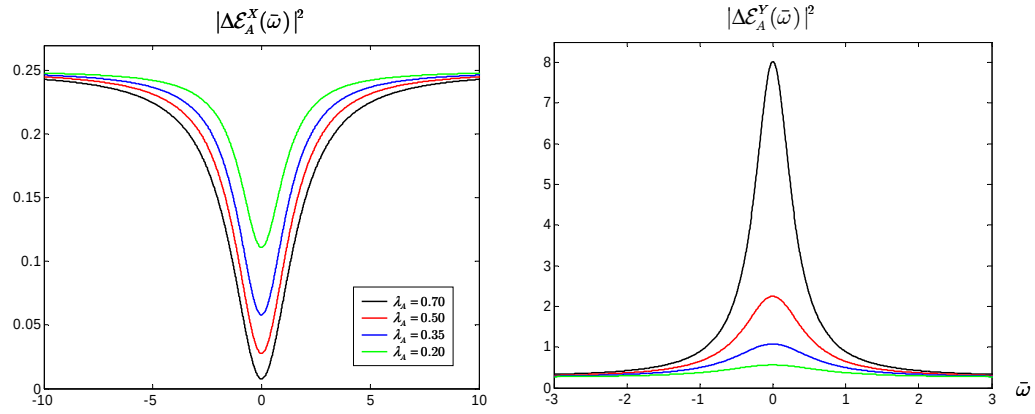

(a) (b)

Fig. 5.1: Squeezing spectra emitted by S_A. (a) The degree of squeezing increases with λ_A. (b) Ideally S_A and S_B should be identical; i.e. they share the same pump and have identical non-linearities, etc ($\lambda_A = \lambda_B$) giving rise to perfectly symmetric outputs $\left|\Delta\mathcal{E}_A^Y(\bar{\omega})\right|^2 = \left|\Delta\mathcal{E}_B^X(\bar{\omega})\right|^2$.

The reader should remember the sign convention adopted in equations (5.17) would give us

$$\left|\Delta\mathcal{E}_A^X(\omega)\right|^2 = \frac{1}{4}\frac{\left[(\kappa_A(1-\lambda_A)\right]^2+\omega^2}{\left[(\kappa_A(1+\lambda_A)\right]^2+\omega^2}\,, \quad \left|\Delta\mathcal{E}_A^Y(\omega)\right|^2 = \frac{1}{4}\frac{\left[(\kappa_A(1+\lambda_A)\right]^2+\omega^2}{\left[(\kappa_A(1-\lambda_A)\right]^2+\omega^2} \tag{5.34a}$$

and

$$\left|\Delta\mathcal{E}_B^X(\omega)\right|^2 = \frac{1}{4}\frac{\left[(\kappa_B(1+\lambda_B)\right]^2+\omega^2}{\left[(\kappa_B(1-\lambda_B)\right]^2+\omega^2}\,, \quad \left|\Delta\mathcal{E}_B^Y(\omega)\right|^2 = \frac{1}{4}\frac{\left[(\kappa_B(1-\lambda_B)\right]^2+\omega^2}{\left[(\kappa_B(1+\lambda_B)\right]^2+\omega^2}\,. \tag{5.34b}$$

Letting $\xi = A$ to be precise, Fig. 5.1 (a) and (b) plots the X- and Y-quadrature intensities given by (5.32). The variance of the squeezed quadrature diminishes as the resonant frequency ($\omega = 0$) is approached. Taking our measure of the spread in frequency for $|\Delta\mathcal{E}_A^X(\omega)|^2$ to be given by the bandwidth $B\bar{W}$ defined as [6]

$$\left|\Delta\mathcal{E}_A^X(B\bar{W}/2)\right|^2 \equiv \frac{1}{2}\left[\frac{1}{4} - \left|\Delta\mathcal{E}_A^X(0)\right|^2\right]\,, \tag{5.35}$$

squeezing is most pronounced within the bandwidth $B\bar{W} \approx 4\kappa$ for $\lambda_A \longrightarrow 1$. As illustrated by Fig. 5.1, and Fig. 5.2 (b) where the X-quadrature intensity is plotted against λ_A for the resonant mode, squeezing increases with increasing pump parameter. One observes that $\left|d\left|\Delta\mathcal{E}_A^X(\bar{\omega})\right|^2/d\lambda_A\right|$ is largest in the range $0 < \lambda_A < 0.4$. For pump parameter values beyond 0.4, there is less decrease in $\left|\Delta\mathcal{E}_A^X(\bar{\omega})\right|^2$ per unit increase in λ_A. It can now be seen that perfect squeezing is restricted to the resonant mode and rather stifled by the required infinite variance of the other quadrature; it is only possible if one has an infinite supply of pump photons, i.e. infinite energy. Finally, (5.19) up to (5.30) reveals that squeezing is "wavicle"; i.e., is strikingly comprehensible in terms of the wave description. Perfect, on resonance squeezing of the radiated field may be interpreted as a result of destructive

[6] Equation (5.35) *is* defined for ω and not $\bar{\omega}$.

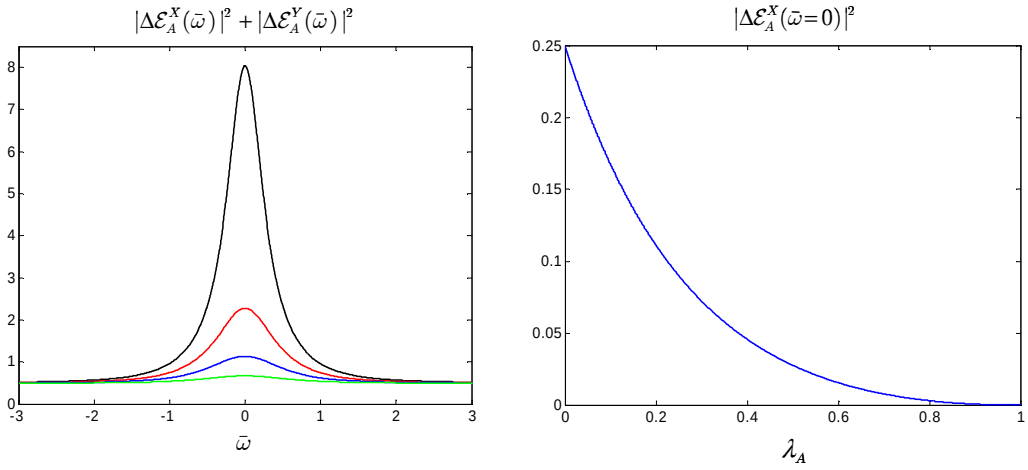

(a) (b)

Fig. 5.2: (a) The optical spectrum. The total power spectral density tends to $|\Delta\mathcal{E}_A^Y(\bar{\omega})|^2$ for large values of the squeezing bandwidth and pump parameter. (b) The X-quadrature variance displays impeded noise suppression (i.e. the gradient of $|\Delta\mathcal{E}_A^Y(\bar{\omega})|^2$ decreases) for $\lambda_A > 0.4$,.

interference between the input and intra-cavity modes:

$$\frac{1}{2}\left\{\tilde{\Lambda}_A(0) + \left[\tilde{\Lambda}_A(0)\right]^*\right\} = \sqrt{\frac{c}{L}}\, x_A(0) + \sqrt{2\kappa}\, X_A(0) = 0\,. \tag{5.36}$$

Continuing with the derivation of the teleported squeezing spectrum for the X-quadrature from (5.26), which now completely determines (5.24) and hence the integral given by (5.23), the important factors in (5.24) follow straightforwardly as

$$\left\langle g(\omega)\left[\sqrt{\frac{c}{L}}\, x_A(\omega) + \sqrt{2\kappa}\, X_A(\omega)\right] g(\omega')\, \bar{\mathcal{I}}_1(\omega')\right\rangle = \frac{1}{4}\,\Omega_A^X(\omega,\omega')\, g(\omega)\, \delta(\omega-\omega')\,, \tag{5.37a}$$

$$\left\langle g(\omega)\left[\sqrt{\frac{c}{L}}\, x_B(\omega) + \sqrt{2\kappa}\, X_B(\omega)\right] g(\omega')\, \bar{\mathcal{I}}_1(\omega')\right\rangle = \frac{1}{4}\,\Omega_B^X(\omega,\omega')\, g(\omega)\, \delta(\omega-\omega')\,. \tag{5.37b}$$

Taking the complex conjugate and letting $\omega \longrightarrow \omega'$ we obtain,

$$\left\langle g(\omega)\left[\bar{\mathcal{I}}_1(\omega)\right]^* g(\omega')\left[\sqrt{\frac{c}{L}}\, x_A(\omega') + \sqrt{2\kappa}\, X_A(\omega')\right]\right\rangle = \frac{1}{4}\left[\Omega_A^X(\omega,\omega')\right]^* g(\omega)\, \delta(\omega-\omega')\,, \tag{5.37c}$$

$$\left\langle g(\omega)\left[\bar{\mathcal{I}}_1(\omega)\right]^* g(\omega')\left[\sqrt{\frac{c}{L}}\, x_B(\omega') + \sqrt{2\kappa}\, X_B(\omega')\right]\right\rangle = \frac{1}{4}\left[\Omega_B^X(\omega,\omega')\right]^* g(\omega)\, \delta(\omega-\omega')\,, \tag{5.37d}$$

$$\Big\langle g(\omega)\left[\bar{\mathcal{I}}_1(\omega)\right]^* g(\omega')\,\bar{\mathcal{I}}_1(\omega')\Big\rangle$$
$$= \frac{1}{4}\left[2\Omega^X_{in}(\omega,\omega') + \Omega^X_A(\omega,\omega') + \Omega^X_B(\omega,\omega')\right] g(\omega)\,\delta(\omega-\omega')\,. \tag{5.37e}$$

Gathering together equations (5.37), the non-zero terms in (5.24) are

$$\begin{aligned}
&\Big\langle g(\omega)\left[\bar{\mathcal{E}}^X_{S3}(\omega)\right]^* g(\omega')\,\bar{\mathcal{E}}^X_{S3}(\omega')\Big\rangle \\
&= \frac{1}{2}\Bigg\{ \left\langle g(\omega)\left[\sqrt{\frac{c}{L}}\,x_A(\omega)+\sqrt{2\kappa}\,X_A(\omega)\right]^* g(\omega')\left[\sqrt{\frac{c}{L}}\,x_A(\omega')+\sqrt{2\kappa}\,X_A(\omega')\right]\right\rangle \\
&\quad + \left\langle g(\omega)\left[\sqrt{\frac{c}{L}}\,x_A(\omega)+\sqrt{2\kappa}\,X_A(\omega)\right]^* g(\omega')\,\bar{\mathcal{I}}_1(\omega')\right\rangle \frac{G_1\big|\bar{\mathcal{E}}_{l1}\big|\,n_1\kappa}{n_1\kappa - i\omega'} \\
&\quad + \left\langle g(\omega)\left[\sqrt{\frac{c}{L}}\,x_B(\omega)+\sqrt{2\kappa}\,X_B(\omega)\right]^* g(\omega')\left[\sqrt{\frac{c}{L}}\,x_B(\omega')+\sqrt{2\kappa}\,X_B(\omega')\right]\right\rangle \\
&\quad - \left\langle g(\omega)\left[\sqrt{\frac{c}{L}}\,x_B(\omega)+\sqrt{2\kappa}\,X_B(\omega)\right]^* g(\omega')\,\bar{\mathcal{I}}_1(\omega')\right\rangle \frac{G_1\big|\bar{\mathcal{E}}_{l1}\big|\,n_1\kappa}{n_1\kappa - i\omega'} \\
&\quad + \left\langle g(\omega)\left[\bar{\mathcal{I}}_1(\omega)\right]^* g(\omega')\left[\sqrt{\frac{c}{L}}\,x_A(\omega')+\sqrt{2\kappa}\,X_A(\omega')\right]\right\rangle \frac{G_1\big|\bar{\mathcal{E}}_{l1}\big|\,n_1\kappa}{n_1\kappa + i\omega} \\
&\quad - \left\langle g(\omega)\left[\bar{\mathcal{I}}_1(\omega)\right]^* g(\omega')\left[\sqrt{\frac{c}{L}}\,x_B(\omega')+\sqrt{2\kappa}\,X_B(\omega')\right]\right\rangle \frac{G_1\big|\bar{\mathcal{E}}_{l1}\big|\,n_1\kappa}{n_1\kappa + i\omega} \\
&\quad + \left\langle g(\omega)\left[\bar{\mathcal{I}}_1(\omega)\right]^* g(\omega')\,\bar{\mathcal{I}}_1(\omega')\right\rangle \frac{(G_1\big|\bar{\mathcal{E}}_{l1}\big|\,n_1\kappa)^2}{(n_1\kappa+i\omega)(n_1\kappa-i\omega')}\Bigg\}
\end{aligned}$$

$$\begin{aligned}
&= \frac{1}{2}\Bigg\{ \Omega^X_A(\omega,\omega') + \Omega^X_B(\omega,\omega') + \frac{G_1\big|\bar{\mathcal{E}}_{l1}\big|\,n_1\kappa}{n_1\kappa - i\omega'}\left[\Omega^X_A(\omega,\omega') - \Omega^X_B(\omega,\omega')\right] \\
&\quad + \frac{G_1\big|\bar{\mathcal{E}}_{l1}\big|\,n_1\kappa}{n_1\kappa + i\omega}\left[\left[\Omega^X_A(\omega,\omega')\right]^* - \left[\Omega^X_B(\omega,\omega')\right]^*\right] \\
&\quad + \frac{(G_1\big|\bar{\mathcal{E}}_{l1}\big|\,n_1\kappa)^2}{(n_1\kappa+i\omega)(n_1\kappa-i\omega')}\left[2\Omega^X_I(\omega,\omega') + \Omega^X_A(\omega,\omega') + \Omega^X_B(\omega,\omega')\right]\Bigg\}\frac{g(\omega)\,\delta(\omega-\omega')}{4}\,.
\end{aligned} \tag{5.38}$$

We are almost finished, since all that is required is to substitute (5.38) into (5.23) and integrate over either ω or ω'. This will give us Bob's output field. To explore bandwidth effects however, it is then necessary to account for filtering in Victor's detection. From (4.45) and (5.22a), the filtered current in terms of the modes at Bob's location gives

$$\begin{aligned}
\Big\langle\left[\mathcal{I}^F_3(t)\right]^* \mathcal{I}^F_3(t+\tau)\Big\rangle &= 4\,G_3^2\left|\bar{\mathcal{E}}_{l3}\right|^2 \int_{-\infty}^{+\infty}\int_{-\infty}^{+\infty}\Big\langle g(\omega)\left[\bar{\mathcal{E}}^X_{S3}(\omega)\right]^* g(\omega')\,\bar{\mathcal{E}}^X_{S3}(\omega')\Big\rangle \\
&\quad\times\frac{(n_3\kappa)^2}{(n_3\kappa+i\omega)(n_3\kappa-i\omega')}\,e^{-i(\omega'-\omega)t}\,e^{-i\omega'\tau}d\omega\,d\omega'\,.
\end{aligned} \tag{5.39}$$

Substituting the density of modes, (5.38) into (5.39) and integrating with respect to ω'; we assert Victor's squeezing spectrum is given by

$$\left|\Delta\mathcal{E}^{XF}_{S3}(\omega)\right|^2 = \frac{1}{2}\left\{\left[\bar{\Omega}^X_A(\omega)+\bar{\Omega}^X_B(\omega)\right] + \frac{2\,G_1\left|\bar{\mathcal{E}}_{l1}\right|(n_1\kappa)^2}{(n_1\kappa)^2+\omega^2}\left[\bar{\Omega}^X_A(\omega)-\bar{\Omega}^X_B(\omega)\right] + \frac{(G_1\left|\bar{\mathcal{E}}_{l1}\right|n_1\kappa)^2}{(n_1\kappa)^2+\omega^2}\left[2\bar{\Omega}^X_I(\omega)+\bar{\Omega}^X_A(\omega)+\bar{\Omega}^X_B(\omega)\right]\right\}\frac{(G_3\left|\bar{\mathcal{E}}_{l3}\right|n_3\kappa)^2}{(n_3\kappa)^2+\omega^2}\,. \tag{5.40}$$

Equation (5.40) is our primary result describing broadband teleportation. The form of (5.40) is sensible when we consider how the energy of the optical fields is distributed within the teleporter (Fig. 3.1) and how the different stages of filtering are organized. The Lorentzian appearing outside the curly braces is the intensity transfer function for Victor's homodyne filter. The first square bracket term is simply the intensity sent directly to Bob from the entanglement source. The last collection of terms in (5.40) is the filtered power spectrum of Alice's field $\mathcal{E}^X_{S1}(t)$, which of course must turn up here as Bob's displacement of $\mathcal{E}_{B'}(t)$. Note the coefficient of $\bar{\Omega}^X_I(\omega)$ is twice that for $\left[\bar{\Omega}^X_A(\omega)+\bar{\Omega}^X_B(\omega)\right]$, as it should due to energy division through the beam-splitters.

The second square bracket term in (5.40) arises from the cross terms in (5.38). First, the minus sign between $\bar{\Omega}^X_A(\omega)$ and $\bar{\Omega}^X_B(\omega)$ arises from the beam-splitter transformation for amplitudes $\mathcal{E}_A(t)$ and $\mathcal{E}_B(t)$, and secondly; in passing from (5.39) to (5.40), the cross terms in (5.38) add to give us a factor of two appearing in front of $\left[\bar{\Omega}^X_A(\omega)-\bar{\Omega}^X_B(\omega)\right]$. These two features, along with unit-gain, provide us with an explanation of broadband teleportation.

To obtain the Y-quadrature spectrum $\left|\Delta\bar{\mathcal{E}}^{YF}_{S3}(\omega)\right|^2$, we recall that the real and imaginary parts of $\mathcal{E}_A(t)$ and $\mathcal{E}_B(t)$ are squeezed symmetrically. Reducing the fluctuations of $\mathcal{E}^X_A(t)$ will simultaneously reduce the fluctuations of $\mathcal{E}^Y_B(t)$ by the same amount. This amounts to the following equalities for the intensities

$$\bar{\Omega}^X_A(\omega)=\bar{\Omega}^Y_B(\omega)\,,\quad \bar{\Omega}^X_B(\omega)=\bar{\Omega}^Y_A(\omega)\,. \tag{5.41}$$

Since the input field $\mathcal{E}_I(t)$ is squeezed independently of the entanglement source we make the replacement

$$\bar{\Omega}^X_I(\omega)\longrightarrow\bar{\Omega}^Y_I(\omega)\equiv\frac{\left[(\kappa_I(1\pm\lambda_I)\right]^2+\omega^2}{\left[(\kappa_I(1\mp\lambda_I)\right]^2+\omega^2}\,. \tag{5.42}$$

Lastly, noting that it is $\mathcal{I}^F_2(t)$ which contributes to $\mathcal{E}^Y_{S3}(t)$, we require another replacement in the subscripts of (5.40), namely $1\longrightarrow 2$. With these modifications the Y-quadrature spectrum seen by Victor is

$$\left|\Delta\mathcal{E}^{YF}_{S3}(\omega)\right|^2 = \frac{1}{2}\left\{\left[\bar{\Omega}^Y_A(\omega)+\bar{\Omega}^Y_B(\omega)\right] - \frac{2\,G_2\left|\bar{\mathcal{E}}_{l2}\right|(n_2\kappa)^2}{(n_2\kappa)^2+\omega^2}\left[\bar{\Omega}^Y_A(\omega)-\bar{\Omega}^Y_B(\omega)\right] + \frac{(G_2\left|\bar{\mathcal{E}}_{l2}\right|n_2\kappa)^2}{(n_2\kappa)^2+\omega^2}\left[2\bar{\Omega}^Y_I(\omega)+\bar{\Omega}^Y_A(\omega)+\bar{\Omega}^Y_B(\omega)\right]\right\}\frac{(G_3\left|\bar{\mathcal{E}}_{l3}\right|n_3\kappa)^2}{(n_3\kappa)^2+\omega^2}\,. \tag{5.43}$$

Equivalent comments to those regarding (5.40) can be made about (5.43).[7] Note that for $\lambda_I = 0$, (5.41) reproduces the coherent state property,

$$\left|\Delta\mathcal{E}_{S3}^{XF}(\omega)\right|^2 = \left|\Delta\mathcal{E}_{S3}^{YF}(\omega)\right|^2 \ . \tag{5.44}$$

5.3 Verification — Broadband Teleportation

5.3.1 Quantifying Teleportation

A discussion of teleportation necessitates one to introduce a measure for the quality of teleportation. As mentioned in the preface, we will not use the fidelity defined by the quantum information community [69], [70]. Broadband teleportation requires as large a range of frequencies over which the teleported field is equal to the input as possible. In general this is not sufficient to quantify the quality of teleportation since frequency components closest to $\omega = 0$ (remembering that ω is the deviation from the physical frequency $\omega_{\rm C}$) are the most significant. It is thus possible to consider a scenario where in a spectral range δ that excludes $\omega = 0$, one finds

$$\left|\Delta\mathcal{E}_{S3}^{X}(\omega)\right|^2 = \frac{1}{4}\,\bar{\Omega}_I^X(\omega)\ , \quad \left|\Delta\mathcal{E}_{S3}^{Y}(\omega)\right|^2 = \frac{1}{4}\,\bar{\Omega}_I^Y(\omega) \quad \forall\ \omega \in \delta\ , \tag{5.45a}$$

but the output still bears less resemblance to the input than the situation given by

$$\left|\Delta\mathcal{E}_{S3}^{X}(\omega)\right|^2 = \frac{1}{4}\,\bar{\Omega}_I^X(\omega)\ , \quad \left|\Delta\mathcal{E}_{S3}^{Y}(\omega)\right|^2 = \frac{1}{4}\,\bar{\Omega}_I^Y(\omega) \quad \forall\ \omega \in \vartheta \tag{5.45b}$$

where $\delta > \vartheta$ and $\omega = 0 \in \vartheta$. A possible way of accurately accounting for the quality of teleportation is to consider some weighted distance measure between the teleported field and the input, with the resonant mode carrying the highest weight and weights decrease as one moves away from the resonant mode. Our analysis will not involve ambiguous situations where such a measure is required. In any comparison we make below, the quality of teleportation will always be judged based on the closeness of $\left|\Delta\mathcal{E}_{S3}^{X}(\omega)\right|^2$ to $\bar{\Omega}_I^X(\omega)/4$ and $\left|\Delta\mathcal{E}_{S3}^{Y}(\omega)\right|^2$ to $\bar{\Omega}_I^Y(\omega)/4$. In the following only filtered fields are plotted, i.e. equations (5.40) and (5.43) are compared with the input quadratures passed through a filter with the same bandwidth specified by n_3.

5.3.2 Noise Reduction

Single Mode Teleportation

Do equations (5.40) and (5.43) reproduce ideal teleportation as described in Chap. 3 ? If we demand the conditions of unit-gain[8], infinite squeezing ($\lambda_A = \lambda_B \longrightarrow 1$), and no filtering whatsoever ($n_j \longrightarrow \infty$), then the squeezing spectra given by (5.40) and (5.43) approach those of the input for the resonant mode,

$$\left|\Delta\mathcal{E}_{S3}^{XF}(0)\right|^2 \longrightarrow \bar{\Omega}_I^X(0)\ , \qquad \left|\Delta\mathcal{E}_{S3}^{YF}(0)\right|^2 \longrightarrow \bar{\Omega}_I^Y(0)\ . \tag{5.46}$$

[7] Note that should one choose to let cavity S_B squeeze the X-quadrature of its vacuum input instead of S_A then we may let $\lambda_B \longrightarrow -\lambda_B$ and define $\bar{\Omega}_B^X(\omega) \equiv \left\{[(\kappa(1-\lambda_B)]^2 + \omega^2\right\} / \left\{[(\kappa(1+\lambda_B)]^2 + \omega^2\right\}$ in (5.40) as the X-quadrature spectrum coming directly out of S_B.

[8] Excluding Victor, this may all, or partially be left to Bob. We have divided the job into two parts through the introduction of G_j and the $1/\sqrt{2}$ in (4.42).

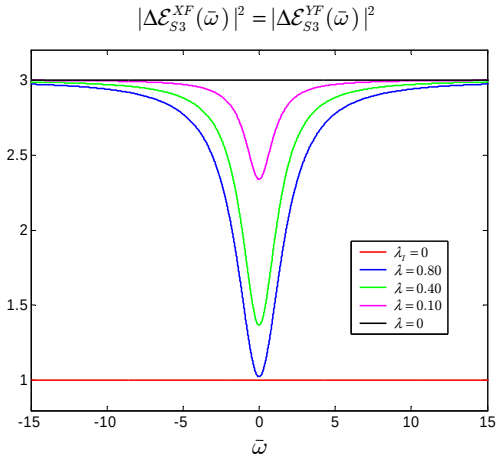

Fig. 5.3: Teleported vacuum modes for different levels of EPR correlations. The red curve is the input spectrum of squeezing and the black curve is the teleported spectrum.

Teleportation is intrinsically multimode, and perfect teleportation is an impossibility dictated by the finite squeezing bandwidth $B\bar{W}$ and our inability to produce unit pump parameters.

Multimode Teleportation

We consider (5.40) and (5.43) with $\lambda_A = \lambda_B \equiv \lambda$, $\kappa_I = \kappa$, and under the conditions of unit-gain and no filtering. Fig. 5.3 displays results for teleportation of a pure coherent vacuum, for which (5.40) and (5.43) are identical. Similarly Fig. 5.4 displays results for various vacuum squeezed states at the input.

With no squeezing applied to the fields distributed to Alice and Bob, the shape of $|\Delta\mathcal{E}_{S3}^{XF}(\omega)|^2$ follows $\bar{\Omega}_I^X(\omega)/4$. In fact, the output noise level is three times that of the input across all frequencies, shown by the separation between the black curve and red curve in Fig. 5.3 and Fig. 5.4. Squeezing serves as a method of noise reduction whereby the modes proximate to (and including) the resonant are driven closer and closer to the input as λ approaches one.

Given the constancy in the separation between the output and input X-quadrature spectra, the right column of Fig. 5.4 might suggest that teleportation becomes better when $\mathcal{E}_I(t)$ has a more intense Y-quadrature. By our measure for the quality of teleportation it is better but it is not because of the teleportation protocol itself. One may think of the red line in the right column of Fig. 5.4 as the optical spectrum of an input coherent state. Thus going down the right column from Fig. 5.4 (a) to (c) is equivalent to teleporting a pure coherent state ($\lambda_I = 0$) whose distance away from the phase-space origin, given by its average photon number, increases while its vacuum fluctuations remain constant. Hence if we return to the case of teleporting a squeezed state whose X- and Y-quadratures are shown by Fig. 5.4, the resemblance of the output field to the input increases as a result of the input becoming more and more defined, i.e. classical. In this case, one would not need to pump so strenuously to achieve the same quality of teleportation. For our squeezed vacuum field input, that energy

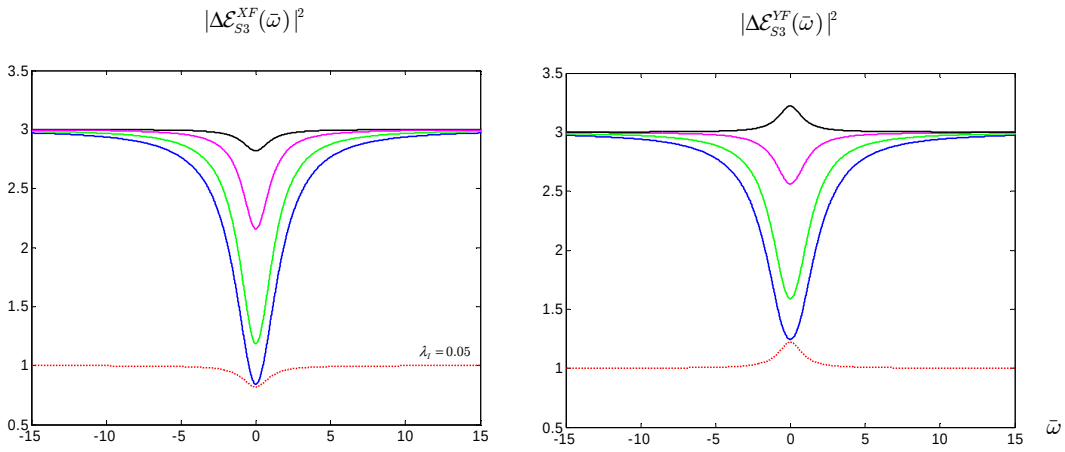

(a)

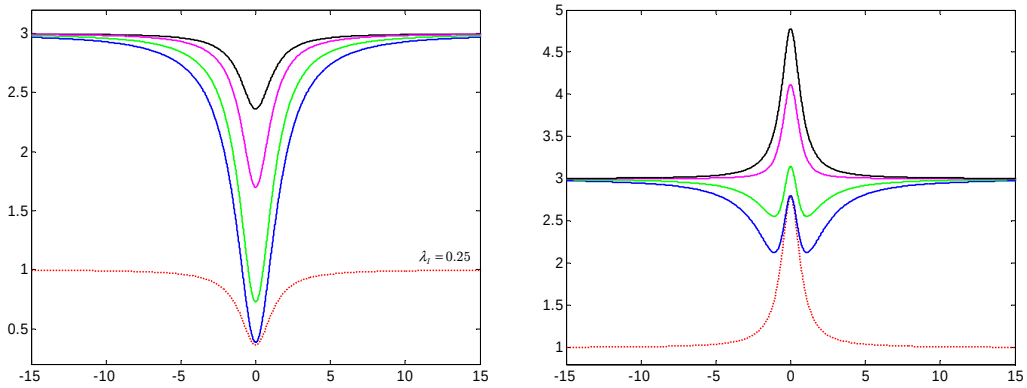

(b)

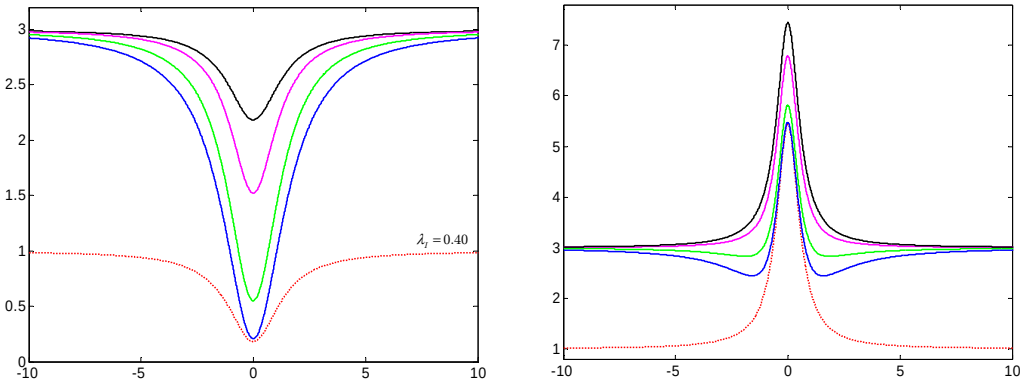

(c)

Fig. 5.4: Teleportation of squeezed vacuum for various degrees of squeezing denoted by λ_I. For concrete analysis, the input is assumed to squeeze the X-quadrature. The same colour key for λ as in Fig. 5.3 applies.

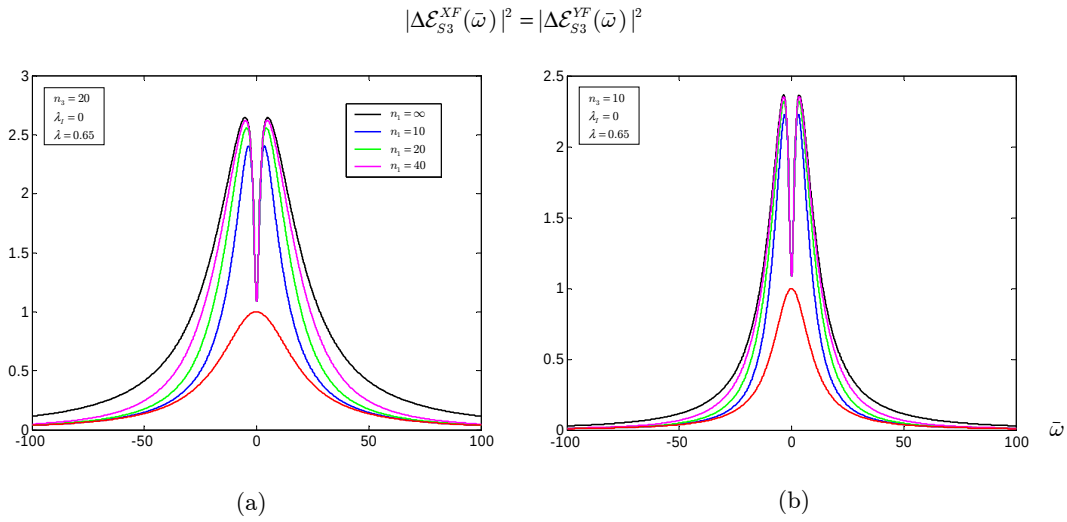

Fig. 5.5: Effects of Alice's filter bandwidth for an unsqueezed input given two different filtering bandwidths at Victor's location. Alice filters symmetrically, $n_1 = n_2$. For the purpose of illustration, Victor has not set a bandwidth as narrow as he should. The same colour code applies to both (a) and (b).

is interpreted to constitute pure statistical uncertainty instead of an increase in photons per mode.

5.3.3 Bandwidth Effects

We discuss the role of bandwidths in teleportation.

Filtering Bandwidths

Teleportation of unsqueezed vacuum modes with applied filtering for constant squeezing power are shown in Fig. 5.5. Noticeably different to Fig. 5.3 or 5.4 are the additional decaying wings, approaching zero for large deviations from resonance. This is simply provided by the asymptotic behaviour of the Lorentzian filters. The black curve in Fig. 5.5 is purely Victor's filtering, and thus for all non-infinite bandwidths set by Alice the output wings must lie within the red and black ones. This is shown for two values of Victor's filter bandwidth.

Passing from Fig. 5.5 (a) to (b) evidently retains the noise power on resonance while lower noise levels appear for all $\bar{\omega} > 0$, or $\bar{\omega} < 0$ given the same degree of filtering by Alice. Mathematically this is expected since we have centred all filtering functions on $\bar{\omega} = 0$; at which point they are unity, and beyond which point they decay quicker for narrower bandwidths. Physically, the result of Fig. 5.5 (b) shows a closer resemblance to the input because Victor has filtered out more noise, particularly significant are those introduced by Bob's displacement of $\mathcal{E}_{B'}(t)$. Victor should look at modes as close to $\bar{\omega} = 0$ as he can since it is only the modes near $\bar{\omega} = 0$ that benefit from the squeezing. There is no bound as to how narrow Victor should set his bandwidth since the resource of squeezing has already been used. However, Alice should be warned not to filter too severely which would degrade the signal-to-noise ratio (for the general case of teleporting arbitrary coherent states) reaching Victor by restricting squeezing to act over a lesser number of modes. In particular, Alice

should set $n_1 > 4$ in the limit of infinite squeezing, since the squeezing bandwidth $B\bar{W}$ was estimated to be 4κ for $\lambda \longrightarrow 1$ from (5.35).

Squeezing Bandwidth

We shall return to teleporting a squeezed vacuum state and be advised by the salient parameter (not to be confused with the density of modes)

$$g \equiv \frac{\kappa_I}{\kappa} \,, \tag{5.47}$$

of bandwidth effects of our EPR source, i.e the squeezing bandwidth of S_A and S_B. We plot in Fig. 5.6, when $\kappa_I = \kappa$, ceteris paribus. Choices from $\kappa = 10\kappa_I$ (Fig. 5.7) to $\kappa = \kappa_I/10$ (Fig. 5.8) are shown below. All plots have the parameter values shown in the legend of Fig. 5.6. It is perspicuous in both the X- and Y-quadratures that the input modes begin to recede from the output as κ diminishes. This is expected since cavity damping rates of S_A and S_B smaller than that for S_I constricts the entanglement source to squeeze over a *relatively* small spectral region, degrading the overlap between output and input. Increasing κ ($g < 1$) then mitigates the shortage of noise reduction per mode suffered by the teleportation protocol, allowing the blue curve to catch up to the red curve.

It is interesting to note the dip in the Y-quadrature for $g = 10$. Fields $\mathcal{E}_{A'}(t)$ and $\mathcal{E}_{B'}(t)$ are no longer a valuable entanglement resource except for the resonant mode, which will always experience the same strength of squeezing. The closeness seen between the output and input for $\bar{\omega} = 0$ will be preserved for any residual damping of S_A and S_B.

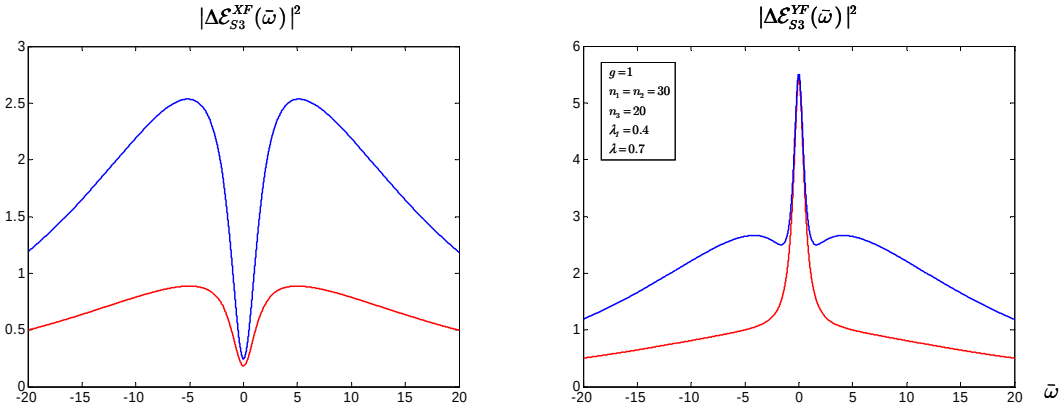

Fig. 5.6: Effects of squeezing bandwidth at $g = 1$ for the parameter values shown in the legend, which are kept constant.

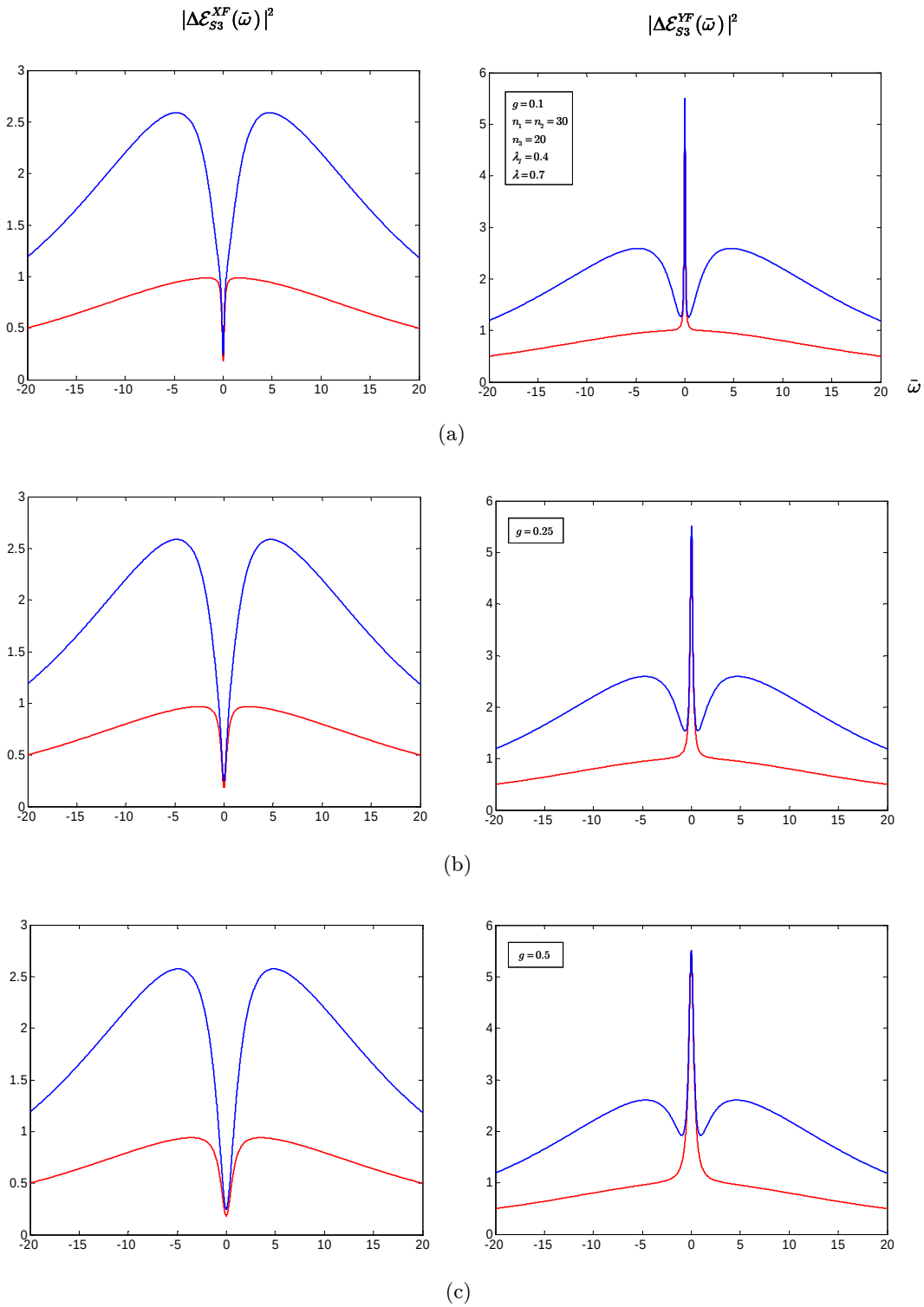

Fig. 5.7: Effects of squeezing bandwidth for $g < 1$.

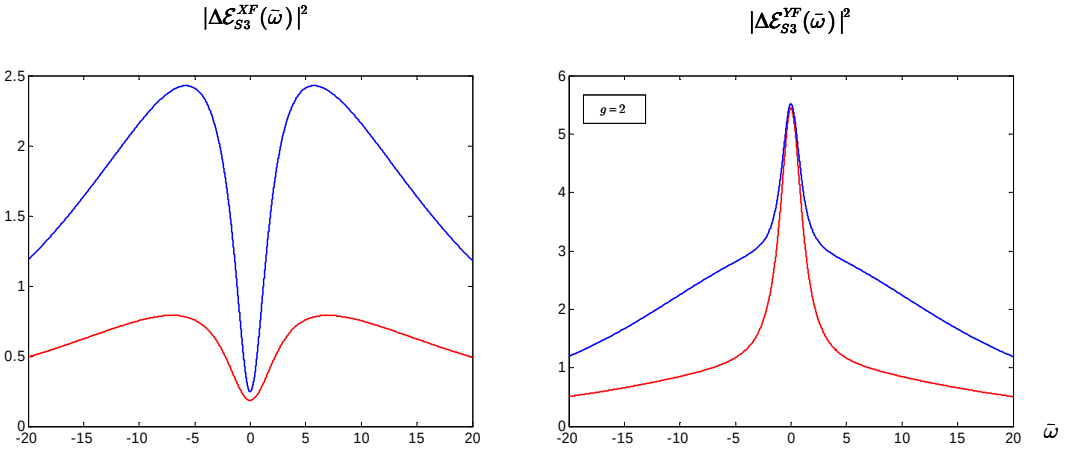

(a)

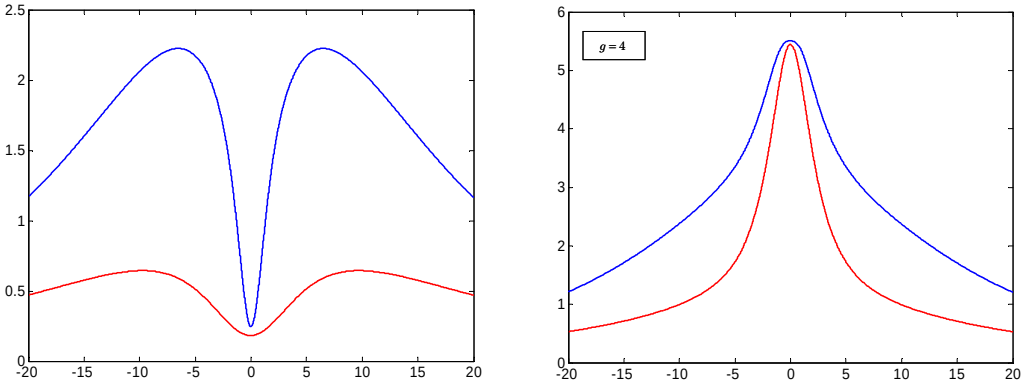

(b)

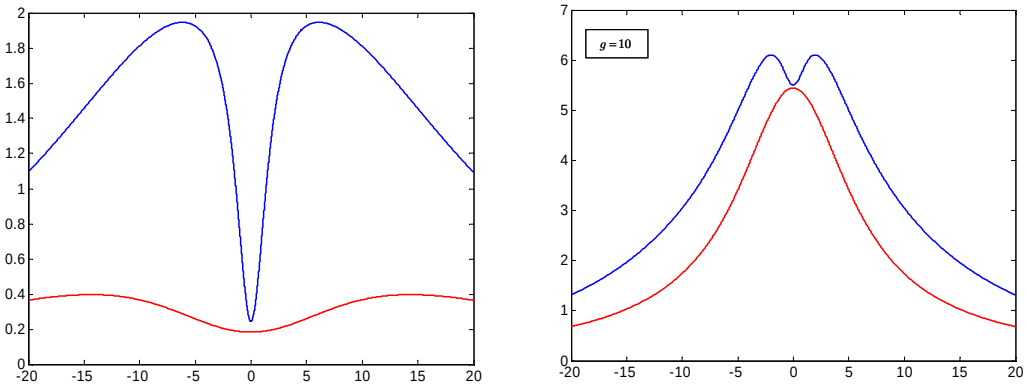

(c)

Fig. 5.8: Effects of squeezing bandwidth for $g > 1$.

5.4 Stochastic Electrodynamics — A Symmetrically Ordered Approach.

As promised, we now digress slightly to demonstrate that SED corresponds to operator averages calculated in the Wigner representation, underlining its failure to account for measurements characterized by a set of normally ordered field operators. Consider the optical spectrum of a coherent state squeezed in the Y-quadrature,

$$\left\langle \hat{\mathcal{E}}^\dagger(t)\,\hat{\mathcal{E}}(t+\tau)\right\rangle = \int_{-\infty}^{+\infty}\int_{-\infty}^{+\infty}\left\langle g(\omega)\hat{\Lambda}^\dagger(\omega)\,g(\omega')\hat{\Lambda}(\omega')\right\rangle e^{i\omega t}\,e^{-i\omega'(t+\tau)}\,d\omega\,d\omega' \tag{5.48}$$

where $\hat{\Lambda}(\omega)$ is defined by (4.22) in operator form. The annihilation and creation operators for the intra-cavity modes may be solved in terms of the external modes from (5.17). After some algebra they are,

$$\hat{\mathcal{A}}(\omega) = \sqrt{\frac{2\kappa c}{L}}\left[\frac{\hat{\bar{f}}(\omega)\,(\kappa-i\omega)+\kappa\lambda\hat{\bar{f}}^\dagger(-\omega)}{(\kappa\lambda)^2-(\kappa-i\omega)^2}\right]. \tag{5.49}$$

With the constants defined by

$$\Upsilon_a(\omega) \equiv \sqrt{\frac{c}{L}}\left[1+\frac{(2\kappa)(\kappa+i\omega)}{(\kappa\lambda)^2-(\kappa-i\omega)^2}\right], \tag{5.50a}$$

$$\Upsilon_b(\omega) \equiv \sqrt{\frac{c}{L}}\left[\frac{(2\kappa)(\kappa\lambda)}{(\kappa\lambda)^2-(\kappa+i\omega)^2}\right], \tag{5.50b}$$

and together with (5.49), the integrand of (5.48) may be written as

$$\begin{aligned}
&\left\langle g(\omega)\hat{\Lambda}^\dagger(\omega)\,g(\omega')\hat{\Lambda}(\omega')\right\rangle \\
&\quad= \left\langle g(\omega)\left[\Upsilon_a^*(\omega)\hat{\bar{f}}^\dagger(\omega)+\Upsilon_b^*(\omega)\hat{\bar{f}}(-\omega)\right]g(\omega')\left[\Upsilon_a(\omega')\hat{\bar{f}}(\omega')+\Upsilon_b(\omega')\hat{\bar{f}}^\dagger(-\omega')\right]\right\rangle \\
&\quad= \Upsilon_a^*(\omega)\Upsilon_a(\omega')\left\langle g(\omega)\hat{\bar{f}}^\dagger(\omega)\,g(\omega')\hat{\bar{f}}(\omega')\right\rangle + \Upsilon_b^*(\omega)\Upsilon_b(\omega')\left\langle g(\omega')\hat{\bar{f}}^\dagger(-\omega')\,g(\omega)\hat{\bar{f}}(-\omega)\right\rangle \\
&\qquad+ \Upsilon_b^*(\omega)\Upsilon_b(\omega')\,g(\omega)\,\delta(\omega-\omega').
\end{aligned} \tag{5.51}$$

We have noted the ensemble averages in (5.28), and the commutator of (5.27c) has been used to write the reservoir modes in normal order. For white noise, the field correlation of (5.48) is

$$\begin{aligned}
\left\langle \hat{\mathcal{E}}^\dagger(t)\,\hat{\mathcal{E}}(t+\tau)\right\rangle &= \int_{-\infty}^{+\infty} g(\omega)\left\{\bar{n}\left[\,|\Upsilon_a(\omega)|^2+|\Upsilon_b(\omega)|^2\right]+|\Upsilon_b(\omega)|^2\right\}e^{-i\omega\tau}\,d\omega \\
&= \frac{1}{2\pi}\int_{-\infty}^{+\infty}\left\{\bar{n}+\frac{(2\bar{n}+1)\left[(2\kappa)(\kappa\lambda)\right]^2}{\left[(\kappa\lambda)^2-(\kappa^2-\omega^2)\right]^2+(2\kappa)^2\omega^2}\right\}e^{-i\omega\tau}\,d\omega\,.
\end{aligned} \tag{5.52}$$

Some rather lengthy algebra in (5.52) has been omitted which leads to

$$|\Upsilon_a(\omega)|^2 = \frac{c}{L}\left\{1+\frac{(2\kappa)^2(\kappa\lambda)^2}{\left[(\kappa\lambda)^2-(\kappa^2-\omega^2)\right]^2+(2\kappa)^2\omega^2}\right\}, \tag{5.53a}$$

$$|\Upsilon_b(\omega)|^2 \;=\; \frac{c}{L}\left\{\frac{(2\kappa)^2(\kappa\lambda)^2}{\left[(\kappa\lambda)^2-(\kappa^2-\omega^2)\right]^2+(2\kappa)^2\omega^2}\right\} \tag{5.53b}$$

with the possibility of writing

$$\frac{(2\kappa)^2(\kappa\lambda)^2}{\left[(\kappa\lambda)^2-(\kappa^2-\omega^2)\right]^2+(2\kappa)^2\omega^2} = \frac{\kappa^2\lambda}{\left[\kappa(1-\lambda)\right]^2+\omega^2} - \frac{\kappa^2\lambda}{\left[\kappa(1+\lambda)\right]^2+\omega^2}\;, \tag{5.53c}$$

if one prefers the resemblance to (5.31). Equation (5.52) derives the correct spectrum as measured by a direct photon count,

$$\mathcal{S}_{\rm QM}(\omega) = \bar{n} + \frac{(2\bar{n}+1)\left[(2\kappa)(\kappa\lambda)\right]^2}{\left[(\kappa\lambda)^2-(\kappa^2-\omega^2)\right]^2+(2\kappa)^2\omega^2}\;. \tag{5.54}$$

Stochastic electrodynamics looks at the free field Hamiltonian and adds the zero-point energy per mode by hand to give us the result of (4.27d). In effect, this reproduces a calculation done in the Wigner representation of operator moments on quantizing our field,

$$\begin{aligned}\left\langle g(\omega)\left[\tilde{f}(\omega)\right]^* g(\omega')\tilde{f}(\omega')\right\rangle &= \left\langle g(\omega)\hat{\tilde{f}}^\dagger(\omega)\, g(\omega')\hat{\tilde{f}}(\omega')\right\rangle_W \\ &\equiv \frac{1}{2}\left[\left\langle g(\omega)\hat{\tilde{f}}^\dagger(\omega)\, g(\omega')\hat{\tilde{f}}(\omega')\right\rangle + \left\langle g(\omega)\hat{\tilde{f}}(\omega)\, g(\omega')\hat{\tilde{f}}^\dagger(\omega')\right\rangle\right] \\ &= \bar{n}+\frac{1}{2}\;.\end{aligned} \tag{5.55}$$

Either using (5.55) for field operators, or (4.27d) for complex random variables, SED predicts the observed photon count to be

$$\mathcal{S}_{\rm SED}(\omega) \;=\; \mathcal{S}_{\rm QM}(\omega) + \frac{1}{2}\;, \tag{5.56}$$

where the subscripts "QM" and "SED" are meant to emphasize that it is in a quantum calculation the operator ordering is kept track of, and not simply the difference between a normally ordered calculation to a symmetrically ordered one. One would accept (5.56) based on a realistic interpretation of vacuum fluctuations, i.e. they *do* contribute to photo-electron generation in a photo-detector.

If we return to our discussion of squeezing in Sect. 5.2.1, in particular (5.29), then it would seem plausible that the quadratures of the DPO output can be accounted for classically if

$$\begin{aligned}&\left\langle g(\omega)\left[\sqrt{\frac{c}{L}}\,\hat{x}^\dagger(\omega)+\sqrt{2\kappa}\,\hat{X}^\dagger(\omega)\right] g(\omega')\left[\sqrt{\frac{c}{L}}\,\hat{x}(\omega')+\sqrt{2\kappa}\,\hat{X}(\omega')\right]\right\rangle \\ &\qquad = \left\langle g(\omega)\left[\sqrt{\frac{c}{L}}\,\hat{x}^\dagger(\omega)+\sqrt{2\kappa}\,\hat{X}^\dagger(\omega)\right] g(\omega')\left[\sqrt{\frac{c}{L}}\,\hat{x}(\omega')+\sqrt{2\kappa}\,\hat{X}(\omega')\right]\right\rangle_W\;.\end{aligned} \tag{5.57}$$

Indeed, (5.57) is true since

$$\left[g(\omega)\hat{x}(\omega), g(\omega')\hat{x}^\dagger(\omega')\right] = \left[g(\omega)\hat{X}(\omega), g(\omega')\hat{X}^\dagger(\omega')\right] = 0\;. \tag{5.58}$$

Although SED manages to produce the correct squeezing spectrum, its calculation of the

optical spectrum still remains erroneous,

$$\begin{aligned}\mathcal{S}_{\text{SED}}(\omega) &= \left|\Delta\mathcal{E}_X(\omega)\right|^2 + \left|\Delta\mathcal{E}_Y(\omega)\right|^2 \\ &= \frac{1}{2}\left(\bar{n}+\frac{1}{2}\right)\left\{\frac{\left[\kappa\left(1+\lambda\right)\right]^2+\omega^2}{\left[\kappa\left(1-\lambda\right)\right]^2+\omega^2}+\frac{\left[\kappa\left(1-\lambda\right)\right]^2+\omega^2}{\left[\kappa\left(1+\lambda\right)\right]^2+\omega^2}\right\} \\ &= \mathcal{S}_{\text{QM}}(\omega)+\frac{1}{2}\,. \end{aligned} \tag{5.59}$$

Perhaps the quickest way to see this is to consider the intensity of $\hat{\tilde{\mathcal{E}}}(t) = \hat{\tilde{\mathcal{E}}}_X(t) + i\hat{\tilde{\mathcal{E}}}_Y(t)$, where $\hat{\tilde{\mathcal{E}}}_X(t)$ and $\hat{\tilde{\mathcal{E}}}_Y(t)$ are Hermitian and non-commuting operators,

$$\left\langle \hat{\tilde{\mathcal{E}}}^{\dagger}(t)\,\hat{\tilde{\mathcal{E}}}(t)\right\rangle = \left\langle \left[\hat{\tilde{\mathcal{E}}}_X(t)\right]^2\right\rangle + \left\langle \left[\hat{\tilde{\mathcal{E}}}_Y(t)\right]^2\right\rangle + i\left[\,\hat{\tilde{\mathcal{E}}}_X(t),\hat{\tilde{\mathcal{E}}}_Y(t)\right]\,. \tag{5.60}$$

In the next chapter we use SED to force a calculation required to be done in the normal ordering of operators.

Chapter 6

The Intensity Correlation Function

In the map given by Fig. 3.1, Victor will now perform a direct photon count. The teleported intensity correlation function will now be calculated. This is the second form of verification that we consider.

6.1 The Classical Intensity Correlation Function

In the following we consider the filtered field of Bob's displaced output. The equation of motion for the filtered field is the classical Langevin equation in the absence of non-linearity in the rotating frame,

$$\frac{d\mathcal{E}_{S3}^{F}}{dt} = -(n_3\kappa)\mathcal{E}_{S3}^{F} - i\sqrt{2n_3\kappa}\,\mathcal{E}_{S3}\ . \tag{6.1}$$

To take advantage of the linearity possessed by our teleporter, $\mathcal{E}_{S3}^{F}(t)$ will be written as a sum of three fields labelled as $\mathcal{E}_1(t)$, $\mathcal{E}_2(t)$, and $\mathcal{E}_3(t)$, where each is directly associated to cavities S_I, S_A, and S_B respectively,

$$\mathcal{E}_{S3}^{F}(t) = \underbrace{\left[\mathcal{E}_1^{X}(t) + i\mathcal{E}_1^{Y}(t)\right]}_{\mathcal{E}_1(t)} + \underbrace{\left[\mathcal{E}_2^{X}(t) + i\mathcal{E}_2^{Y}(t)\right]}_{\mathcal{E}_2(t)} + \underbrace{\left[\mathcal{E}_3^{X}(t) + i\mathcal{E}_3^{Y}(t)\right]}_{\mathcal{E}_3(t)}\ . \tag{6.2}$$

With recourse to (4.43) and (4.44), the real and imaginary parts of each field in (6.2) are

$$\mathcal{E}_1^{X}(t) = \int_{-\infty}^{+\infty} g(\omega)\left[\sqrt{\frac{c}{L}}\,x_I(\omega) + \sqrt{2\kappa_I}\,X_I(\omega)\right]\left(\frac{\alpha_1 n_1\kappa}{n_1\kappa - i\omega}\right)\left(\frac{-i\sqrt{2n_3\kappa}}{n_3\kappa - i\omega}\right)e^{-i\omega t}\,d\omega\ , \tag{6.3a}$$

$$\mathcal{E}_1^{Y}(t) = \int_{-\infty}^{+\infty} g(\omega)\left[\sqrt{\frac{c}{L}}\,x_I(\omega) + \sqrt{2\kappa_I}\,X_I(\omega)\right]\left(\frac{\alpha_2 n_2\kappa}{n_2\kappa - i\omega}\right)\left(\frac{-i\sqrt{2n_3\kappa}}{n_3\kappa - i\omega}\right)e^{-i\omega t}\,d\omega\ , \tag{6.3b}$$

$$\mathcal{E}_2^X(t) = \frac{1}{\sqrt{2}} \int_{-\infty}^{+\infty} g(\omega) \left[\sqrt{\frac{c}{L}}\, x_A(\omega) + \sqrt{2\kappa}\, X_A(\omega) \right] \left(1 + \frac{\alpha_1 n_1 \kappa}{n_1\kappa - i\omega} \right) \left(\frac{-i\sqrt{2n_3\kappa}}{n_3\kappa - i\omega} \right) e^{-i\omega t}\, d\omega \,, \tag{6.3c}$$

$$\mathcal{E}_2^Y(t) = \frac{1}{\sqrt{2}} \int_{-\infty}^{+\infty} g(\omega) \left[\sqrt{\frac{c}{L}}\, y_A(\omega) + \sqrt{2\kappa}\, Y_A(\omega) \right] \left(1 - \frac{\alpha_2 n_2 \kappa}{n_2\kappa - i\omega} \right) \left(\frac{-i\sqrt{2n_3\kappa}}{n_3\kappa - i\omega} \right) e^{-i\omega t}\, d\omega \,, \tag{6.3d}$$

$$\mathcal{E}_3^X(t) = \frac{-1}{\sqrt{2}} \int_{-\infty}^{+\infty} g(\omega) \left[\sqrt{\frac{c}{L}}\, x_B(\omega) + \sqrt{2\kappa}\, X_B(\omega) \right] \left(1 - \frac{\alpha_1 n_1 \kappa}{n_1\kappa - i\omega} \right) \left(\frac{-i\sqrt{2n_3\kappa}}{n_3\kappa - i\omega} \right) e^{-i\omega t}\, d\omega \,, \tag{6.3e}$$

$$\mathcal{E}_3^Y(t) = \frac{-1}{\sqrt{2}} \int_{-\infty}^{+\infty} g(\omega) \left[\sqrt{\frac{c}{L}}\, y_B(\omega) + \sqrt{2\kappa}\, Y_B(\omega) \right] \left(1 + \frac{\alpha_2 n_2 \kappa}{n_2\kappa - i\omega} \right) \left(\frac{-i\sqrt{2n_3\kappa}}{n_3\kappa - i\omega} \right) e^{-i\omega t}\, d\omega \,. \tag{6.3f}$$

where $\alpha_1 \equiv G_1|\bar{\mathcal{E}}_{l1}|$ and $\alpha_2 \equiv G_2|\bar{\mathcal{E}}_{l2}|$. To make use of (6.3), the intensity correlation function requires an orderly decomposition into apprehensible terms. Using (6.2), the expansion is as follows,

$$\begin{aligned}
&\Big\langle \left[\mathcal{E}_{S3}^F(t)\right]^* \mathcal{E}_{S3}^F(t) \left[\mathcal{E}_{S3}^F(t+\tau)\right]^* \mathcal{E}_{S3}^F(t+\tau) \Big\rangle \\
&\quad = \Big\langle \left[\mathcal{E}_1(t)\right]^* \left[\mathcal{E}_1(t+\tau)\right]^* \Big\rangle \Big\langle \mathcal{E}_2(t)\, \mathcal{E}_2(t+\tau) \Big\rangle + \Big\langle \left[\mathcal{E}_2(t)\right]^* \left[\mathcal{E}_2(t+\tau)\right]^* \Big\rangle \Big\langle \mathcal{E}_1(t)\, \mathcal{E}_1(t+\tau) \Big\rangle \\
&\qquad + \Big\langle \left[\mathcal{E}_1(t)\right]^* \left[\mathcal{E}_1(t+\tau)\right]^* \Big\rangle \Big\langle \mathcal{E}_3(t)\, \mathcal{E}_3(t+\tau) \Big\rangle + \Big\langle \left[\mathcal{E}_3(t)\right]^* \left[\mathcal{E}_3(t+\tau)\right]^* \Big\rangle \Big\langle \mathcal{E}_1(t)\, \mathcal{E}_1(t+\tau) \Big\rangle \\
&\qquad + \Big\langle \left[\mathcal{E}_2(t)\right]^* \left[\mathcal{E}_2(t+\tau)\right]^* \Big\rangle \Big\langle \mathcal{E}_3(t)\, \mathcal{E}_3(t+\tau) \Big\rangle + \Big\langle \left[\mathcal{E}_3(t)\right]^* \left[\mathcal{E}_3(t+\tau)\right]^* \Big\rangle \Big\langle \mathcal{E}_2(t)\, \mathcal{E}_2(t+\tau) \Big\rangle \\
&\qquad + \Big\langle \left[\mathcal{E}_1(t)\right]^* \mathcal{E}_1(t) \Big\rangle \Big\langle \left[\mathcal{E}_3(t+\tau)\right]^* \mathcal{E}_3(t+\tau) \Big\rangle + \Big\langle \left[\mathcal{E}_3(t)\right]^* \mathcal{E}_3(t) \Big\rangle \Big\langle \left[\mathcal{E}_1(t+\tau)\right]^* \mathcal{E}_1(t+\tau) \Big\rangle \\
&\qquad + \Big\langle \left[\mathcal{E}_1(t)\right]^* \mathcal{E}_1(t) \Big\rangle \Big\langle \left[\mathcal{E}_2(t+\tau)\right]^* \mathcal{E}_2(t+\tau) \Big\rangle + \Big\langle \left[\mathcal{E}_2(t)\right]^* \mathcal{E}_2(t) \Big\rangle \Big\langle \left[\mathcal{E}_1(t+\tau)\right]^* \mathcal{E}_1(t+\tau) \Big\rangle \\
&\qquad + \Big\langle \left[\mathcal{E}_2(t)\right]^* \mathcal{E}_2(t) \Big\rangle \Big\langle \left[\mathcal{E}_3(t+\tau)\right]^* \mathcal{E}_3(t+\tau) \Big\rangle + \Big\langle \left[\mathcal{E}_3(t)\right]^* \mathcal{E}_3(t) \Big\rangle \Big\langle \left[\mathcal{E}_2(t+\tau)\right]^* \mathcal{E}_2(t+\tau) \Big\rangle \\
&\qquad + \Big\langle \left[\mathcal{E}_1(t)\right]^* \mathcal{E}_1(t+\tau) \Big\rangle \Big\langle \mathcal{E}_2(t) \left[\mathcal{E}_2(t+\tau)\right]^* \Big\rangle + \Big\langle \left[\mathcal{E}_2(t)\right]^* \mathcal{E}_2(t+\tau) \Big\rangle \Big\langle \mathcal{E}_1(t) \left[\mathcal{E}_1(t+\tau)\right]^* \Big\rangle \\
&\qquad + \Big\langle \left[\mathcal{E}_1(t)\right]^* \mathcal{E}_1(t+\tau) \Big\rangle \Big\langle \mathcal{E}_3(t) \left[\mathcal{E}_3(t+\tau)\right]^* \Big\rangle + \Big\langle \left[\mathcal{E}_3(t)\right]^* \mathcal{E}_3(t+\tau) \Big\rangle \Big\langle \mathcal{E}_1(t) \left[\mathcal{E}_1(t+\tau)\right]^* \Big\rangle \\
&\qquad + \Big\langle \left[\mathcal{E}_2(t)\right]^* \mathcal{E}_2(t+\tau) \Big\rangle \Big\langle \mathcal{E}_3(t) \left[\mathcal{E}_3(t+\tau)\right]^* \Big\rangle + \Big\langle \left[\mathcal{E}_3(t)\right]^* \mathcal{E}_3(t+\tau) \Big\rangle \Big\langle \mathcal{E}_2(t) \left[\mathcal{E}_2(t+\tau)\right]^* \Big\rangle \\
&\qquad + \Big\langle \left[\mathcal{E}_1(t)\right]^* \mathcal{E}_1(t) \left[\mathcal{E}_1(t+\tau)\right]^* \mathcal{E}_1(t+\tau) \Big\rangle + \Big\langle \left[\mathcal{E}_2(t)\right]^* \mathcal{E}_2(t) \left[\mathcal{E}_2(t+\tau)\right]^* \mathcal{E}_2(t+\tau) \Big\rangle \\
&\qquad + \Big\langle \left[\mathcal{E}_3(t)\right]^* \mathcal{E}_3(t) \left[\mathcal{E}_3(t+\tau)\right]^* \mathcal{E}_3(t+\tau) \Big\rangle \,.
\end{aligned} \tag{6.4}$$

In (6.4) we have noted the statistical independence of $\mathcal{E}_i(t)$ and $\mathcal{E}_j(t)$ for $i, j = 1, 2, 3$ and $i \neq j$. Thus all fourth order terms formed by pairs of fields with $i \neq j$ factorize immediately to products of second order. For example,

$$\Big\langle \left[\mathcal{E}_i(t)\right]^* \mathcal{E}_i(t+\tau)\, \mathcal{E}_j(t) \left[\mathcal{E}_j(t+\tau)\right]^* \Big\rangle = \Big\langle \left[\mathcal{E}_i(t)\right]^* \mathcal{E}_i(t+\tau) \Big\rangle \Big\langle \mathcal{E}_j(t) \left[\mathcal{E}_j(t+\tau)\right]^* \Big\rangle \,. \tag{6.5}$$

Furthermore, the symmetry of the vacuum spectrum deduces all second order correlation functions in (6.4) to be real. More precisely, all ensemble averages between the vacuum quadratures $\left\langle g(\omega)\left[x_\xi(\omega)\right]^* g(\omega')y_\xi(\omega')\right\rangle$ vanish if we note that

$$\left\langle g(\omega)\left[\bar{f}_\xi(\omega)\right]^* g(\omega')\bar{f}_\xi(\omega')\right\rangle = \left\langle g(\omega)\left[\bar{f}_\xi(-\omega)\right]^* g(\omega')\bar{f}_\xi(-\omega')\right\rangle = \frac{1}{2}\, g(\omega)\,\delta(\omega-\omega')\,. \tag{6.6}$$

Consequently the cross terms in a field correlation function such as

$$\begin{aligned}\left\langle \left[\mathcal{E}_j(t)\right]^* \mathcal{E}_j(t+\tau)\right\rangle &= \left\langle \mathcal{E}_j^X(t)\,\mathcal{E}_j^X(t+\tau)\right\rangle + \left\langle \mathcal{E}_j^Y(t)\,\mathcal{E}_j^Y(t+\tau)\right\rangle \\ &\quad + i\left[\left\langle \mathcal{E}_j^X(t)\,\mathcal{E}_j^Y(t+\tau)\right\rangle - \left\langle \mathcal{E}_j^Y(t)\,\mathcal{E}_j^X(t+\tau)\right\rangle\right]\end{aligned} \tag{6.7}$$

are zero. Hence all second order terms in (6.4) are encompassed by

$$\begin{aligned}\left\langle \left[\mathcal{E}_i(t)\right]^* \mathcal{E}_i(t+\tau)\right\rangle &= \left\langle \mathcal{E}_i(t)\left[\mathcal{E}_i(t+\tau)\right]^*\right\rangle \\ &= \left\langle \mathcal{E}_i^X(t)\,\mathcal{E}_i^X(t+\tau)\right\rangle + \left\langle \mathcal{E}_i^Y(t)\,\mathcal{E}_i^Y(t+\tau)\right\rangle, \end{aligned} \tag{6.8a}$$

$$\begin{aligned}\left\langle \left[\mathcal{E}_i(t)\right]^*\left[\mathcal{E}_i(t+\tau)\right]^*\right\rangle &= \left\langle \mathcal{E}_i(t)\,\mathcal{E}_i(t+\tau)\right\rangle \\ &= \left\langle \mathcal{E}_i^X(t)\,\mathcal{E}_i^X(t+\tau)\right\rangle - \left\langle \mathcal{E}_i^Y(t)\,\mathcal{E}_i^Y(t+\tau)\right\rangle. \end{aligned} \tag{6.8b}$$

By virtue of the assumed stationarity of $\tilde{\mathcal{E}}_\xi(t)$, (6.8) are only functions in the variable τ. The intensities in lines four, five and six of (6.4) are then (6.8a) at $\tau = 0$,

$$\begin{aligned}\left\langle \left[\mathcal{E}_i(t)\right]^* \mathcal{E}_i(t)\right\rangle &= \left\langle \left[\mathcal{E}_i(t+\tau)\right]^* \mathcal{E}_i(t+\tau)\right\rangle \\ &= \left\langle \left[\mathcal{E}_i^X(t)\right]^2\right\rangle + \left\langle \left[\mathcal{E}_i^Y(t)\right]^2\right\rangle, \end{aligned} \tag{6.8c}$$

which are constants.

However, the last three terms of (6.4) simply do not submit to factorizations such as (6.5). The Gaussian moment theorem allows us to digest these apparently intractable fourth order terms [71].

Excursion 6.1 The Gaussian moment theorem states that for any set of Gaussian random variables $\{\nu_1, \nu_2, \ldots, \nu_k\}$:

$$\langle \Delta\nu_1 \Delta\nu_2 \cdots \Delta\nu_k\rangle = \sum_{\substack{\text{All } (k-1)!! \\ \text{pairings}}} \langle \Delta\nu_1\Delta\nu_2\rangle \langle \Delta\nu_3\Delta\nu_4\rangle \cdots \langle \Delta\nu_{k-1}\Delta\nu_k\rangle \quad \text{if } k \text{ is an even number}\,,$$

$$\langle \Delta\nu_1 \Delta\nu_2 \cdots \Delta\nu_k\rangle = 0 \quad \text{if } k \text{ is an odd number}\,,$$

where $\Delta\nu_k \equiv \nu_k - \langle\nu_k\rangle$.

Hence we consider the case with $k = 4$,

$$\begin{aligned}\langle \Delta\nu_1\, \Delta\nu_2\, \Delta\nu_3\, \Delta\nu_4\rangle &= \sum_{\substack{\text{All 3!!}\\ \text{pairings}}} \langle \Delta\nu_1\, \Delta\nu_2\rangle\, \langle \Delta\nu_3\, \Delta\nu_4\rangle \\ &= \langle \Delta\nu_1\, \Delta\nu_2\rangle\, \langle \Delta\nu_3\, \Delta\nu_4\rangle + \langle \Delta\nu_1\, \Delta\nu_3\rangle\, \langle \Delta\nu_2 \Delta\, \nu_4\rangle \\ &\quad + \langle \Delta\nu_1\, \Delta\nu_4\rangle\, \langle \Delta\nu_2\, \Delta\nu_3\rangle\ .\end{aligned}$$

Since all fields have zero mean, we obtain

$$\begin{aligned}&\Big\langle\, [\mathcal{E}_i(t)]^*\, \mathcal{E}_i(t)\, [\mathcal{E}_i(t+\tau)]^*\, \mathcal{E}_i(t+\tau)\Big\rangle \\ &\quad = \Big\langle\, [\mathcal{E}_i(t)]^*\, \mathcal{E}_i(t)\Big\rangle\Big\langle\, [\mathcal{E}_i(t+\tau)]^*\, \mathcal{E}_i(t+\tau)\Big\rangle + \Big\langle\, [\mathcal{E}_i(t)]^*\, [\mathcal{E}_i(t+\tau)]^*\, \Big\rangle\Big\langle \mathcal{E}_i(t)\, \mathcal{E}_i(t+\tau)\Big\rangle \\ &\qquad + \Big\langle\, [\mathcal{E}_i(t)]^*\, \mathcal{E}_i(t+\tau)\Big\rangle\Big\langle \mathcal{E}_i(t)\, [\mathcal{E}_i(t+\tau)]^*\, \Big\rangle \\ &\quad = \Big\langle\, [\mathcal{E}_i(t)]^*\, \mathcal{E}_i(t)\Big\rangle^2 + \Big\langle \mathcal{E}_i(t)\, \mathcal{E}_i(t+\tau)\Big\rangle^2 + \Big\langle\, [\mathcal{E}_i(t)]^*\, \mathcal{E}_i(t+\tau)\Big\rangle^2\ . \end{aligned} \tag{6.9}$$

By (6.9) and (6.8), the number of terms in (6.4) quickly reduces. In fact, (6.9) and (6.8) allows us to factorize all second order terms to yield three squared sums:

$$\begin{aligned}&\Big\langle\, \big[\mathcal{E}^F_{S3}(t)\big]^*\, \mathcal{E}^F_{S3}(t)\, \big[\mathcal{E}^F_{S3}(t+\tau)\big]^*\, \mathcal{E}^F_{S3}(t+\tau)\Big\rangle \\ &\qquad = \bigg\{\Big\langle\, [\mathcal{E}_1(t)]^*\, \mathcal{E}_1(t+\tau)\Big\rangle + \Big\langle\, [\mathcal{E}_2(t)]^*\, \mathcal{E}_2(t+\tau)\Big\rangle + \Big\langle\, [\mathcal{E}_3(t)]^*\, \mathcal{E}_3(t+\tau)\Big\rangle\bigg\}^2 \\ &\qquad\quad + \bigg\{\Big\langle \mathcal{E}_1(t)\, \mathcal{E}_1(t+\tau)\Big\rangle + \Big\langle \mathcal{E}_2(t)\, \mathcal{E}_2(t+\tau)\Big\rangle + \Big\langle \mathcal{E}_3(t)\, \mathcal{E}_3(t+\tau)\Big\rangle\bigg\}^2 \\ &\qquad\quad + \bigg\{\Big\langle\, [\mathcal{E}_1(t)]^*\, \mathcal{E}_1(t)\Big\rangle + \Big\langle\, [\mathcal{E}_2(t)]^*\, \mathcal{E}_2(t)\Big\rangle + \Big\langle\, [\mathcal{E}_3(t)]^*\, \mathcal{E}_3(t)\Big\rangle\bigg\}^2\ . \end{aligned} \tag{6.10}$$

This is then more manageably expressible in terms of (6.8),

$$\begin{aligned}&\Big\langle\, \big[\mathcal{E}^F_{S3}(t)\big]^*\, \mathcal{E}^F_{S3}(t)\, \big[\mathcal{E}^F_{S3}(t+\tau)\big]^*\, \mathcal{E}^F_{S3}(t+\tau)\Big\rangle \\ &\qquad = 2\bigg\{\Big[\Big\langle \mathcal{E}^X_1(t)\, \mathcal{E}^X_1(t+\tau)\Big\rangle + \Big\langle \mathcal{E}^X_2(t)\, \mathcal{E}^X_2(t+\tau)\Big\rangle + \Big\langle \mathcal{E}^X_3(t)\, \mathcal{E}^X_3(t+\tau)\Big\rangle\Big]^2 \\ &\qquad\quad + \Big[\Big\langle \mathcal{E}^Y_1(t)\, \mathcal{E}^Y_1(t+\tau)\Big\rangle + \Big\langle \mathcal{E}^Y_2(t)\, \mathcal{E}^Y_2(t+\tau)\Big\rangle + \Big\langle \mathcal{E}^Y_3(t)\, \mathcal{E}^Y_3(t+\tau)\Big\rangle\Big]^2\bigg\} \\ &\qquad\quad + \Big\langle\, \big[\mathcal{E}^X_1(t)\big]^2 + \big[\mathcal{E}^X_2(t)\big]^2 + \big[\mathcal{E}^X_3(t)\big]^2 + \big[\mathcal{E}^Y_1(t)\big]^2 + \big[\mathcal{E}^Y_2(t)\big]^2 + \big[\mathcal{E}^Y_3(t)\big]^2\, \Big\rangle^2\ . \end{aligned} \tag{6.11}$$

It can already be seen that the intensity correlation function will have an offset from zero given by the last sum of constants. Equation (6.11), along with (6.4), is general except for the assumed beam-splitter transformations, hence the $1/\sqrt{2}$ in Bob's phase-space displacement which in part contributes to unit-gain teleportation. It now remains to calculate (6.11) from (6.3). From (6.3), and after some computation, all second order terms may be listed as follows. The X-quadrature field correlations are

$$\Big\langle \mathcal{E}^X_1(t)\, \mathcal{E}^X_1(t+\tau)\Big\rangle = \frac{1}{2\pi}\int_{-\infty}^{+\infty} \bar{\Omega}^X_I(\omega)\bigg\{\frac{(\alpha_1 n_1\kappa)^2}{(n_1\kappa)^2+\omega^2}\bigg\}\bigg\{\frac{2n_3\kappa}{(n_3\kappa)^2+\omega^2}\bigg\}e^{-i\omega\tau}\, d\omega\ , \tag{6.12a}$$

$$\left\langle \mathcal{E}_2^X(t)\,\mathcal{E}_2^X(t+\tau)\right\rangle = \frac{1}{2\pi}\int_{-\infty}^{+\infty}\bar{\Omega}_A^X(\omega)\left\{\frac{[n_1\kappa(1+\alpha_1)]^2+\omega^2}{(n_1\kappa)^2+\omega^2}\right\}\left\{\frac{n_3\kappa}{(n_3\kappa)^2+\omega^2}\right\}e^{-i\omega\tau}\,d\omega\ , \tag{6.12b}$$

$$\left\langle \mathcal{E}_3^X(t)\,\mathcal{E}_3^X(t+\tau)\right\rangle = \frac{1}{2\pi}\int_{-\infty}^{+\infty}\bar{\Omega}_B^X(\omega)\left\{\frac{[n_1\kappa(1-\alpha_1)]^2+\omega^2}{(n_1\kappa)^2+\omega^2}\right\}\left\{\frac{n_3\kappa}{(n_3\kappa)^2+\omega^2}\right\}e^{-i\omega\tau}\,d\omega\ . \tag{6.12c}$$

Similarly for the Y-quadrature, we have

$$\left\langle \mathcal{E}_1^Y(t)\,\mathcal{E}_1^Y(t+\tau)\right\rangle = \frac{1}{2\pi}\int_{-\infty}^{+\infty}\bar{\Omega}_I^Y(\omega)\left\{\frac{(\alpha_2 n_2\kappa)^2}{(n_2\kappa)^2+\omega^2}\right\}\left\{\frac{2n_3\kappa}{n_3\kappa+\omega^2}\right\}e^{-i\omega\tau}\,d\omega\ , \tag{6.13a}$$

$$\left\langle \mathcal{E}_2^Y(t)\,\mathcal{E}_2^Y(t+\tau)\right\rangle = \frac{1}{2\pi}\int_{-\infty}^{+\infty}\bar{\Omega}_A^Y(\omega)\left\{\frac{[n_2\kappa(1-\alpha_2)]^2+\omega^2}{(n_2\kappa)^2+\omega^2}\right\}\left\{\frac{n_3\kappa}{(n_3\kappa)^2+\omega^2}\right\}e^{-i\omega\tau}\,d\omega\ , \tag{6.13b}$$

$$\left\langle \mathcal{E}_3^Y(t)\,\mathcal{E}_3^Y(t+\tau)\right\rangle = \frac{1}{2\pi}\int_{-\infty}^{+\infty}\bar{\Omega}_B^Y(\omega)\left\{\frac{[n_2\kappa(1+\alpha_2)]^2+\omega^2}{(n_2\kappa)^2+\omega^2}\right\}\left\{\frac{n_3\kappa}{(n_3\kappa)^2+\omega^2}\right\}e^{-i\omega\tau}\,d\omega\ . \tag{6.13c}$$

In order to avoid diversion into ungainly computation, we call upon the results of Appendix A and leave the details therein. With faith, equations (6.12) integrate to,

$$\begin{aligned}
&\left\langle \mathcal{E}_1^X(t)\,\mathcal{E}_1^X(t+\tau)\right\rangle \\
&= [\alpha_1(n_1\kappa)]^2\,(n_3\kappa)\left\{\frac{(n_3\kappa)e^{-n_1\kappa|\tau|}-(n_1\kappa)e^{-n_3\kappa|\tau|}}{(n_1\kappa)(n_3\kappa)\left[(n_3\kappa)^2-(n_1\kappa)^2\right]}\right. \\
&\quad+\left(\gamma_{-\lambda_I}^2-\gamma_{\lambda_I}^2\right)\left(\frac{e^{-n_1\kappa|\tau|}}{(n_1\kappa)\left[\gamma_{\lambda_I}^2-(n_1\kappa)^2\right]\left[(n_3\kappa)^2-(n_1\kappa)^2\right]}\right. \\
&\quad\left.\left.+\frac{e^{-n_1\kappa|\tau|}}{\gamma_{\lambda_I}\left[(n_1\kappa)^2-\gamma_{\lambda_I}^2\right]\left[(n_3\kappa)^2-\gamma_{\lambda_I}^2\right]}+\frac{e^{-n_3\kappa|\tau|}}{(n_3\kappa)\left[\gamma_{\lambda_I}^2-(n_3\kappa)^2\right]\left[(n_1\kappa)^2-(n_3\kappa)^2\right]}\right)\right\}\ ,
\end{aligned} \tag{6.14a}$$

$$\begin{aligned}
&\left\langle \mathcal{E}_2^X(t)\,\mathcal{E}_2^X(t+\tau)\right\rangle \\
&= \frac{(n_3\kappa)}{2}\left\{\frac{e^{-n_3\kappa|\tau|}}{n_3\kappa}+\frac{n_1\kappa\left[(1+\alpha_1)^2-1\right]\left[(n_1\kappa)\,e^{-n_3\kappa|\tau|}-(n_3\kappa)\,e^{-n_1\kappa|\tau|}\right]}{(n_3\kappa)\left[(n_1\kappa)^2-(n_3\kappa)^2\right]}\right. \\
&\quad+\frac{\left(\gamma_{-\lambda}^2-\gamma_\lambda^2\right)\left(n_3\kappa\,e^{-\gamma_\lambda|\tau|}-\gamma_\lambda\,e^{-n_3\kappa|\tau|}\right)}{\gamma_\lambda(n_3\kappa)\left[(n_3\kappa)^2-\gamma_\lambda^2\right]} \\
&\quad+\left(\gamma_{-\lambda}^2-\gamma_\lambda^2\right)(n_1\kappa)^2\left[(1+\alpha_1)^2-1\right]\left(\frac{e^{-n_1\kappa|\tau|}}{(n_1\kappa)\left[\gamma_\lambda^2-(n_1\kappa)^2\right]\left[(n_3\kappa)^2-(n_1\kappa)^2\right]}\right. \\
&\quad\left.\left.+\frac{e^{-\gamma_\lambda|\tau|}}{\gamma_\lambda\left[(n_1\kappa)^2-\gamma_\lambda^2\right]\left[(n_3\kappa)^2-\gamma_\lambda^2\right]}+\frac{e^{-n_3\kappa|\tau|}}{(n_3\kappa)\left[\gamma_\lambda^2-(n_3\kappa)^2\right]\left[(n_1\kappa)^2-(n_3\kappa)^2\right]}\right)\right\}\ ,
\end{aligned} \tag{6.14b}$$

$$\Big\langle \mathcal{E}_3^X(t)\,\mathcal{E}_3^X(t+\tau)\Big\rangle$$
$$= \frac{(n_3\kappa)}{2}\Bigg\{ \frac{e^{-n_3\kappa|\tau|}}{n_3\kappa} + \frac{n_1\kappa\left[(1-\alpha_1)^2-1\right]\left[(n_1\kappa)\,e^{-n_3\kappa|\tau|}-(n_3\kappa)\,e^{-n_1\kappa|\tau|}\right]}{(n_3\kappa)\left[(n_1\kappa)^2-(n_3\kappa)^2\right]}$$
$$+\frac{\left(\gamma_\lambda^2-\gamma_{-\lambda}^2\right)\left(n_3\kappa\,e^{-\gamma_{-\lambda}|\tau|}-\gamma_{-\lambda}\,e^{-n_3\kappa|\tau|}\right)}{\gamma_{-\lambda}(n_3\kappa)\left[(n_3\kappa)^2-\gamma_{-\lambda}^2\right]}$$
$$+\left(\gamma_\lambda^2-\gamma_{-\lambda}^2\right)(n_1\kappa)^2\left[(1-\alpha_1)^2-1\right]\Bigg(\frac{e^{-n_1\kappa|\tau|}}{(n_1\kappa)\left[\gamma_{-\lambda}^2-(n_1\kappa)^2\right]\left[(n_3\kappa)^2-(n_1\kappa)^2\right]}$$
$$+\frac{e^{-\gamma_{-\lambda}|\tau|}}{\gamma_{-\lambda}\left[(n_1\kappa)^2-\gamma_{-\lambda}^2\right]\left[(n_3\kappa)^2-\gamma_{-\lambda}^2\right]}+\frac{e^{-n_3\kappa|\tau|}}{(n_3\kappa)\left[\gamma_{-\lambda}^2-(n_3\kappa)^2\right]\left[(n_1\kappa)^2-(n_3\kappa)^2\right]}\Bigg)\Bigg\}\,. \tag{6.14c}$$

We have introduced in (6.14), for ease of writing,

$$\gamma_\lambda \equiv \kappa\,(1+\lambda)\ , \quad \gamma_{\lambda_I} \equiv \kappa_I\,(1+\lambda_I)\ .$$

Letting $\lambda \longrightarrow -\lambda$, $\lambda_I \longrightarrow -\lambda_I$, and also $\alpha_1 \longrightarrow -\alpha_2$, $n_1 \longrightarrow n_2$, equations (6.13) are,

$$\Big\langle \mathcal{E}_1^Y(t)\,\mathcal{E}_1^Y(t+\tau)\Big\rangle$$
$$= [\alpha_2(n_2\kappa)]^2\,(n_3\kappa)\Bigg\{\frac{(n_3\kappa)e^{-n_2\kappa|\tau|}-(n_2\kappa)e^{-n_3\kappa|\tau|}}{(n_2\kappa)(n_3\kappa)\left[(n_3\kappa)^2-(n_2\kappa)^2\right]}$$
$$+\left(\gamma_{\lambda_I}^2-\gamma_{-\lambda_I}^2\right)\Bigg(\frac{e^{-n_2\kappa|\tau|}}{(n_2\kappa)\left[\gamma_{-\lambda_I}^2-(n_2\kappa)^2\right]\left[(n_3\kappa)^2-(n_2\kappa)^2\right]}$$
$$+\frac{e^{-n_2\kappa|\tau|}}{\gamma_{-\lambda_I}\left[(n_2\kappa)^2-\gamma_{-\lambda_I}^2\right]\left[(n_3\kappa)^2-\gamma_{-\lambda_I}^2\right]}+\frac{e^{-n_3\kappa|\tau|}}{(n_3\kappa)\left[\gamma_{-\lambda_I}^2-(n_3\kappa)^2\right]\left[(n_2\kappa)^2-(n_3\kappa)^2\right]}\Bigg)\Bigg\}\,, \tag{6.15a}$$

$$\Big\langle \mathcal{E}_2^Y(t)\,\mathcal{E}_2^Y(t+\tau)\Big\rangle$$
$$= \frac{(n_3\kappa)}{2}\Bigg\{ \frac{e^{-n_3\kappa|\tau|}}{n_3\kappa} + \frac{n_2\kappa\left[(1-\alpha_2)^2-1\right]\left[(n_2\kappa)\,e^{-n_3\kappa|\tau|}-(n_3\kappa)\,e^{-n_2\kappa|\tau|}\right]}{(n_3\kappa)\left[(n_2\kappa)^2-(n_3\kappa)^2\right]}$$
$$+\frac{\left(\gamma_\lambda^2-\gamma_{-\lambda}^2\right)\left(n_3\kappa\,e^{-\gamma_{-\lambda}|\tau|}-\gamma_{-\lambda}\,e^{-n_3\kappa|\tau|}\right)}{\gamma_{-\lambda}(n_3\kappa)\left[(n_3\kappa)^2-\gamma_{-\lambda}^2\right]}$$
$$+\left(\gamma_\lambda^2-\gamma_{-\lambda}^2\right)(n_2\kappa)^2\left[(1-\alpha_2)^2-1\right]\Bigg(\frac{e^{-n_2\kappa|\tau|}}{(n_2\kappa)\left[\gamma_{-\lambda}^2-(n_2\kappa)^2\right]\left[(n_3\kappa)^2-(n_2\kappa)^2\right]}$$
$$+\frac{e^{-\gamma_{-\lambda}|\tau|}}{\gamma_{-\lambda}\left[(n_2\kappa)^2-\gamma_{-\lambda}^2\right]\left[(n_3\kappa)^2-\gamma_{-\lambda}^2\right]}+\frac{e^{-n_3\kappa|\tau|}}{(n_3\kappa)\left[\gamma_{-\lambda}^2-(n_3\kappa)^2\right]\left[(n_2\kappa)^2-(n_3\kappa)^2\right]}\Bigg)\Bigg\}\,, \tag{6.15b}$$

$$\Big\langle \mathcal{E}_3^Y(t)\,\mathcal{E}_3^Y(t+\tau)\Big\rangle$$
$$= \frac{(n_3\kappa)}{2}\Bigg\{ \frac{e^{-n_3\kappa|\tau|}}{n_3\kappa} + \frac{n_2\kappa\left[(1+\alpha_2)^2-1\right]\left[(n_2\kappa)\,e^{-n_3\kappa|\tau|}-(n_3\kappa)\,e^{-n_2\kappa|\tau|}\right]}{(n_3\kappa)\left[(n_2\kappa)^2-(n_3\kappa)^2\right]}$$

$$+\frac{\left(\gamma_{-\lambda}^2-\gamma_\lambda^2\right)\left(n_3\kappa\, e^{-\gamma_\lambda|\tau|}-\gamma_\lambda\, e^{-n_3\kappa|\tau|}\right)}{\gamma_\lambda(n_3\kappa)\left[(n_3\kappa)^2-\gamma_\lambda^2\right]}$$
$$+\left(\gamma_{-\lambda}^2-\gamma_\lambda^2\right)(n_2\kappa)^2\left[(1+\alpha_2)^2-1\right]\left(\frac{e^{-n_2\kappa|\tau|}}{(n_2\kappa)\left[\gamma_\lambda^2-(n_2\kappa)^2\right]\left[(n_3\kappa)^2-(n_2\kappa)^2\right]}\right.$$
$$\left.\left.+\frac{e^{-\gamma_\lambda|\tau|}}{\gamma_\lambda\left[(n_2\kappa)^2-\gamma_\lambda^2\right]\left[(n_3\kappa)^2-\gamma_\lambda^2\right]}+\frac{e^{-n_3\kappa|\tau|}}{(n_3\kappa)\left[\gamma_\lambda^2-(n_3\kappa)^2\right]\left[(n_2\kappa)^2-(n_3\kappa)^2\right]}\right)\right\}. \tag{6.15c}$$

The average intensities follow by simply setting $\tau = 0$ in the above equations. Alice may help Bob complete the unit-gain by setting $\alpha_1 = \alpha_2 = 1$. She may further set $n_1 = n_2$ in which case,

$$\left\langle \mathcal{E}_2^X(t)\,\mathcal{E}_2^X(t+\tau)\right\rangle = \left\langle \mathcal{E}_3^Y(t)\,\mathcal{E}_3^Y(t+\tau)\right\rangle, \tag{6.16a}$$
$$\left\langle \mathcal{E}_2^Y(t)\,\mathcal{E}_2^Y(t+\tau)\right\rangle = \left\langle \mathcal{E}_3^X(t)\,\mathcal{E}_3^X(t+\tau)\right\rangle. \tag{6.16b}$$

If one intends to teleport a coherent vacuum state ($\lambda_I = 0$), then

$$\left\langle \mathcal{E}_1^X(t)\,\mathcal{E}_1^X(t+\tau)\right\rangle = \left\langle \mathcal{E}_1^Y(t)\,\mathcal{E}_1^Y(t+\tau)\right\rangle. \tag{6.17}$$

Properties (6.16) and (6.17) may of course also be read off directly from (6.14) and (6.15). Under conditions (6.16) and (6.17) the intensity correlation function may be further simplified to,

$$\left\langle \left[\mathcal{E}_{S3}^F(t)\right]^*\mathcal{E}_{S3}^F(t)\left[\mathcal{E}_{S3}^F(t+\tau)\right]^*\mathcal{E}_{S3}^F(t+\tau)\right\rangle$$
$$= 4\left[\left\langle \mathcal{E}_1^X(t)\,\mathcal{E}_1^X(t+\tau)\right\rangle+\left\langle \mathcal{E}_2^X(t)\,\mathcal{E}_2^X(t+\tau)\right\rangle+\left\langle \mathcal{E}_3^X(t)\,\mathcal{E}_3^X(t+\tau)\right\rangle\right]^2$$
$$+4\left\langle \left[\mathcal{E}_1^X(t)\right]^2+\left[\mathcal{E}_2^X(t)\right]^2+\left[\mathcal{E}_3^X(t)\right]^2\right\rangle^2. \tag{6.18}$$

It is more preferable to consider the normalized correlation function, denoted by

$$g_{\text{SED}}^{(2)}(\tau) \equiv \frac{\left\langle \left[\mathcal{E}_{S3}^F(t)\right]^*\mathcal{E}_{S3}^F(t)\left[\mathcal{E}_{S3}^F(t+\tau)\right]^*\mathcal{E}_{S3}^F(t+\tau)\right\rangle}{\left\langle \left[\mathcal{E}_{S3}^F(t)\right]^*\mathcal{E}_{S3}^F(t)\right\rangle^2}$$
$$= 1+\left\{\frac{\left\langle \mathcal{E}_1^X(t)\,\mathcal{E}_1^X(t+\tau)\right\rangle+\left\langle \mathcal{E}_2^X(t)\,\mathcal{E}_2^X(t+\tau)\right\rangle+\left\langle \mathcal{E}_3^X(t)\,\mathcal{E}_3^X(t+\tau)\right\rangle}{\left\langle \left[\mathcal{E}_1^X(t)\right]^2+\left[\mathcal{E}_2^X(t)\right]^2+\left[\mathcal{E}_3^X(t)\right]^2\right\rangle}\right\}^2. \tag{6.19}$$

6.2 Stochastic Electrodynamics vs Quantum Trajectories

We now compare the above intensity correlations derived using stochastic electrodynamics with those obtained from a quantum trajectory formulation [52]. A quantum calculation necessarily requires a normally ordered treatment,

$$g_{\text{QT}}^{(2)}(\tau) \equiv \frac{\left\langle \left[\hat{\mathcal{E}}_{S3}^F(t)\right]^\dagger\left[\hat{\mathcal{E}}_{S3}^F(t+\tau)\right]^\dagger\hat{\mathcal{E}}_{S3}^F(t+\tau)\,\hat{\mathcal{E}}_{S3}^F(t)\right\rangle}{\left\langle \left[\hat{\mathcal{E}}_{S3}^F(t)\right]^\dagger\hat{\mathcal{E}}_{S3}^F(t)\right\rangle^2} \tag{6.20}$$

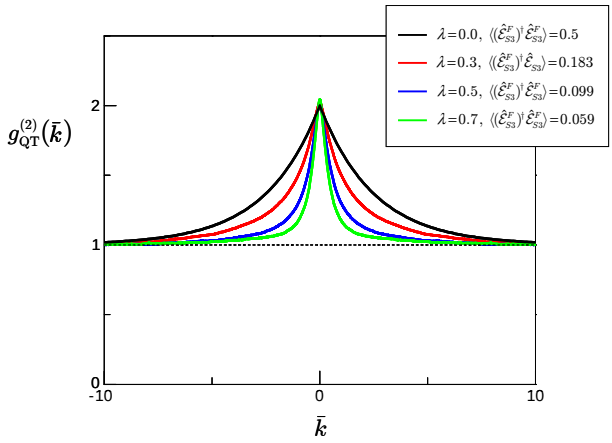

Fig. 6.1: Simulation results of $g^{(2)}_{\rm QT}$ from quantum trajectories for various values of squeezing given the filter bandwidths specified by $n_1 = n_2 = 10$ and $n_3 = 0.2$ [52].

to coincide with the measurement of photo-detection. The important equations describing broadband teleportation of a coherent vacuum state when Victor performs a direct photon count at the teleporter output are neatly summarized in Ref. [52]. We will not be bothered with the explicit form of these equations. We are interested in the final form of $g^{(2)}_{\rm QT}(\tau)$, qualitatively, and quantitatively in the teleported photon numbers seen by Victor. Only the modes closest to the resonant are considered.

In Fig. 6.1 we plot the normalized correlation function as measured by Victor against $\bar{k} \equiv \kappa\tau$ for different values of λ. The figure also displays the corresponding to the mean photon numbers inside his filter cavity given by $\langle(\hat{\mathcal{E}}^F_{S3})^\dagger\hat{\mathcal{E}}^F_{S3}\rangle$. Only the modes closest to the resonant are considered. The analytical results of (6.19) and (6.14) are shown in Fig. 6.2.

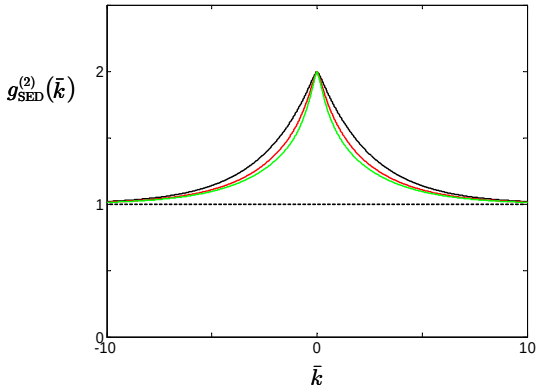

Fig. 6.2: Normalized intensity correlations as predicted by SED, i.e. (6.19). The same colour code to Fig. 6.1 is kept and for clarity the $\lambda = 0.5$ curve, which lies between those for $\lambda = 0.3$ and $\lambda = 0.7$, has been omitted.

A discrepancy is observed in the intensity correlations calculated by quantum trajectories and SED. Clearly, SED does not predict any significant change in the intensity correlation of the teleported field when one increases the pumping of S_A and S_B. The change in $g^{(2)}_{\rm SED}(\tau)$ is almost negligible for values of the pump parameter beyond 0.5. Had we not

been given the quantum result of Fig. 6.1, it certainly would have been tempting to argue that it is essentially the situation depicted by Fig. 5.2 (b), i.e. the squeezing undergoes insignificant changes for values of the pump parameter greater than 0.5. As anticipated, the problem arises from an incorrect account of operator ordering when the measured quantity is normally ordered. Stochastic electrodynamics would add one half to the photon numbers given in Fig. 6.1. A photon number calculation within SED should come out of the above results.

To give a comprehensive discussion of the implications brought about by a quantum field as opposed to a classical field with a real fluctuating zero-point energy on the observed photocurrent would drag us to a theory of measurement. This is beyond the scope of the thesis.

Chapter 7

Conclusion

It is fitting that we begin by recapitulating the intended scope of this report: to use SED as a means of obtaining a broadband description for teleportation of the two quadrature phase amplitudes belonging to an optical field. In particular, teleportation of vacuum modes have been examined where analytical expressions for the teleported squeezing spectra and intensity correlation function were obtained for both squeezed and coherent inputs.

7.1 Broadband Teleportation

Teleportation is broadband, limited by the bandwidth of an ideal EPR source. The process of verifying broadband teleportation was made viable by our ability to relate the Fourier components seen by Victor to those impinging on the input cavity, and the cavities preparing the EPR correlations. Collett's and Gardiner's input-output theory in the Heisenberg picture was pivotal in facilitating our derivation of the linear mapping with random variables. The mapping may be summarized by equations (4.45), (4.46), and (4.47), together with (5.17) and (5.18). These equations provide a continuous-time description of the teleporter; this is to say that all the necessary steps required to accomplish teleportation occur uninterruptedly. One may like to think of the input field as having an interminable temporal extension, made to entangle continuously with one of the EPR beams via a beam-splitter. In this way, our scheme, the scheme of Fig. 3.1 in the long-time limit, has no identifiable *sequence* in which a particular procedure should be activated. Every processing unit (e.g. Alice's BSM and filtering) of the teleporter operates concurrently with each other.

7.2 Classicality and the Wigner Distribution

The validity of a classical description by SED hinges on the positivity of the Wigner distribution and the measurement schemes intrinsic to the teleportation protocol. The general class of Gaussian states — coherent and squeezed states — all have a positive-definite Wigner distribution. The realistic interpretation of a non-negative Wigner distribution can only predict correctly the results of quadrature measurements and no other. We have demonstrated this benchmark with the example of SED by showing that it is capable of describing the entanglement resource consisting of vacuum squeezed states, and teleportation (of Gaussian states) in its entirety only when Victor performs a quadrature measurement at the output.

Finally, for teleportation of Gaussian states using the standard protocol considered in this report, SED provides a local hidden-variable interpretation of teleportation.

7.3 Quadrature Teleportation Revisited

Equations (5.40) and (5.43) are our basic results describing teleportation of the X- and Y-quadrature for a vacuum input. Teleportation with homodyning at the output may be succinctly summarized by the parameters; $g \equiv \kappa_I/\kappa$, λ, n_1 and n_3. The parameters g and λ are *the* features of quantum teleportation and hence the most important parameters of the teleporter. Dismissing the classical channel capabilities, what is at stake are the properties empowering an accurate replication of $\mathcal{E}_I(t)$ at the teleporter output. These properties are g and λ.

- **Squeezing bandwidth**

  The squeezing bandwidth should be made larger than the bandwidth of the input. The larger the better. This is summarized by Figs. 5.6, 5.7, and 5.8. This is obvious since we have resolved the EPR correlations frequency by frequency, where the degree of correlation is indicated by λ. Thus the input modes outside the squeezing bandwidth have no useful partner to be entangled with.

- **Pump parameter**

  The pump parameter indicates the amount of squeezing per unit bandwidth. The closer λ is to one the better the teleportation. This is expected since the stronger the squeezing in S_A and S_B, the stronger the entanglement between $\mathcal{E}_A(t)$ and $\mathcal{E}_B(t)$. This point is demonstrated by Figs. 5.3 and 5.4. However, the observable effect of squeezing on the similitude between output and input decreases as the cavities are pumped more and more intensely, as shown in Fig. 5.2.

7.4 Intensity Correlation and Photon Number at the Output

Photon counts, and therefore intensity correlation measurements at the teleporter output can not be accounted for within SED. Commutation relations are called for to legitimately keep track of the vacuum energy. A natural extension from here would be to subtract the vacuum fluctuations to produce the correct teleported photon number and intensity correlation function. We recognize this quantitatively by (5.56), and qualitatively in the interpretation of the vacuum as a real fluctuating field causing photo-electrons to be emitted by photo-detectors.

Appendix A

Fourier Integrals of Lorentzian Products

The necessary integral identities for the classical intensity correlation function of Chap. 6 are derived. Note that equations (6.12) or (6.13) demand only integrals of the form

$$I_1 \equiv \int_{-\infty}^{+\infty} \frac{a^2+\omega^2}{(b^2+\omega^2)(c^2+\omega^2)(d^2+\omega^2)}\, e^{-i\omega\tau}\, d\omega\ , \tag{A.1a}$$

$$I_2 \equiv \int_{-\infty}^{+\infty} \frac{(a^2+\omega^2)(c^2+\omega^2)}{(b^2+\omega^2)(d^2+\omega^2)(q^2+\omega^2)}\, e^{-i\omega\tau}\, d\omega \tag{A.1b}$$

where a, b, c, d and q are all constants. Let us first work out I_2. Note the integrand may be written, either by the method of partial fractions, or by an algebraic manipulation performed below as,

$$\begin{aligned} I_2 &= \int_{-\infty}^{+\infty} \left(\frac{a^2-b^2+b^2+\omega^2}{b^2+\omega^2}\right)\left(\frac{c^2-d^2+d^2+\omega^2}{d^2+\omega^2}\right)\frac{1}{q^2+\omega^2}\, e^{-i\omega\tau}\, d\omega \\ &= \int_{-\infty}^{+\infty} \left[\frac{1}{q^2+\omega^2} + \frac{a^2-b^2}{(b^2+\omega^2)(q^2+\omega^2)} + \frac{c^2-d^2}{(d^2+\omega^2)(q^2+\omega^2)}\right. \\ &\quad \left. + \frac{(a^2-b^2)(c^2-d^2)}{(b^2+\omega^2)(d^2+\omega^2)(q^2+\omega^2)}\right] e^{-i\omega\tau}\, d\omega\ . \end{aligned} \tag{A.2}$$

Integrals of this form may be computed on the complex plane by defining ω (β) to be the real (imaginary) part of

$$z \equiv \omega + i\beta = |z|\,(\cos\phi + i\sin\phi)\ , \tag{A.3}$$

with $\phi \equiv \arg(z)$. One may wish to then define a function of the complex variable z,

$$f(z) \equiv \frac{e^{-iz\tau}}{(b^2+z^2)(d^2+z^2)(q^2+z^2)} \tag{A.4}$$

and express it in terms of ϕ,

$$f(z) = \frac{e^{-i|z|\tau\cos\phi} e^{|z|\tau\sin\phi}}{(z^2+b^2)(z^2+d^2)(z^2-q^2)} \; . \tag{A.5}$$

To be justified shortly by (A.8), we now write each piece of I_2 as a contour integral where an appropriate choice of contour must be effected depending on the parameter τ. Let us consider

$$\int_{-\infty}^{+\infty} \frac{e^{-i\omega\tau}\, d\omega}{(b^2+\omega^2)(d^2+\omega^2)(q^2+\omega^2)} = \lim_{|z|\to\infty} \oint_{\mathrm{C}} f(z)\, dz \; . \tag{A.6}$$

For convergence of the right hand side of (A.6), the following parameterizations for C are hinted by (A.5):

$$\phi \in [0, \pi] \; , \quad \text{for } \tau < 0 \; , \tag{A.7a}$$

$$\phi \in [0, -\pi] \; , \quad \text{for } \tau > 0 \; . \tag{A.7b}$$

For $\tau < 0$, C is the closed anticlockwise contour (also said to be traversed in the positive sense) shown by the dashed semicircle in Fig. A.1 (b). Equation (A.6) can be understood by writing the closed line integral as

$$\oint_{\mathrm{C}} f(z)\, dz = \int_{\mathrm{C}_1} f(z)\, dz + \int_{\mathrm{C}_2} f(z)\, dz \; . \tag{A.8}$$

In the limit $|z| \longrightarrow \infty$, **Jordan's lemma** asserts the second integral over the entire arc of C to be zero [72]. The left hand side of (A.8) then amounts to an integral over the real line stretching from $-\infty$ to $+\infty$, as originally intended in (A.6). For $\tau > 0$, C may be chosen to be a semicircle traversed clockwise enclosing the negative pure imaginary poles in the lower half plane. This is shown in Fig. A.1 (a).

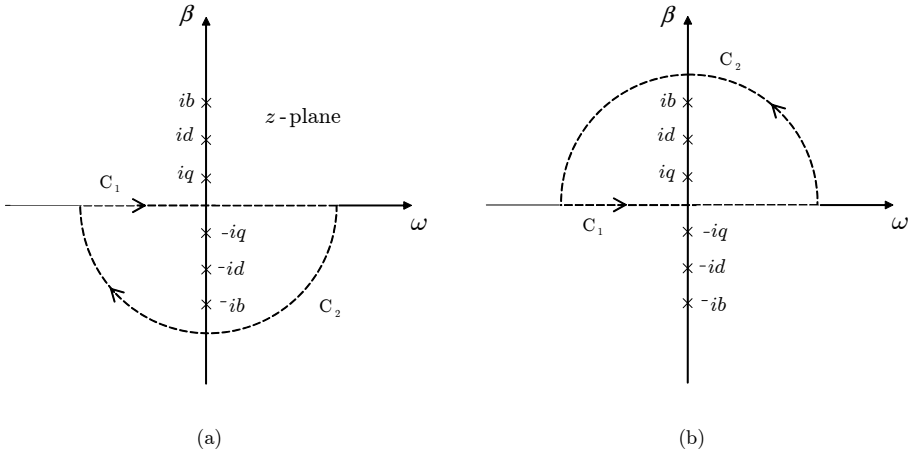

Fig. A.1: Contour integral for calculating I_2. (a) $\tau > 0$. (b) $\tau < 0$.

The line integral around C is now straightwardly computable by the **Residue theorem** [73]. For $\tau > 0$, the theorem states

$$\lim_{|z|\to\infty} \oint_{\mathrm{C}} f(z)\, dz \; = \; -2\pi i \lim_{|z|\to\infty} \Big(\text{sum over enclosed residues}\Big) \; , \tag{A.9}$$

where for some function F of a complex variable z, the residue at a pole z_p is denoted by $\mathrm{Res}(F; z_p)$. For a simple pole

$$\mathrm{Res}(F; z_p) = \lim_{z \to z_p} (z - z_p)\, F(z)\ . \tag{A.10}$$

Hence (A.9) is given by,

$$\begin{aligned}\lim_{|z|\to\infty} \oint_{\mathrm{C}} f(z)\, dz \;&=\; \pm\, 2\pi i \lim_{|z|\to\infty} \Big[\mathrm{Res}(f; -id) + \mathrm{Res}(f; -ib) + \mathrm{Res}(f; -iq)\Big] \\ &= \pi \left[\frac{e^{\pm d\tau}}{d(b^2 - d^2)(q^2 - d^2)} + \frac{e^{\pm b\tau}}{b(d^2 - b^2)(q^2 - b^2)} \right. \\ &\quad \left. + \frac{e^{\pm q\tau}}{q(b^2 - q^2)(d^2 - q^2)} \right]\ ,\end{aligned} \tag{A.11}$$

where we take the positive or negative sign for $\tau > 0$ or $\tau < 0$ respectively in the exponents. By similar means, the remaining terms in (A.2) are

$$\int_{-\infty}^{+\infty} \frac{e^{-i\omega\tau}\, d\omega}{(b^2 + \omega^2)(q^2 + \omega^2)} \;=\; \frac{\pi \left(q\, e^{\pm b\tau} - b\, e^{\pm q\tau}\right)}{bq(q^2 - b^2)}\ , \tag{A.12}$$

$$\int_{-\infty}^{+\infty} \frac{e^{-i\omega\tau}}{q^2 + \omega^2}\, d\omega \;=\; \frac{\pi e^{\pm q\tau}}{q}\ . \tag{A.13}$$

Combining (A.11), (A.12), and (A.13) we can write I_2 for all τ as,

$$\begin{aligned}&\int_{-\infty}^{+\infty} \frac{(a^2 + \omega^2)(c^2 + \omega^2)}{(b^2 + \omega^2)(d^2 + \omega^2)(q^2 + \omega^2)}\, e^{-i\omega\tau}\, d\omega \\ &\quad = \pi \left\{ \frac{e^{-q|\tau|}}{q} + \frac{\left(a^2 - b^2\right)\left(q\, e^{-b|\tau|} - b\, e^{-q|\tau|}\right)}{bq(q^2 - b^2)} + \frac{\left(c^2 - d^2\right)\left(d\, e^{-q|\tau|} - q\, e^{-d|\tau|}\right)}{qd(d^2 - q^2)} \right. \\ &\qquad + \left(a^2 - b^2\right)\left(c^2 - d^2\right) \left[\frac{e^{-d|\tau|}}{d(b^2 - d^2)(q^2 - d^2)} + \frac{e^{-b|\tau|}}{b(d^2 - b^2)(q^2 - b^2)} \right. \\ &\qquad \left. \left. + \frac{e^{-q|\tau|}}{q(b^2 - q^2)(d^2 - q^2)} \right] \right\}\ .\end{aligned} \tag{A.14}$$

Let us quote I_1 and leave the details as an exercise for the reader,

$$\begin{aligned}&\int_{-\infty}^{+\infty} \frac{a^2 + \omega^2}{(b^2 + \omega^2)(c^2 + \omega^2)(d^2 + \omega^2)}\, e^{-i\omega\tau}\, d\omega \\ &\qquad = \pi \left\{ \frac{\left(d\, e^{-c|\tau|} - c\, e^{-d|\tau|}\right)}{cd(d^2 - c^2)} + (a^2 - b^2) \left[\frac{e^{-c|\tau|}}{c(b^2 - c^2)(d^2 - c^2)} \right. \right. \\ &\qquad \left. \left. + \frac{e^{-b|\tau|}}{b(c^2 - b^2)(d^2 - b^2)} + \frac{e^{-d|\tau|}}{d(b^2 - d^2)(c^2 - d^2)} \right] \right\}\ .\end{aligned} \tag{A.15}$$

Bibliography

[1] A. Einstein, B. Podolsky, and N. Rosen, *Phys. Rev.* **47**, 777 (1935).

[2] H. Kragh, *Quantum Generations*, Chap. 14 (Princeton University Press, 1999)

[3] D. Bohm and Y. Aharonov, *Phys. Rev.* **108**, 1070 (1957)

[4] E. Schrödinger, *Die Naturwissenschaften* **23**, 807 (1935).

[5] W. Moore, *Schrödinger*, Chap. 8 (Cambridge University Press, 1989, 1990).

[6] E. Schrödinger, *Proc. Cambridge Phil. Soc.* **31**, 555 (1935).

[7] G. Auletta, *Foundations and Interpretation of Quantum Mechanics*, Chap. 3, (World Scientific, 2001).

[8] J. von Neumann, *Mathematische Grundlagen der Quanten-mechanik*, (Julius Springer-Verlag, 1932).

[9] D. Bohm, *Phys. Rev.* **85**, 166 (1952).

[10] D. Bohm, *Phys. Rev.* **85**, 180 (1952).

[11] J. S. Bell, *Physics* **1**, 195 (1964).

[12] J. S. Bell, *Rev. Mod. Phys.* **38**, 447 (1966).

[13] J. F. Clauser, M. A. Horne, A. Shimony, and R. A. Holt, *Phys. Rev. Lett.* **23**, 880 (1969).

[14] D. M. Greenberger, M. A. Horne, and A. Zeilinger, *Bell's Theorem, Quantum Theory, and Conceptions of the Universe*, (Kluwer Academics, 1989).

[15] D. M. Greenberger, M. A. Horne, A. Shimony, and A. Zeilinger, *Am. J. Phys.* **58**, 1131 (1990).

[16] D. Bouwmeester, J.-W. Pan, M. Daniell, H. Weinfurter, and A. Zeilinger, *Phys. Rev. Lett.* **82**, 1345 (1999).

[17] S. J. Freedman and J. F. Clauser, *Phys. Rev. Lett.* **28**, 938 (1972).

[18] A. Aspect, P. Grangier, and G. Roger, *Phys. Rev. Lett.* **47**, 460 (1981).

[19] A. Aspect, J. Dalibard, and G. Roger, *Phys. Rev. Lett.* **49**, 1804 (1982).

[20] A, Aspect, P. Grangier, and G. Roger, *Phys. Rev. Lett.* **49**, 91 (1982).

[21] W. Tittel, J. Brendel, H. Zbinden, and N. Gisin, *Phys. Rev. Lett.* **81**, 3563 (1998).

[22] M. A. Nielson, *Sci. Am.* **13** No.1, 25 (2003).

[23] M. A. Nielson and I. L. Chuang, *Quantum Computation and Quantum Information*, Chap. 12 (Cambridge University Press, 2000).

[24] D. Bouwmeester, A. Ekert, and A. Zeilinger (Eds.), *The Physics of Quantum Information*, (Springer-Verlag, 2000).

[25] C. H. Bennett, G. Brassard, C. Crépeau, R. Jozsa, A. Peres, and W. K. Wooters, *Phys. Rev. Lett.* **70**, 1895 (1993).

[26] W. K. Wootters and W. H. Zurek, *Nature* **299**, 802, (1982).

[27] S. L. Braunstein, A. Mann, and M. Revzen, *Phys. Rev. Lett.* **68**, 3259 (1992).

[28] C. H. Bennett and S. J. Wiesner, *Phys. Rev. Lett.* **69**, 2881 (1992).

[29] S. Popescu, *LANL e-print*, quant-ph 9501020 (1995).

[30] D. Boschi, S. Branca, F. De Martini, L. Hardy, and S. Popescu, *Phys. Rev. Lett.* **80**, 1121 (1998).

[31] M. Żukowski, A. Zeilinger, M. A. Horne, and A. K. Ekert, *Phys. Rev. Lett.* **71**, 4287 (1993).

[32] S. Bose, V. Vedral, and P. L. Knight, *Phys. Rev.* **A 57**, 822 (1998).

[33] J.-W. Pan, D. Bouwmeester, H. Weinfurter, and A. Zeilinger, *Phys. Rev. Lett.* **80**, 3891 (1998).

[34] D. Bouwmeester, J.-W. Pan, K. Mattle, M. Eibl, H. Weinfurter, and A. Zeilinger, *Nature* **390**, 575 (1997).

[35] L. Vaidman, *Phys. Rev.* **A 49**, 1473 (1994).

[36] S. L. Braunstein and H. J. Kimble, *Phys. Rev. Lett* **80**, 869 (1998).

[37] P. van Loock, S. L. Braunstein, and H. J. Kimble, *Phys. Rev.* **A 62**, 022309 (2000).

[38] A. Furusawa, J. L. Sørensen, S. L. Braunstein, C. A. Fuchs, H. J. Kimble, and E. S. Polzik, *Science* **282**, 706 (1998).

[39] T. C. Zhang, K. W. Goh, C. W. Chou, P. Lodahl, and H. J. Kimble, *Phys. Rev.* **A 67**, 033802 (2003).

[40] W. P. Bowen, N. Treps, B. C. Buchler, R. Schnabel, T. C. Ralph, H.-A. Bachor, T. Symul, and P. K. Lam, *Phys. Rev.* **A 67**, 032302 (2003).

[41] M. O. Scully and M. S. Zubairy, *Quantum Optics*, Chap. 4 (Cambridge University Press, 1997).

[42] H. P. Yuen and V. W. S. Chan, *Opt. Lett.* **8**, 177 (1982).

[43] T. W. Marshall and E. Santos, *Found. Phys* **18**, 185 (1988).

[44] T. W. Marshall, *Proc. R. Soc. London* **276**, 475 (1963).

[45] T. H. Boyer, *Phys. Rev.* **A 5**, 1799 (1972).

[46] T. H. Boyer, *Phys. Rev.* **174**, 1631 (1968).

[47] L. de la Pẽna-Auerbach and A. M. Cetto, *Phys. Lett.* **A 47**, 183 (1974).

[48] L. J. Landau, *Phys. Rev.* **A 37**, 4449 (1988).

[49] L. de la Pẽna-Auerbach and A. M. Cetto, *J. Math. Phys.* **18**, 1612 (1977).

[50] H. J. Carmichael and H. Nha, *J. Opt. B* **6**, S645 (2004).

[51] P. Heszler, D. Abbott, J. R. Gea-Banacloche, and P. R. Hemmer (Eds.), *Fluctutations and Noise in Photonics and Quantum Optics II*, *Proc. SPIE* **5468**, 282 (2004).

[52] H. J. Carmichael, *Continuous Variable Teleportation of Quantum Fields*, *Proc.* 1^{st} *Asia-Pacific Conf. QI Sci* (World Scientific, 2005) in press.

[53] J. S. Bell, *New Techniques and Ideas in Quantum Measurement Theory*, (New York Academy of Sciences, 1986).

[54] K. Banaszek and Wódkiewicz, *Phys. Rev.* **A 58**, 4345 (1998).

[55] C. W. Gardiner, *Handbook of Stochastic Methods for Physics, Chemistry and the Natural Sciences 3rd edition*, Chap. 4 (Spinger-Verlag, 2004).

[56] P. Hannaford, A. Sidorov, H. Bachor, and K. Baldwin (Eds.), *Laser Spectroscopy*, *Proc. XVI Intl. Con. Laser Spectroscopy*, 324 (World Scientific, 2004).

[57] W. P. Schleich, *Quantum Optics in Phase Space*, Chap. 13 (WILEY-VCH Verlag, 2001).

[58] H. J. Carmichael, *Statistical Methods in Quantum Optics 1*, Chap. 7 (Springer-Verlag, 2002).

[59] C. M. Caves and B. L. Schumaker, *Phys. Rev.* **A 31**, 3068 (1985).

[60] B. L. Schumaker and C. M. Caves, *Phys. Rev.* **A 31**, 3093 (1985).

[61] M. J. Collett and C. W. Gardiner, *Phys. Rev.* **A 30**, 1386 (1984).

[62] C.W. Gardiner and M. J. Collet, *Phys. Rev.* **A 31**, 3761 (1985).

[63] B. Yurke and J. S. Denker, *Phys. Rev.* **A 29**, 1419 (1984).

[64] P.D. Drummond and Z. Ficek (Eds.), *Quantum Squeezing*, Chap. 3 (Springer-Verlag, 2004).

[65] G. Milburn and D. F. Walls, *Opt. Commun.* **39**, 401 (1981).

[66] B. Yurke, *Phys. Rev.* **A 29**, 408 (1984).

[67] C. M. Caves, *Phys. Rev.* **D 26**, 1817 (1982).

[68] Philippe Réfrégier, *Noise Theory and Application to Physics*, Chap. 3 (Springer-Verlag, 2003).

[69] B. Schumaker, *Phys. Rev.* **A 51**, 2783 (1995).

[70] S. L. Braunstein, C. A. Fuchs, and H. J. Kimble, *J. Mod. Opt* **47**, 267 (2000).

[71] L. Mandel and E. Wolf, *Optical Coherence and Quantum Optics*, Chap. 1 (Cambridge University Press, 1995).

[72] G. B. Arfken and H. J. Weber, *Mathematical Methods for Physicists 5th edition*, Chap. 5 (Academic Press, 2001).

[73] A. D. Osbourne, *Complex Variables and their Applications*, Chap. 5 (Addison Wesley Longman Limited, 1999)